GENOMIC AND EPIDEMIOLOGICAL ANALYSES OF *CANDIDA AURIS*: UNRAVELING INSIGHTS INTO A CRITICAL HUMAN FUNGAL PATHOGEN

GENOMIC AND EPIDEMIOLOGICAL ANALYSES OF *CANDIDA AURIS*: UNRAVELING INSIGHTS INTO A CRITICAL HUMAN FUNGAL PATHOGEN

by

YUE WANG, B.Sc.

A Thesis
Submitted to the School of Graduate Studies
in Partial Fulfillment of the Requirements
for the Degree of
Doctor of Philosophy

McMaster University

DOCTOR OF PHILOSOPHY (2023) McMaster University
(Biology) Hamilton, Ontario, Canada

TITLE:	Genomic and Epidemiological Analyses of *Candida auris*: Unraveling Insights into a Critical Human Fungal Pathogen
AUTHOR:	Yue Wang
	B.Sc. (Bioinformatics)
	Soochow University, Suzhou, China
SUPERVISOR:	Dr. Jianping Xu
NUMBER OF PAGES:	x, 169

Abstract

Fungi are vital microbes present throughout the biosphere. Many species are essential decomposers in the ecosystem, breaking down organic materials and nourishing other lives. Moreover, some have directly influenced human civilization by providing beneficial products, such as edible mushrooms, brewer's yeast, baker's yeast, and antibiotics. However, it's important to note that this group of organisms can also have a “dark side”. Each year, fungal pathogens cause approximately 150 million severe infections and 1.7 million deaths. The high rate of infection is compounded by the limited availability of antifungal drugs and the increasing prevalence of antifungal resistance. In response to the global burden of fungal diseases, the World Health Organization published a list of priority fungal pathogens in 2022 and highlighted strategies such as surveillance, sustainable research investments, and public health interventions to combat the increasing fungal threats. My PhD research has focused on surveillance and genomic analyses of several human fungal pathogens, particularly *Candida auris*. *Candida auris* is an emerging multidrug-resistant yeast that causes systemic infections with high mortality rates. While initially recognized as a nosocomial pathogen, our genomic analyses of strains isolated from clinical environments, tropical wetlands, fruit surfaces, and dog ears revealed potential transmission routes between diverse environments and patients, including a potential driver for the prevalence of antifungal resistance. Furthermore, our research indicated limited genetic exchange within and between lineages of *Candida auris*. Through genome-wide association analyses of global *Candida auris* strains, several known and novel genomic variants were identified associated with susceptibility to azoles, echinocandins, and amphotericin B. Overall, our studies underscore the importance of continuous surveillance to understand potential routes of *Candida auris* transmission and the urgent need for innovative approaches to treat multidrug-resistant *Candida auris* infections.

Acknowledgments

I joined Dr. Jianping (JP) Xu's lab in 2018 as a master student studying genomic variation in one of the important human fungal pathogen *Cryptococcus neoformans*, and have since then been passionate about fungal genomics, curious about how fungal pathogens evolve to cause diseases. I would like to express my heartfelt gratitude to JP. Without his guidance, I would have never had the opportunity to explore and appreciate the wonders of fungi. He has been the most patient and supportive supervisor, providing continuous guidance and support. I sincerely appreciate his invaluable contribution to my personal and professional growth as a better person and researcher.

I also want to extend my gratitude to my supervisory committee members, Dr. Golding Brian, and Dr. James Quinn, who have witnessed every milestone I accomplished in my PhD career and provided me with valuable advice and inspiration. I am appreciative to the previous lab members, Adrian Forsythe, Himeshi Samarasinghe, Lijun Liu, Sarah Sandor, Yuying Fan, Man You, Meagan Archer, who have helped me with my research and the adaptation to the new environment, as well as the current lab members, Gregory Korfanty, Chadabhorn Insuk, Megan Hitchcock, Veronica Thorn, Viraj Whabi, and Nicolas Popescu, for our remarkable camaraderie and support. A special thanks to Heather Yoell, who is very hospitable and warm-hearted. I will miss those parties and her special banana brownie.

Moreover, I would like to thank Dr. Anuradha Chowdhary and her lab members, who have made noteworthy contributions to my thesis work. Without their participation, I would not be able to complete those projects efficiently and comprehensively. I wish them all the best in their future and research.

At last, I must thank my parents for their love and support throughout my life, and Jing Wang for the love and companionship during the past five years.

Table of Contents

List of Figures

List of Tables

Chapter 1

Introduction

1.1 Fungal Diversity and their Ecological Role

Fungi represent a very diverse group of eukaryotic microbes that exist in almost every ecological niche on earth. There are estimated at 2.2 to 3.8 million species in the fungal kingdom, although only 140,000 have been officially recognized and named (Hawksworth et al., 2017). A substantial portion of fungal species are decomposers, with different fungi serving different roles during decomposition from consuming simple sugars to breaking down lignin and other organic residues. In addition, fungi and bacteria can collaborate to break down and transform complex molecules into nutrients that can be utilized by plants and other organisms in the soil (Lubbe et al., 2012). Furthermore, plants and fungi can form symbiotic relationship known as mycorrhizae. Through this association, fungi can get direct and constant access to carbohydrates, while plants absorb water and mineral nutrients easier through mycorrhizae (Kottke et al., 2005). It is estimated that roughly 92% of plant families form mycorrhizae, and mycorrhizal plants exhibit more resistance to diseases, drought, and salinity than plants without mycorrhizae (Rivero et al., 2018; Aroca et al., 2013; B. Wang et al., 2006).

1.2 Benefits of Fungi for Humans

The relationship between humans and fungi started since before recorded history. In September 1991, a mummy of a man who lived between 3350 and 3105 BC was discovered in Europe and among his possessions included two species of mushrooms, which were believed to be used as an anthelmintic and a tinder (Capasso, 1998). Mushrooms are macroscopic fungal fruiting bodies typically generated by members of *Basidiomycota* and *Agaricomycetes*. It is estimated that 140,000 species of mushrooms exist in nature, yet only 14,000 (10%) have been described (Wasser, 2002). Approximately 25 of them are

commonly cultivated and consumed, including *Agaricus bisporus*, *Lentinula edodes* (shiitake), *Pleurotus spp*, and *Flammulina velutipes* (enoki). Due to the high protein, vitamin, mineral, yet low calories, carbohydrates, and fat contents, edible mushrooms are considered as an excellent source of nutrition (Mattila et al., 2001; Barros et al., 2008). In addition, there is a long history of using mushrooms as traditional medicine. *Ganoderma lucidum* was listed in the oldest official book of 365 medicinal substances, Shennong Bencao Jing. It has been used for at least 2000 years to enhance physical constitution, prevent diseases, and to slow aging, which was considered an elixir of life. Current studies have shown that metabolites of mushrooms present a wide spectrum of biological activity, such as antimicrobial, immunomodulatory, and antineoplastic properties (Alves et al., 2012; Chang et al., 2012; Wasser, 2002; Zhao et al., 2020). Additionally, due to their ability to convert sugars into alcohol and carbon dioxide, yeasts have been extensively utilized in the food industry for fermentation processes involved in making bread, beer, wine, and various other beverages (Querol and Fleet, 2006).

1.3 The Dark Side of Fungi

Plant fungal pathogens inflict substantial damages to crops, leading to significant annual crop losses ranging from 10% to 20% (Xu, 2022). The economic impact of these losses amounts to a staggering $100 to $200 billion ("Food Security: How Do Crop Plants Combat Pathogens?", 2022). Similarly, approximately 30% of harvested fruit and vegetables is lost to fungal infections each year (Sirivatanapa, 2006; Bano et al., 2023). Furthermore, fungal infections in humans have been occurring at an alarming rate, with a significant increase in recent years (Kainz et al., 2020). According to data from the Centers for Disease Control and Prevention (CDC) in the US, fungal infections caused by the yeast strain *Candida auris* (*C. auris*) have experienced a threefold increase nationally, rising from 476 cases in 2019 to 1,471 cases in 2021 (Nirappil, 2023). On the other hand, global warming effect boosts the adaptation of soil-dwelling fungi to human body temperatures (Gusa et al., 2023; Gadre et al., 2022). As a result, previously uncommon fungal pathogens, such as *Lodderomyces elongisporus* and *C. auris*, have emerged and been identified as the cause of nosocomial

outbreaks in healthcare settings in recent years (Casadevall et al., 2019; Sathyapalan et al., 2021; Ben Abid et al., 2023). This situation is further exacerbated by a concerning rise in antifungal resistance resulted by the extensively application of antifungal agents in agriculture field and clinics (Vitiello et al., 2023). In October 2022, the World Health Organization (WHO) made a significant milestone by publishing the first-ever priority list of human fungal pathogens. Four species include *Cryptococcus neoformans, C. albicans, Aspergillus fumigatus,* and *C. auris* have been classified as critical human pathogens, due to their significant impact on human health. They all have ability to cause life-threatening systemic diseases, present increasing drug resistance, posing significant threat to public health (Lionakis et al., 2023).

1.4 *Candida auris*: A Rising Fungal Pathogen

C. auris was a recently identified novel species and human fungal pathogen (Satoh et al., 2009a). Since then, it has caused numerous infection outbreaks in many countries at an alarming rate. In India, *C. auris* has caused sporadic outbreaks and a multicenter study conducted in 2011 across 27 intensive care units (ICUs), reported that the fungus was the causative agent in approximately 5.3% (74 out of 1400) of candidemia episodes, ranking as the fifth most common pathogen responsible for candidemia cases (Chakrabarti et al., 2015; Rudramurthy et al., 2017; Chowdhary et al., 2013; Chowdhary et al., 2014; Lockhart et al., 2022). The initial major outbreak in Europe occurred in a London hospital and involved a total of 72 cases between 2015 and 2016 (Schelenz et al., 2016). Approximately half of these cases were related to colonization without infection, while the remaining cases were associated with actual fungal infections (Schelenz et al., 2016). During the years 2020 and 2021, there was a notable increase in the number of reported cases and outbreaks of *C. auris* infection or carriage in Europe (Kohlenberg et al., 2022). In 2020, eight countries reported a total of 335 cases, and in 2021, this number rose to 655 cases reported by 13 countries (Kohlenberg et al., 2022). In the United States, based on recent surveillance data released by CDC, *C. auris* has spread to a total of 27 states since its initial report in 2006 (Lyman et al., 2023). From 2019 to 2021, there was a sudden surge in reported cases,

comprising a total of 3,270 clinical cases and 7,413 screening cases (Lyman et al., 2023). Notably, in 2021, the number of *C. auris* cases resistant to echinocandins was approximately three times higher than in 2016 and 2017 (Lyman et al., 2023). Compounding the problem further, this fungus commonly exhibits multidrug resistance, with roughly 90% of clinical isolates resistant to fluconazole, 30% to amphotericin B, 4% to echinocandins, and 2% to flucytosine with some variation across different studies (Jacobs et al., 2022). It is worth noting that the current available antifungal drugs comprise four main classes: azoles, polyenes, echinocandins, and antimetabolites, and certain strains of *C. auris* can exhibit pan-resistance to three of four classes of them, highlighting the need for ongoing research and the development of new antifungal agents to combat drug-resistant *C. auris* infections. The growing prevalence of *C. auris* infections and drug resistance in *C. auris* underscores the importance of surveillance and infection control measures to prevent further spread of this emerging pathogen.

C. auris demonstrates a preference for colonizing the skin of patients and exhibits high transmissibility within healthcare facilities. It can easily spread from patients to various surfaces such as bed rails, hospital curtains, and floors, where it can persist for extended periods of up to a month (Yadav et al., 2021; Lyman et al., 2023). Moreover, this species has been recently identified in diverse sources, including wetlands, fruits, and animals (Yadav et al., 2022; Arora et al., 2021). This discovery implies the potential for transmission between clinical settings and various other environments, highlighting the importance of understanding the ecological factors contributing to its spread and the potential for cross-contamination between different settings.

C. auris belongs to the *Candida* genus and is genetically closely related to species in the *C. haemulonii* Clade, but it is distinct from other *Candida* species, such as *C. albicans* and *C. glabrata* (Muñoz et al., 2018a). Research findings indicate that certain *C. haemulonii* or other yeast species, initially identified using traditional phenotypic methods for yeast identification, were in fact *C. auris* (Snayd et al., 2018). Therefore, more advanced

techniques, such as DNA sequencing and matrix-assisted laser desorption ionization-time-of-flight mass spectrometry (MALDI-TOF MS), are required for accurate identification of this pathogen (Lockhart et al., 2022).

According to genomic data analysis, clinical isolates of *C. auris* can been categorized into five separate clades. Each of the five clades displays specific phylogeographic patterns. Specifically, Clade I strains were primarily isolated from South Asia, Clade II from East Asia and Oceania, Clade III from Africa and Europe, and Clade IV from Americas (Chow et al., 2020). Meanwhile, only 5-7 isolates have been reported as Clade V which were exclusively isolated from Iran (Chow et al., 2019; Armaki et al., 2021; Safari et al., 2022). However, global travel for medical purposes has resulted in the coexistence of strains from different clades in the same geographical areas, as reported in various studies (Chow et al., 2020; 2018). Of note, isolates within each of the clades of *C. auris* exhibit a high degree of clonality, with variations ranging from several to thousands of single nucleotide polymorphisms (SNPs) (Wang et al., 2022). However, interclade variations can vary more extensively, spanning from tens of thousands to hundreds of thousands of SNPs (Wang et al., 2022). Additionally, genomic rearrangements have been observed between the different clades of *C. auris*. These rearrangements involve changes in the organization and arrangement of genetic material within the genome (Muñoz et al., 2021). Thus, it is crucial to delve into the genomic architecture of each clade to gain a deeper understanding of how these variations may impact factors such as virulence and the development of antifungal resistance. Results from such research are vital for informing strategies to combat *C. auris* infections and develop effective treatment approaches.

1.5 Thesis Outline

My PhD thesis is focused on expanding our current understanding of *C. auris*. I aim to investigate various aspects of this pathogenic fungus, including its ecological niches, genomic characteristics, mechanisms of antifungal resistance, and epidemiology. My thesis consists of six chapters that provide a comprehensive exploration of the research topic. The

detailed descriptions of each chapter can be found in chapters two to six. In chapter 2, I focused on analyzing genomic data from isolated Andaman Islands to investigate the origin of *C. auris*. In chapter 3 of my thesis, the focus was on exploring the ecological niche of *C. auris* in apples and examining the genomic relationships between these isolates and previously documented strains from India. In chapter 4, I conducted metabarcoding analysis on samples isolated from dog ears to investigate the yeast diversity and the presence of *C. auris*. In chapter 5, I carried out four-gamete tests and linkage disequilibrium analyses on genomic data of 1,285 samples retrieved from NCBI database to investigate the evidence of recombination in *C. auris* populations. In chapter 6, I performed genome wide association analyses on multiple antifungal agents within Clade I, III and IV samples to identify genomic variants associated with antifungal susceptibility in individual clades of *C. auris*.

References

Abid, Fatma Ben, Husam Salah, Sathyavathi Sundararaju, Lamya Dalil, Ayman H. Abdelwahab, Sarah Salameh, Emad B. Ibrahim, et al. 2023. "Molecular Characterization of *Candida auris* Outbreak Isolates in Qatar from Patients with COVID-19 Reveals the Emergence of Isolates Resistant to Three Classes of Antifungal Drugs." *Clinical Microbiology and Infection* 0 (0). https://doi.org/10.1016/j.cmi.2023.04.025.

Alves, Mariajosé, Isabelc F.R. Ferreira, Joana Dias, Vânia Teixeira, Anabela Martins, and Manuela Pintado. 2012. "A Review on Antimicrobial Activity of Mushroom (Basidiomycetes) Extracts and Isolated Compounds." *Planta Medica* 78 (16): 1707–18. https://doi.org/10.1055/S-0032-1315370.

Armaki, Mojtaba Taghizadeh, Saeid Mahdavi Omran, Keyvan Kiakojuri, Shaghayegh Khojasteh, Jalal Jafarzadeh, Mahin Tavakoli, Hamid Badali, et al. 2021. "First Fluconazole-Resistant *Candida auris* Isolated from Fungal Otitis in Iran." *Current Medical Mycology* 7 (1): 51. https://doi.org/10.18502/CMM.7.1.6243.

Aroca, Ricardo, Juan Manuel Ruiz-Lozano, ángel María Zamarreño, José Antonio Paz, José María García-Mina, María José Pozo, and Juan Antonio López-Ráez. 2013. "Arbuscular Mycorrhizal Symbiosis Influences Strigolactone Production under Salinity and Alleviates Salt Stress in Lettuce Plants." *Journal of Plant Physiology* 170 (1): 47–55. https://doi.org/10.1016/J.JPLPH.2012.08.020.

Arora, Parth, Prerna Singh, Yue Wang, Anamika Yadav, Kalpana Pawar, Ashutosh Singh, Gadi Padmavati, Jianping Xu, and Anuradha Chowdhary. 2021. "Environmental Isolation of *Candida auris* from the Coastal Wetlands of Andaman Islands, India." Edited by Leah E. Cowen. *MBio* 12 (2): 1–9. https://doi.org/10.1128/mBio.03181-20.

Bano, Ambreen, Anmol Gupta, Manas Ranjan Prusty, and Manoj Kumar. 2023. "Elicitation of Fruit Fungi Infection and Its Protective Response to Improve the Postharvest Quality of Fruits." *Stresses 2023, Vol. 3, Pages 231-255* 3 (1): 231–55. https://doi.org/10.3390/STRESSES3010018.

Barros, Lillian, Daniela M. Correia, Isabel C.F.R. Ferreira, Paula Baptista, and Celestino Santos-Buelga. 2008. "Optimization of the Determination of Tocopherols in Agaricus Sp. Edible Mushrooms by a Normal Phase Liquid Chromatographic Method." *Food Chemistry* 110 (4): 1046–50. https://doi.org/10.1016/J.FOODCHEM.2008.03.016.

Nirappil, Fenit. 2023 "*Candida auris* Fungal Infection Rapidly Spreading in U.S. - The Washington Post." n.d. Accessed June 21, 2023. https://www.washingtonpost.com/health/2023/03/20/candida-auris-fungus-infection/.

Capasso, L. 1998. "5300 Years Ago, the Ice Man Used Natural Laxatives and Antibiotics." *Lancet (London, England)* 352 (9143): 1864. https://doi.org/10.1016/S0140-6736(05)79939-6.

Casadevall, Arturo, Dimitrios P. Kontoyiannis, and Vincent Robert. 2019. "On the Emergence of *Candida auris*: Climate Change, Azoles, Swamps, and Birds." *MBio* 10 (4). https://doi.org/10.1128/MBIO.01397-19/ASSET/79702525-66F1-4B50-916F-0748CD812B4B/ASSETS/GRAPHIC/MBIO.01397-19-F0002.JPEG.

Chakrabarti, Arunaloke, Prashant Sood, Shivaprakash M. Rudramurthy, Sharon Chen, Harsimran Kaur, Malini Capoor, Deepinder Chhina, et al. 2015. "Incidence, Characteristics and Outcome of ICU-Acquired Candidemia in India." *Intensive Care Medicine* 41 (2): 285–95. https://doi.org/10.1007/s00134-014-3603-2.

Chang, Shu Ting, and Solomon P. Wasser. 2012. "The Role of Culinary-Medicinal Mushrooms on Human Welfare with a Pyramid Model for Human Health." *International Journal of Medicinal Mushrooms* 14 (2): 95–134. https://doi.org/10.1615/INTJMEDMUSHR.V14.I2.10.

Chow, Nancy A., Lalitha Gade, Sharon V. Tsay, Kaitlin Forsberg, Jane A. Greenko, Karen L. Southwick, Patricia M. Barrett, et al. 2018. "Multiple Introductions and Subsequent Transmission of Multidrug-Resistant *Candida auris* in the USA: A Molecular Epidemiological Survey." *The Lancet Infectious Diseases* 18 (12): 1377–84. https://doi.org/10.1016/S1473-3099(18)30597-8.

Chow, Nancy A., Theun De Groot, Hamid Badali, Mahdi Abastabar, Tom M. Chiller, and Jacques F. Meis. 2019. "Potential Fifth Clade of *Candida auris*, Iran, 2018." *Emerging Infectious Diseases* 25 (9): 1780–81. https://doi.org/10.3201/eid2509.190686.

Chow, Nancy A., José F. Muñoz, Lalitha Gade, Elizabeth L. Berkow, Xiao Li, Rory M. Welsh, Kaitlin Forsberg, et al. 2020. "Tracing the Evolutionary History and Global Expansion of *Candida auris* Using Population Genomic Analyses." *MBio* 11 (2). https://doi.org/10.1128/MBIO.03364-19.

Chowdhary, A., V. Anil Kumar, C. Sharma, A. Prakash, K. Agarwal, R. Babu, K. R. Dinesh, et al. 2014. "Multidrug-Resistant Endemic Clonal Strain of *Candida auris* in India." *European Journal of Clinical Microbiology & Infectious Diseases: Official Publication of the European Society of Clinical Microbiology* 33 (6): 919–26. https://doi.org/10.1007/S10096-013-2027-1.

Chowdhary, Anuradha, Cheshta Sharma, Shalini Duggal, Kshitij Agarwal, Anupam Prakash, Pradeep Kumar Singh, Sarika Jain, et al. 2013. "New Clonal Strain of *Candida auris*, Delhi, India." *Emerging Infectious Diseases* 19 (10): 1670–73. https://doi.org/10.3201/EID1910.130393.

"Food Security: How Do Crop Plants Combat Pathogens? : USDA ARS." 2022. Accessed June 21, 2023. https://www.ars.usda.gov/oc/dof/food-security-how-do-crop-plants-combat-pathogens/.

Gadre, Aditi, Wendemagegn Enbiale, Louise K Andersen, and Sarah J Coates. 2022. "The Effects of Climate Change on Fungal Diseases with Cutaneous Manifestations: A Report from the International Society of Dermatology Climate Change Committee." *The Journal of Climate Change and Health* 6 (May): 100156. https://doi.org/10.1016/J.JOCLIM.2022.100156.

Gusa, Asiya, Vikas Yadav, Cullen Roth, Jonathan D. Williams, Eva Mei Shouse, Paul Magwene, Joseph Heitman, and Sue Jinks-Robertson. 2023. "Genome-Wide Analysis of Heat Stress-Stimulated Transposon Mobility in the Human Fungal Pathogen Cryptococcus deneoformans." *Proceedings of the National Academy of Sciences of the United States of America* 120 (4): e2209831120. https://www.pnas.org/doi/10.1073/pnas.2209831120.

Hawksworth, David L., and Robert Lücking. 2017. "Fungal Diversity Revisited: 2.2 to 3.8 Million Species." *Microbiology Spectrum* 5 (4). https://journals.asm.org/doi/10.1128/microbiolspec.FUNK-0052-2016.

Jacobs, Samantha E., Jonathan L. Jacobs, Emily K. Dennis, Sarah Taimur, Meenakshi Rana, Dhruv Patel, Melissa Gitman, et al. 2022. "*Candida auris* Pan-Drug-Resistant to Four Classes of Antifungal Agents." *Antimicrobial Agents and Chemotherapy* 66 (7). https://journals.asm.org/doi/10.1128/aac.00053-22

Kainz, Katharina, Maria A. Bauer, Frank Madeo, and Didac Carmona-Gutierrez. 2020. "Fungal Infections in Humans: The Silent Crisis." *Microbial Cell* 7 (6): 143. https://doi.org/10.15698/MIC2020.06.718.

Kohlenberg, Anke, Dominique L. Monnet, Diamantis Plachouras, Birgit Willinger, Katrien Lagrou, Ivva Philipova, Ana Budimir, et al. 2022. "Increasing Number of Cases and Outbreaks Caused by *Candida auris* in the EU/EEA, 2020 to 2021." *Eurosurveillance* 27 (46). https://doi.org/10.2807/1560-7917.ES.2022.27.46.2200846.

Kottke, Ingrid, and Martin Nebel. 2005. “The Evolution of Mycorrhiza-like Associations in Liverworts: An Update.” *New Phytologist* 167 (2): 330–34. https://doi.org/10.1111/J.1469-8137.2005.01471.X.

Lionakis, Michail S., Rebecca A. Drummond, and Tobias M. Hohl. 2023. “Immune Responses to Human Fungal Pathogens and Therapeutic Prospects.” *Nature Reviews Immunology 2023 23:7* 23 (7): 433–52. https://doi.org/10.1038/s41577-022-00826-w.

Lockhart, Shawn R., Meghan M. Lyman, and D. Joseph Sexton. 2022. “Tools for Detecting a ‘Superbug’: Updates on *Candida auris* Testing.” *Journal of Clinical Microbiology* 60 (5). https://doi.org/10.1128/jcm.00808-21.

Lubbe, Andrea, and Valdon R. Smith. 2012. “Field Soil Respiration Rate on a Sub-Antarctic Island: Its Relation to Site Characteristics and Response to Added C, N and P.” *Open Journal of Soil Science* 02 (02): 187–95. https://doi.org/10.4236/OJSS.2012.22023.

Lyman, Meghan, Kaitlin Forsberg, D. Joseph Sexton, Nancy A. Chow, Shawn R. Lockhart, Brendan R. Jackson, and Tom Chiller. 2023. “Worsening Spread of *Candida auris* in the United States, 2019 to 2021.” *Https://Doi.Org/10.7326/M22-3469* 176 (4): 489–95. https://doi.org/10.7326/M22-3469.

Mattila, Pirjo, Karoliina Könkö, Merja Eurola, Juha Matti Pihlava, Jouni Astola, Liisa Vahteristo, Veli Hietaniemi, Jorma Kumpulainen, Meli Valtonen, and Vieno Piironen. 2001. “Contents of Vitamins, Mineral Elements, and Some Phenolic Compounds in Cultivated Mushrooms.” *Journal of Agricultural and Food Chemistry* 49 (5): 2343–48. https://doi.org/10.1021/JF001525D.

Muñoz, José F., Lalitha Gade, Nancy A. Chow, Vladimir N. Loparev, Phalasy Juieng, Elizabeth L. Berkow, Rhys A. Farrer, Anastasia P. Litvintseva, and Christina A. Cuomo. 2018. “Genomic Insights into Multidrug-Resistance, Mating and Virulence in *Candida auris* and Related Emerging Species.” *Nature Communications* 9 (1): 1–13. https://doi.org/10.1038/s41467-018-07779-6.

Muñoz, José F., Rory M. Welsh, Terrance Shea, Dhwani Batra, Lalitha Gade, Dakota Howard, Lori A. Rowe, Jacques F. Meis, Anastasia P. Litvintseva, and Christina A.

Cuomo. 2021. “Clade-Specific Chromosomal Rearrangements and Loss of Subtelomeric Adhesins in *Candida auris*.” *Genetics* 218 (1). https://doi.org/10.1093/GENETICS/IYAB029.

Rivero, Javier, Domingo Álvarez, Víctor Flors, Concepción Azcón-Aguilar, and María J. Pozo. 2018. “Root Metabolic Plasticity Underlies Functional Diversity in Mycorrhiza-Enhanced Stress Tolerance in Tomato.” *The New Phytologist* 220 (4): 1322–36. https://doi.org/10.1111/NPH.15295.

Rudramurthy, Shivaprakash M., Arunaloke Chakrabarti, Raees A. Paul, Prashant Sood, Harsimran Kaur, Malini R. Capoor, Anupma J. Kindo, et al. 2017. “*Candida auris* Candidaemia in Indian ICUs: Analysis of Risk Factors.” *Journal of Antimicrobial Chemotherapy* 72 (6): 1794–1801. https://doi.org/10.1093/JAC/DKX034.

Safari, Fatemeh, Mahboobeh Madani, Hamid Badali, Amir Abbas Kargoshaie, Hamed Fakhim, Majid Kheirollahi, Jacques F. Meis, and Hossein Mirhendi. 2022. “A Chronic Autochthonous Fifth Clade Case of *Candida auris* Otomycosis in Iran.” *Mycopathologia* 187 (1): 121–27. https://doi.org/10.1007/s11046-021-00605-6.

Sathyapalan, Dipu Thareparambil, Remya Antony, Vrinda Nampoothiri, Anil Kumar, Nandita Shashindran, Jini James, Jisha Thomas, et al. 2021. “Evaluating the Measures Taken to Contain a *Candida auris* Outbreak in a Tertiary Care Hospital in South India: An Outbreak Investigational Study.” *BMC Infectious Diseases* 21 (1): 1–10. https://doi.org/10.1186/S12879-021-06131-6.

Satoh, Kazuo, Koichi Makimura, Yayoi Hasumi, Yayoi Nishiyama, Katsuhisa Uchida, and Hideyo Yamaguchi. 2009. “*Candida auris*, a Novel Ascomycetous Yeast Isolated from the External Ear Canal of an Inpatient in a Japanese Hospital.” *Microbiology and Immunology* 53 (1): 41–44. https://doi.org/10.1111/J.1348-0421.2008.00083.X.

Schelenz, Silke, Ferry Hagen, Johanna L. Rhodes, Alireza Abdolrasouli, Anuradha Chowdhary, Anne Hall, Lisa Ryan, et al. 2016. “First Hospital Outbreak of the Globally Emerging *Candida auris* in a European Hospital.” *Antimicrobial Resistance and Infection Control* 5 (1). https://doi.org/10.1186/S13756-016-0132-5.

Sirivatanapa, Somjate. 2006. “Postharvest Management of Fruit and Vegetables in the Asia-Pacific Region Reports of the APO Seminar on Reduction of Postharvest Losses of Fruit and Vegetables Held in India, 5-11 October 2004 and Marketing and Food Safety: Challenges in Postharvest Manag.” *Apo-Tokyo.Org*, 43–48. www.apo-tokyo.org.

Snayd, Mary, Feliciano Dias, Raymond W. Ryan, Donna Clout, and David B. Banach. 2018. “Misidentification of *Candida auris* by RapID Yeast Plus, a Commercial, Biochemical Enzyme-Based Manual Rapid Identification System.” *Journal of Clinical Microbiology* 56 (5). https://doi.org/10.1128/JCM.00080-18.

Vitiello, Antonio, Francesco Ferrara, Mariarosaria Boccellino, Annarita Ponzo, Carla Cimmino, Emilio Comberiati, Andrea Zovi, Salvatore Clemente, and Michela Sabbatucci. 2023. “Antifungal Drug Resistance: An Emergent Health Threat.” *Biomedicines* 11 (4): 1063. https://doi.org/10.3390/BIOMEDICINES11041063.

Wang, B., and Y. L. Qiu. 2006. “Phylogenetic Distribution and Evolution of Mycorrhizas in Land Plants.” *Mycorrhiza* 16 (5): 299–363. https://doi.org/10.1007/S00572-005-0033-6/METRICS.

Wang, Yue, and Jianping Xu. 2022. “Population Genomic Analyses Reveal Evidence for Limited Recombination in the Superbug *Candida auris* in Nature.” *Computational and Structural Biotechnology Journal* 20 (January): 3030–40. https://doi.org/10.1016/J.CSBJ.2022.06.030.

Wasser, S. 2002. “Medicinal Mushrooms as a Source of Antitumor and Immunomodulating Polysaccharides.” *Applied Microbiology and Biotechnology* 60 (3): 258–74. https://doi.org/10.1007/S00253-002-1076-7/METRICS.

Xu, Jianping. 2022. “Assessing Global Fungal Threats to Humans.” *MLife* 1 (3): 223–40. https://doi.org/10.1002/MLF2.12036.

Yadav, Anamika, Kusum Jain, Yue Wang, Kalpana Pawar, Hardeep Kaur, Krishan Kumar Sharma, Vandana Tripathy, Ashutosh Singh, Jianping Xu, and Anuradha Chowdhary. 2022. “*Candida auris* on Apples: Diversity and Clinical Significance.” Edited by Leah E. Cowen. *MBio* 13 (2). https://doi.org/10.1128/MBIO.00518-22.

Yadav, Anamika, Anubhav Singh, Yue Wang, Merlijn Hi Van Haren, Ashutosh Singh, Theun De Groot, Jacques F. Meis, Jianping Xu, and Anuradha Chowdhary. 2021. "Colonisation and Transmission Dynamics of *Candida auris* among Chronic Respiratory Diseases Patients Hospitalised in a Chest Hospital, Delhi, India: A Comparative Analysis of Whole Genome Sequencing and Microsatellite Typing." *Journal of Fungi* 7 (2): 81. https://doi.org/10.3390/JOF7020081.

Querol, Amparo and Fleet, Graham H. 2006. *Yeasts in Food and Beverages*. https://doi.org/10.1007/978-3-540-28398-0.

Zhao, Shuang, Qi Gao, Chengbo Rong, Shouxian Wang, Zhekun Zhao, Yu Liu, and Jianping Xu. 2020. "Immunomodulatory Effects of Edible and Medicinal Mushrooms and Their Bioactive Immunoregulatory Products." *Journal of Fungi* 6 (4): 1–37. https://doi.org/10.3390/JOF6040269.

Chapter 2

Environmental Isolation of *Candida auris* from the Coastal Wetlands of Andaman Islands, India

Abstract *Candida auris* is a multidrug resistant pathogen that presents a serious global threat to human health. As *C. auris* is a newly emerged pathogen, several questions regarding its ecological niche remain unexplored. While species closely related to *C. auris* have been detected in different environmental habitats, little is known about the natural habitat(s) of *C. auris*. Here, we explored the virgin habitats around the very isolated Andaman Islands in the Indian Ocean for evidence of *C. auris*. We sampled coastal wetlands, including rocky shores, sandy beaches, tidal marshes, and mangrove swamps, around the Andaman group of the Andaman & Nicobar Islands, Union Territory, in India. Forty-eight samples of sediment soil and seawater were collected from eight sampling sites representing the heterogeneity of intertidal habitats across the east and west coast of South Andaman district. *C. auris* was isolated from two of the eight sampling sites, a salt marsh and a sandy beach. Interestingly, both multidrug-susceptible and multidrug-resistant *C. auris* isolates were found in the sample. Whole-genome sequencing analysis clustered the *C. auris* isolates into clade I, showing close similarity to other isolates from South Asia. Isolation of *C. auris* from the tropical coastal environment suggests its association with the marine ecosystem. The fact that viable *C. auris* was detected in the marine habitat confirms *C. auris* survival in harsh wetlands. However, the ecological significance of *C. auris* in salt marsh wetland and sandy beaches to human infections remains to be explored.

Importance *Candida auris* is a recently emerged multidrug-resistant fungal pathogen capable of causing severe infections in hospitalized patients. Despite its recognition as a human pathogen a decade ago, so far the natural ecological niche(s) of *C. auris* remains enigmatic. A previous hypothesis suggested that *C. auris* might be native to wetlands, that its emergence as a human pathogen might have been linked to global warming effects on

wetlands, and that its enrichment in that ecological niche was favored by the ability of *C. auris* for thermal tolerance and salinity tolerance. To understand the mystery of environmental niches of *C. auris*, we explored the coastal wetland habitat around the very isolated Andaman Islands in the Indian Ocean. *C. auris* was isolated from the virgin habitats of salt marsh area with no human activity and from a sandy beach. *C. auris* isolation from the marine wetlands suggests that prior to its recognition as a human pathogen, it existed as an environmental fungus.

For the study in this chapter, I conducted the bioinformatic analyses. The following paper has been published in mBio:
Arora, P., Singh, P., Wang, Y., Yadav, A., Pawar, K., Singh, A., Padmavati, G., Xu. J. and Chowdhary, A. 2021. "Environmental Isolation of *Candida auris* from the Coastal Wetlands of Andaman Islands, India." mBio 12(2):e03181-20.

2.1 Observation

Candida auris is a multidrug-resistant fungal pathogen that presents a serious threat to patients and health care facilities worldwide (Caceres et al., 2019). Due to the widespread clinical and economic impact of difficult-to-treat *C. auris* infections, the U.S. Centers for Disease Control and Prevention in 2019 have classified *C. auris* as an urgent threat to public health (Solomon et al., n.d.). An escalating number of infections across the globe in health care facilities have been attributed to the unique characteristics of this yeast in that it can survive and persist within the hospital environment for prolonged periods. Its ability to survive on dry environmental surfaces for prolonged periods suggests that this yeast is well adapted to survival outside human host settings (Chowdhary et al., 2017). *Candida auris* belongs to the *Candida haemulonii* clade of the Metschnikowiaceae family of the order Saccharomycetales. The related species of the Metschnikowiaceae family have been detected in plants, insects, and aquatic environments, as well as from human body sites (Sipiczki et al., 2016; Madden et al., 2018). The closest known relative of *C. auris* is *C. haemulonii*, which was first discovered in 1962 from the gut of a blue-striped grunt fish

(Haemulon sciurus), the skin of dolphins, and the seawater off the coast of Portugal (van Uden et al., 1962). In contrast to the related species, *C. auris* has not been reported from natural environments. The retrospective analyses of clinical yeasts showed that the earliest known clinical isolates of *C. auris* date back to 1996 in South Korea and 1997 in Japan (Lee et al., 2011; Iguchi et al., 2019; Satoh et al., 2009). However, unlike the clinical settings, the detection of *C. auris* in the natural environment has not been explored (Jackson et al., 2019).

Candida auris is capable of growing at higher temperatures than most of its closely related species and can tolerate hypersaline environments more than most *Candida* species (Welsh et al., 2017). The thermotolerance of *C. auris* has led to the hypothesis by Casadevall et al. that its emergence may be linked to climate change and global temperature changes (Casadevall et al., 2019). Indeed, the authors proposed that prior to its recognition as a human pathogen and being prevalent in hospital environments; *C. auris* was an environmental fungus that might have previously existed as a plant saprophyte in specialized ecosystems, such as wetlands. Its emergence might have been linked to global warming effects on wetlands, and its enrichment in that ecological niche was the result of *C. auris*'s combined thermal tolerance and salinity tolerance. Wetlands are among the crucial natural habitats distributed throughout the world and contain an enormous diversity of organisms, including yeast species. Following the prediction of Casadevall's hypothesis, we undertook the present study to explore the environmental niches of *C. auris* in the marine environment encompassing coastal wetlands including rocky shores, tidal marshes, and mangrove swamps of the Andaman Islands, Union Territory of India.

The Andaman & Nicobar Islands of the Union Territory of India are a chain of islands located in the southeastern Bay of Bengal and are surrounded by the Andaman Sea to the east and the Bay of Bengal to the west. The climate of these islands is tropical, with hot and humid conditions. In the present study, eight sampling sites including six on the east coast of South Andaman district and two on the west coast were selected to represent the

heterogeneity of intertidal habitats and accessibility for specimen collections (Figure 2. 1). The coastal zone of the South Andaman district is endowed with sandy beaches and mangrove vegetation interspersed with rocky outcrops. Corals, seaweeds, and seagrasses are common in this region. Due to its unique location and tribal culture, few people visit these islands. Thus, we expect little impacts of direct human activities on their yeast distributions.

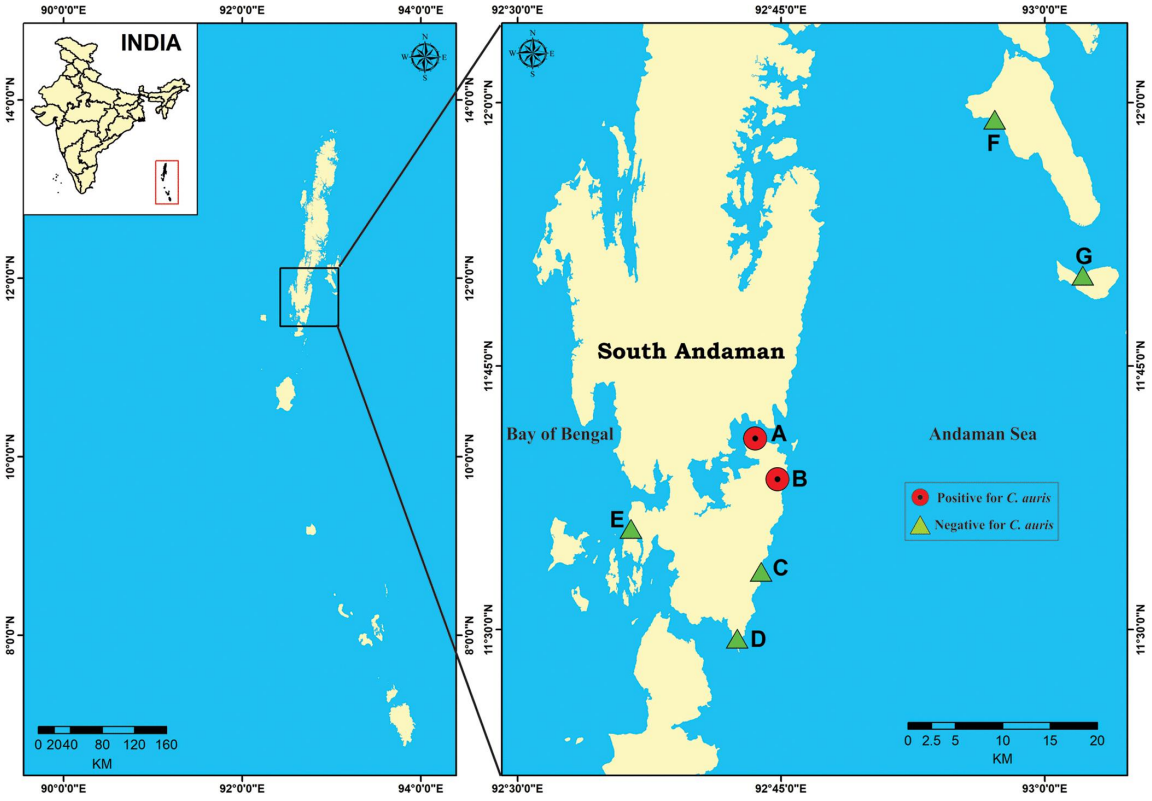

Figure 2. 1. Map showing location of sampling sites (n = 8; sites E1 and E2 collectively depicted as E) of South Andaman district, Andaman & Nicobar Islands, Union Territory of India.

Candida auris was isolated from two of the eight locations investigated in the present study: a salt marsh wetland site (site A, Chatham) and a sandy beach site (site B, Corbyn's Cove) as detailed in Table 2. 1. *Candida auris* strains at site A were isolated from the sediment samples while those at site B were from both the sediment and water samples. Site A is a bay tidal salt marsh which is directly in contact with seawater of the Andaman Sea, and the

marsh was exposed only during low tide. The intertidal area is separated from the terrestrial land by a seawall. The habitat is characterized by a mixture of sandy-muddy substratum and an abundant vegetation of seagrass. The area is inhabited by sea birds and experiences no known human activity. The Corbyn's Cove beach site that yielded *C. auris* was an upper middle intertidal zone with the shore characterized by the presence of fine sand sediment and uprooted seaweeds. In total, two colonies of *C. auris* were found at site A, and both were from the composite soil sediment. In contrast, 22 colonies were found at site B, and they were distributed in both the sediment and water samples. Further, both sites A and B had low yeast diversity with only *C. auris* and Trichosporon asahii cultured from site A samples and *C. auris* and *Candida parapsilosis* from site B samples.

Table 2. 1. Description of study area locations and distribution of yeast speciesisolated from the South Andaman district (SAD), Andaman & Nicobar Islands, Union Territory of India

Sampling location	Sampling station	Yeast species isolated (no. of colonies isolated)	Station description
Location I (South Andaman Island)	A (Chatham salt marsh)	***Candida auris*** (n = 2)[a] *Trichosporon asahii* (n = 4) *Arthrographis kalrae*[c] (n = 2)	Intertidal habitat along the east coast of SAD, characterized by marshy sediment on the abundant seagrass bed with seabirds; negligible human activity.
	B (Corbyn's Cove)	***Candida auris*** (n = 22)[b] *Candida parapsilosis* (n = 2)	Upper middle intertidal zone, east coast of SAD, a tourist beach with fine sand sediment
	C (Burmanallah rocky shore)	*Candida tropicalis* (n=5)	Rocky shore, intertidal habitat, coarse sediment, rocky substratum with dead corals
	D (Chidiyatapu)	*Candida parapsilosis* (n=6)	Southernmost tip of SAD, surrounded by waters of Andaman Sea and Bay of Bengal, sediment comprised of granules and pebbles, coastal birds, crocodile-prone area, with fewer human activities
	E_1 (Wandoor)	*Candida parapsilosis* (n=10) *Trichosporon asahii* (n=5)	West coast of SAD, crocodile-inhabited area, coastal birds, minimal human activity
	E_2 (Wandoor mangrove)	*Candida catenulata* (n=5) *Candida tropicalis* (n=2)	West coast of SAD
Location II (Swaraj Dweep Island)	F (Radhanagar)	None	Tourist beach
Location III (Shaheed Dweep Island)	G (Bharatpur)	*Candida parapsilosis* (n = 11) *Candida palmioleophila* (n = 1) *Issatchenkia siamensis* (n = 1) *Kluyveromyces siamensis* (n = 1) *Kluyveromyces aestuarii* (n = 1)	Beach with water sports activities

[a] Number of colonies isolated from the sediment suspension. Boldface highlights the isolation of *C. auris* from site A and site B.

[b] Number of colonies isolated from the sediment suspension and seawater.

[c] Hyaline mold.

Antifungal susceptibility testing by the CLSI broth microdilution method showed that 23 of the 24 *C. auris* isolates had high MICs of fluconazole (MIC of >256 mg/liter) and amphotericin B (MIC range of 2 to 4 mg/liter) while a single isolate (VPCI/E/AN/176/20) had low MICs against all tested antifungal drugs (e.g., fluconazole MIC of 8 mg/liter and amphotericin B MIC of 1 mg/liter) (see Table 2. S1 in the supplemental material) (Rex et al., 2008). This susceptible isolate was recovered from the salt marsh (site A). Interestingly, the other *C. auris* isolate from the same salt marsh exhibited high MIC values against azoles and amphotericin B. Also, all 22 *C. auris* isolates from the beach site were resistant to multiple antifungal drugs (Table 2. S1). The susceptible and resistant isolates, when grown on agar plates containing serial dilutions of fluconazole, showed inhibition of growth of the susceptible isolate on the agar plate containing 16 mg/liter of fluconazole (Figure 2. 2). All of the *C. auris* isolates grew well at 42°C; however, the susceptible isolate (VPCI/E/AN/176/20) from the salt marsh grew slower than other isolates at both 37°C and 42°C. For example, isolate VPCI/E/AN/176/20 had a growth rate r of 0.212 and r of 0.117 in liquid media at 37°C and 42°C, respectively, which was lower than those of other isolates from site A ($n = 1$) and site B ($n = 3$) (37°C, $r > 0.249$, $P = 0.03$, versus 42°C, $r > 0.143$, $P = 0.04$). (Figure 2. S1). Further, isolate VPCI/E/AN/176/20 was highly susceptible to cycloheximide with 99% inhibition at 0.01 mg/liter whereas other *C. auris* isolates were inhibited only at a concentration of 2 to 4 mg/liter. Whole-genome sequencing (WGS) of 13 *C. auris* isolates including both isolates from site A and 11 from site B showed that they all clustered into clade I. However, they differed from all known south Asian clade I strains. Interestingly, while the Andaman isolates differed from the reference clade I strain B8441 from Pakistan by 829 to 904 single nucleotide polymorphisms (SNPs), they showed closer relationships to clinical strains from mainland India (Figure 2. 3). Interestingly, while the two isolates from site A were genetically different from each other by 77 SNP differences, all 11 isolates from site B were genetically very similar to each other, with no or 1 SNP difference across the whole genome, likely representing recent clonal descendants of a single ancestor genotype. Further, the two site A isolates differed from site B isolates by 77 to 78 SNPs.

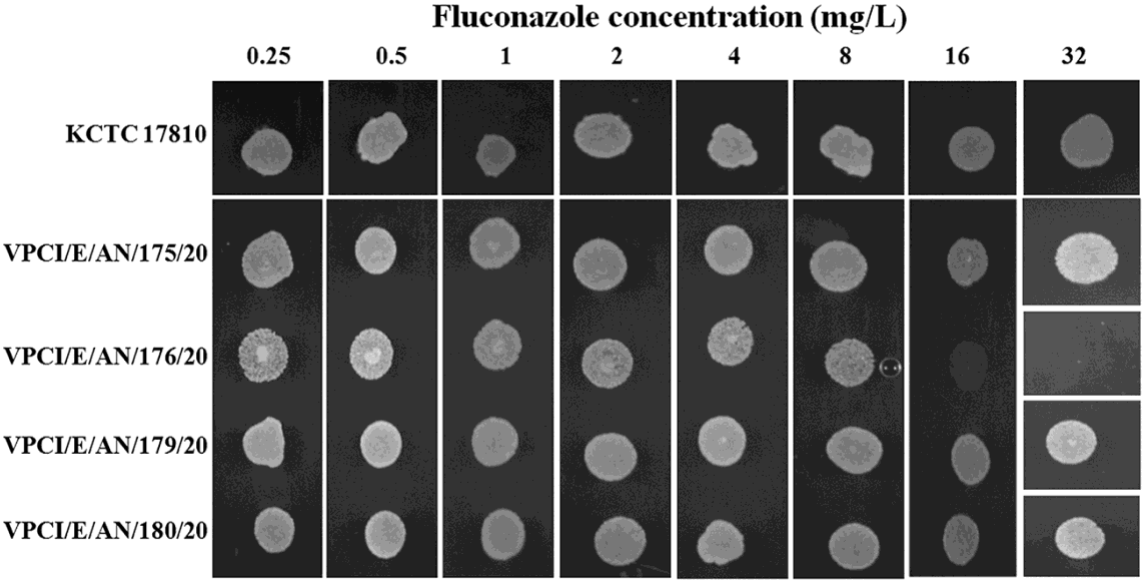

Figure 2. 2. Representation of fluconazole susceptibility profile by spot assay on fluconazole-containing agar plates. Fluconazole concentrations used are depicted horizontally. Both fluconazole-susceptible (VPCI/E/AN/176/20) and -resistant (VPCI/E/AN/175/20) *C. auris* strains from site A and two resistant strains from site B (VPCI/E/AN/179/20 and VPCI/E/AN/180/20) of South Andaman District, Andaman & Nicobar Islands, Union Territory of India, were spot inoculated. The KCTC 17810 (clade II) strain of *C. auris* was used as a reference strain. Spots on the plate indicate growth of *C. auris* at that concentration.

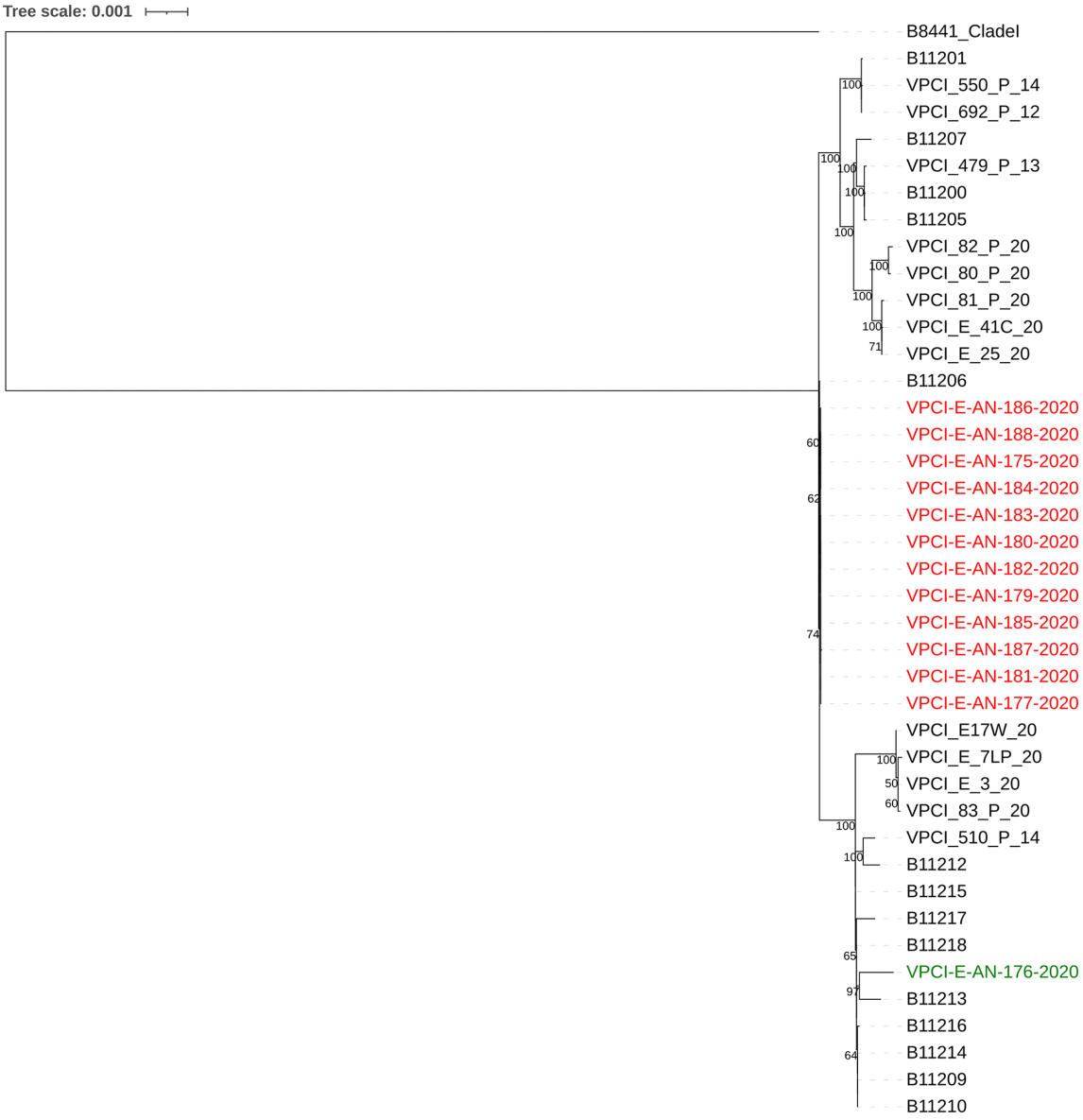

Figure 2. 3. Maximum likelihood phylogenetic tree constructed based on whole-genome SNPs using RAxML. Included in the phylogenetic tree are 13 *Candida auris* strains isolated from South Andaman district, Andaman & Nicobar Islands (VPCI/E/AN/175/20 to AN/177/20 and VPCI/E/AN/179/20 to AN/188/20). Red text in the figure represents resistant strains (fluconazole geometric mean [GM] MIC, 256 mg/liter; amphotericin B GM MIC, 4 mg/liter) from both sites A and B, and the green text represents a single susceptible strain (fluconazole MIC, 8 mg/liter; amphotericin B MIC, 1 mg/liter) from site A. The remaining strains depicted include 9 recent isolates from patients and their immediate environments (VPCI/80/P/20 to VPCI/82/P/20, VPCI/E/41C/20, VPCI/E/25/20, VPCI/E/17W/20, VPCI/E/7LP/20, VPCI/E/3/20, and VPCI/83/P/20), 18 previously published Indian *C. auris* strains (B11200, B11201, B11205 to B11207, B11209, B11210, B11212 to B11218, VPCI/510/P/14, VPCI/692/P/12, VPCI/550/P/14, and VPCI/479/P/13), and reference clade I strain B8441 from Pakistan.

For comparative analyses, we also included the WGS data of 18 strains from India published previously and nine clinical *C. auris* strains recently obtained from patients' body sites and their hospital environment from the V. P. Chest Institute. A range of SNP differences were found. For example, there were 67 to 153 SNPs between our Andaman wetland strains and our nine hospital clinical strains. Similar genetic variability was noted among the Andaman isolates and four previously published *C. auris* strains (SNP differences, 46 to 126) from candidemia patients collected from 4 different hospitals of North and South India (Sharma et al., 2016). Similarly, the Andaman isolates differed from 14 other Indian clade I isolates reported by Lockhart et al. (2017) by 1 to 131 SNPs. Together, these results suggest that the Andaman isolates are genetically distinct but part of the broad *C. auris* population from India.

Our analyses identified that all 13 sequenced isolates were mating type a. Identification of genetic determinants of antifungal susceptibilities showed the presence of previously known amino acid substitution Y132F in the *ERG11* gene of all the 13 *C. auris* isolates. Interestingly, the *TAC1B* gene (a zinc-cluster transcription factor-encoding gene) had previously known amino acid substitution A583S in site A susceptible *C. auris* strain VPCI/E/AN/176/20. All *C. auris* isolates showed amino acid substitution L351M in the ERG7 gene (ergosterol biosynthetic gene) and harbored the K719N amino acid substitution in the STE6 gene, which is an ABC family transporter expressed in MTLa-carrying strains and exports the a-factor pheromone in *Saccharomyces cerevisiae* and *Candida albicans*.

2.2 Discussion

The present study reports the isolation of *C. auris* from the tropical marine ecosystems in India. The isolation of *C. auris* from this natural environment is noteworthy considering that until now this yeast has not been identified outside hospital environmental settings. Remarkably, *C. auris* was isolated from two different habitats, i.e., salt marsh wetland and sandy beach of the Andaman Islands, India. However, the ecological significance of the presence of *C. auris* in these habitats to human infections remains to be explored.

Previously, *Candida* spp. of the *Metschnikowia* clade, namely, *C. haemulonii*, *C. pseudointermedia*, *C. intermedia*, *C. melibiosica*, and *C. torresii*, have been isolated from seawater and other coastal habitats from different geographical areas (Buzzini et al., 2017). The fact that many environmental isolations of *Candida* spp. of the *Metschnikowia* clade have occurred in tropical areas, predominantly in South and Southeast Asia, suggests potentially greater yeast diversity in tropical rather than temperate regions (Tedersoo et al., 2014). The Andaman & Nicobar Islands have unique untouched ecology in terms of anthropogenic activities, and salt marsh and mangroves are the only wetland types in these islands that have vegetation. The isolation of *C. auris* from the salt marsh with extensive vegetation is consistent with the hypothesis that *C. auris* probably existed as a plant saprophyte in the wetlands (Casadevall et al., 2019). Notably, isolation of the drug-susceptible *C. auris* strain from this aquatic habitat with no known human activity probably indicates that *C. auris* existed as a drug-susceptible pathogen and developed multidrug-resistant traits after its adaptation in humans. Further, the drug-susceptible isolate grew slowly at high temperature, suggesting that environmental strains could acquire thermal tolerance quickly. The isolation of *C. auris* from the sediment of the nearshore environment may also be related to human activities and/or its close association with plants and soils in these environments. Regardless, the isolation of viable *C. auris* in both the marine habitats confirms that *C. auris* is capable of surviving harsh wetlands.

The environmental strains from the two sites had several genotypes and belonged to the South Asia clade I, similar to the *C. auris* clinical strains reported from India. Interestingly, *Candida albicans* was isolated from oak trees in an ancient wood pasture (Bensasson et al., 2019). *Candida albicans* is traditionally regarded as an obligate commensal of humans and other mammals, but the genomic sequences of the oak strains were closely related to those from humans. The high genetic diversity of *C. albicans* from old oaks shows that they can live in this environment for extended periods of time. Similarly, isolation of *C. auris* from the marine environment suggests wetlands as a niche for *C. auris* outside its human host.

The exploration of further ecological niches will determine if new clades of *C. auris* exist in these natural habitats.

2.3 Experimental Procedures

(i) Sampling sites. The Andaman & Nicobar group of islands (6°45′ N and 13°45′ N latitude and 92°12′ E and 93°57′ E longitude), Union Territory of India, are a chain of 572 islands/islets located in the southeastern Bay of Bengal at a distance of 1,200 km from mainland India with a coast line of 1,962 km. The islands are surrounded by the Andaman Sea to the east and the Bay of Bengal to the west. The Andaman group has 325 islands which cover an area of 6,170 km2. The temperature variation is slight, between 22°C and 30°C, and average relative humidity is 79%. Eight locations distributed on three islands detailed in Table 2. 1 and Figure 2. 1 were investigated.

(ii) Environmental sampling. At each site, three replicate samples of sediments and seawaters were collected during low tides within a period of 1 month in the dry season (February to March 2020). The sediment samples were taken from a depth of 5 cm using a sterile plastic PVC corer of 5 cm in diameter and placed in sterile zip-lock pouches. The triplicate sediment samples collected from one site were then mixed, representing one composite sediment sample for each sampling site. For collection of the seawater, 50-ml sterile bottles were used and the seawater samples were maintained separately. The samples were transported to the laboratory at 4°C.

(iii) Processing of environmental samples and identification of yeast isolates. To isolate yeasts from these samples, 2 g of sediments (retaining the natural content of water) was suspended in 8 ml of 0.85% NaCl, vortexed, and allowed to settle. Four hundred microliters of the suspension was plated in triplicate on Sabouraud dextrose agar plates supplemented with chloramphenicol (50 mg/liter) and gentamicin (0.75 ml/liter) (SDA-CG) and incubated at 28°C up to 7 days. The seawater samples were filtered using sterile 0.45-μm membrane filters, and the membranes were plated on SDA-CG plates and incubated at 28°C

up to 7 days. The physical-chemical parameters of soil and water samples such as salinity, temperature, and pH were recorded, and dissolved oxygen were obtained using the modified Winkler method (Strickland and Parson., 1972).

The SDA-CG plates were examined periodically after 24 h, and yeast-like colonies were subcultured on CHROMagar *Candida* medium for preliminary identification. All yeast isolates were identified by matrix-assisted laser desorption ionization-time of flight mass spectrometry (MALDI-TOF MS) (Bruker Biotyper OC version 3.1; Daltonics, Bremen, Germany) using the ethanol-formic acid extraction method (20). Molecular identification of all isolates was performed by sequencing the internal transcribed spacer (ITS) regions and the D1D2 region of the ribosomal DNA (rDNA) as described previously (Prakash et al., 2016). All *C. auris* isolates were screened for growth characteristics at 37°C and 42°C, and their ability to assimilate sugars and sensitivity to cycloheximide was determined as described previously (Kurtzman et al., 2011). Antifungal susceptibility testing of *C. auris* was done using the broth microdilution method according to CLSI M27-A3 (Rex et al., 2008). Antifungals tested were fluconazole, voriconazole, posaconazole, isavuconazole, micafungin, anidulafungin, and amphotericin B.

(iv) Spot assay on fluconazole-containing SDA plates. To perform the spot assay, SDA plates were prepared containing 2-fold serial dilutions of fluconazole. Briefly, a freshly prepared stock solution of fluconazole in dimethyl sulfoxide (DMSO) was used to prepare fluconazole-containing agar dilution plates of 2-fold dilution from 0.25 mg/liter to 32 mg/liter. Inoculum was prepared by streaking the isolate on freshly prepared SDA plates (without antifungal) and incubated at 37°C for a period of 18 to 24 h. The colonies obtained from the overnight culture were directly suspended into sterile 0.85% saline, and optical density (OD) was adjusted to 0.1 (~106 cells/ml) at 625 nm. Five microliters each of the fluconazole-susceptible strain (VPCI/E/AN/176/20), three fluconazole-resistant strains (VPCI/E/AN/175/20, VPCI/E/AN/179/20, and VPCI/E/AN/180/20), and reference *C. auris* KCTC 17810 (clade II) were spot inoculated on the fluconazole-containing agar

plates. The plates were left undisturbed to air dry under aseptic conditions and were incubated at 37°C for 24 h.

(v) Growth profiling. The growth profiles were studied for four *C. auris* strains, including the two *C. auris* strains from site A and two representative *C. auris* strains from site B. All four *C. auris* strains were first grown in Sabouraud dextrose (SD) broth overnight at 30°C. From the overnight culture, cells corresponding to an optical density of 0.1 at 625 nm (OD625) were inoculated into fresh SD broth in a microtiter plate. The plate was then incubated at 37°C and 42°C up to 72 h. The optical density was recorded in an Infinite 200 Pro (Tecan, Switzerland) microplate reader at regular intervals (2 h). The OD625 values versus time were plotted.

(vi) Genome sequencing. *Candida auris* was subjected to whole-genome sequencing using Illumina HiSeq 4000. Sequencing libraries were prepared as described elsewhere (Singh et al., 2019). For comparative analyses, we also included 18 previously published genomes of Indian *C. auris* strains (B11200, B11201, B11205 to B11207, B11209, B11210, B11212 to B11218, VPCI/510/P/14, VPCI/692/P/12, VPCI/550/P/14, and VPCI/479/P/13), 9 recent isolates from patients and their immediate environments admitted to V. P. Chest Institute (VPCI/82/P/20, VPCI/80/P/20, VPCI/81/P/20, VPCI/E/41C/20, VPCI/E/25/20, VPCI/E/17W/20, VPCI/E/7LP/20, VPCI/E/3/20, and VPCI/83/P/20), and reference clade I strain B8441 from Pakistan.

The genome-wide single nucleotide polymorphisms (SNPs) were identified using the NASP pipeline (Northern Arizona SNP Pipeline, http://tgennorth.github.io/NASP/). Reads were trimmed using Trimmomatic v0.39 (Bolger et al., 2014) and aligned against the reference genome using BWA v0.7.17 (Li, 2013). SNP sites were identified using GATK v2.7.4 (McKenna et al., 2010). The SNP sites were filtered out if they were located in the repetitive regions of the reference genome, had a coverage lower than 10×, or had less than 90% variant allele calls. For the phylogenetic analysis, all the 1,154 identified SNP sites

among the 41 strains were concatenated. The maximum likelihood tree was constructed using RAxML based on 1,000 bootstrap replicates and the ASC_GTRCAT nucleotide substitution model. The phylogeny was visualized using an online tool, iTOL.

(vii) Data availability. The genome sequences of all 13 *Candida auris* strains isolated in the present study from the South Andaman district, Andaman & Nicobar Islands, Union Territory of India, are accessible through BioProject number PRJNA679832.

Acknowledgments

We are thankful to the authorities of Pondicherry University for providing the facilities and the University fellowship to Parth Arora. Y.W. acknowledges the MacData Fellowship, and J.X. acknowledges McMaster University's Global Science Initiative and IIDR.
All other authors declare no potential conflicts of interest. We alone are responsible for the content and writing of the paper.

Supplemental Material

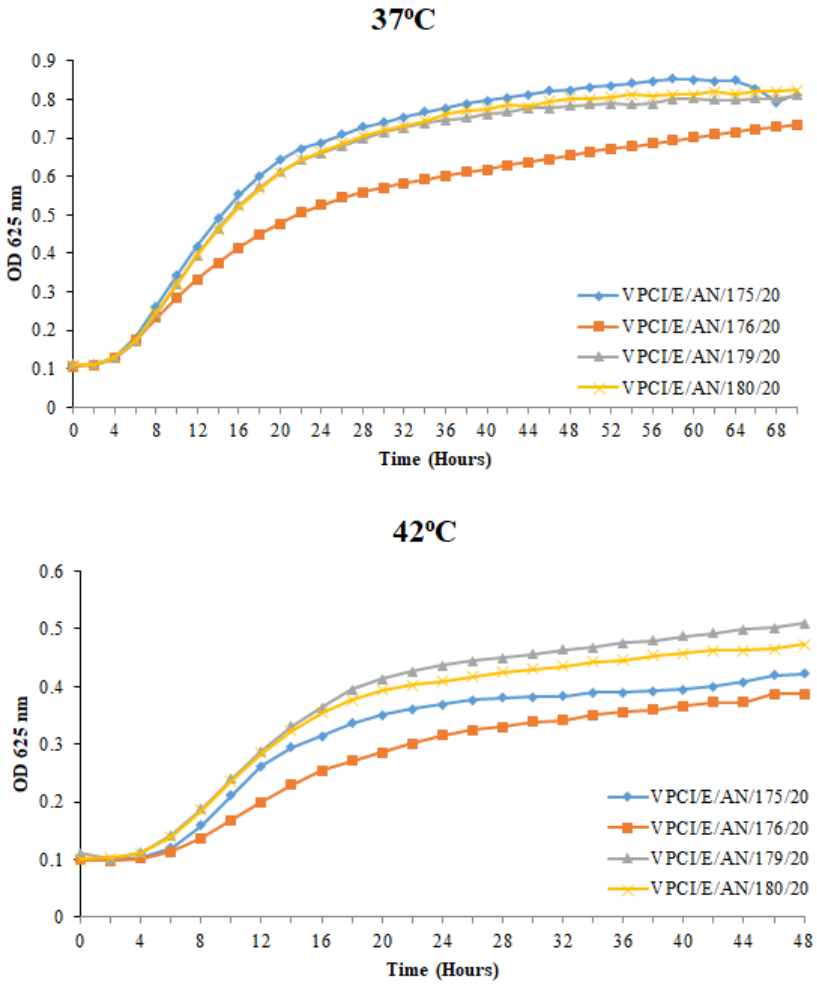

Figure 2. S1. The graph illustrates the growth curve (optical density versus time plot) of *Candida auris* strains isolated from the South Andaman district (SAD), Andaman & Nicobar Islands, Union Territory of India, at 37°C and 42°C.

Table 2. S1. MIC distribution of *Candida auris* (n = 24) isolated from the South Andaman district (SAD), Andaman & Nicobar Islands, Union territory of India against 9 antifungal drugs tested using CLSI-BMD method.

Site (number of isolates)	Isolate ID	Parameters	MIC (mg/L)							
			FLU	ITC	VRC	ISA	POS	AMB	MFG	AFG
#A (n=2)	VPCI/E/AN/176/20	MIC	8	0.25	0.125	<0.015	0.06	1	0.25	0.125
	VPCI/E/AN/175/20	MIC	>256	1	2	0.5	0.25	2	0.125	0.125

B (n= 22)	VPCI/E/AN/177/20-VPCI/E/AN/198/20	Range	256->256	0.5-1	1-2	0.5	0.25	2-4	0.125-0.25	0.125
		GM MIC	256	0.97	1.71	0.5	0.25	4	0.19	0.125
		MIC_{50}	256	1	2	0.5	0.25	4	0.25	0.125
		MIC_{90}	256	1	2	0.5	0.25	4	0.25	0.125

[#] Site A, Salt Marsh; Site B, Tourist Beach

MIC, Minimum Inhibitory Concentration; GM, Geometric Mean; MIC50, MIC at which 50% of test isolates were inhibited; MIC90, MIC at which 90% of test isolates were inhibited; FLU, Fluconazole; ITC, Itraconazole; VRC, Voriconazole; ISA, Isavuconazole; POS, Posaconazole; AMB, Amphotericin B; MFG, Micafungin; AFG, Anidulafungin.

References

Strickland, J.D.H. and Parsons, T.R. (1972) A Practical Handbook of Seawater Analysis. 2nd edition. Ottawa, Canada, Fisheries Research Board of Canada, 310pp. (Bulletin Fisheries Research Board of Canada, Nr. 167 (2nd ed)). DOI: https://repository.oceanbestpractices.org/handle/11329/1994.

Bensasson, Douda, Jo Dicks, John M. Ludwig, Christopher J. Bond, Adam Elliston, Ian N. Roberts, and Stephen A. James. 2019. "Diverse Lineages of *Candida albicans* Live on Old Oaks." *Genetics* 211 (1): 277–88. https://doi.org/10.1534/GENETICS.118.301482.

Bolger, Anthony M., Marc Lohse, and Bjoern Usadel. 2014. "Trimmomatic: A Flexible Trimmer for Illumina Sequence Data." *Bioinformatics (Oxford, England)* 30 (15): 2114–20. https://doi.org/10.1093/BIOINFORMATICS/BTU170.

Buzzini, P, MA Lachance, and A Yurkov. 2017. *Yeasts in Natural Ecosystems: Diversity*. https://link.springer.com/content/pdf/10.1007/978-3-319-62683-3.pdf.

Caceres, Diego H., Kaitlin Forsberg, Rory M. Welsh, David Joseph Sexton, Shawn R. Lockhart, Brendan R. Jackson, and Tom Chiller. 2019. "*Candida auris*: A Review of Recommendations for Detection and Control in Healthcare Settings." *Journal of Fungi (Basel, Switzerland)* 5 (4). https://doi.org/10.3390/JOF5040111.

Casadevall, Arturo, Dimitrios P. Kontoyiannis, and Vincent Robert. 2019. "On the Emergence of *Candida auris*: Climate Change, Azoles, Swamps, and Birds." *MBio* 10 (4). https://doi.org/10.1128/MBIO.01397-19.

Chowdhary, Anuradha, Cheshta Sharma, and Jacques F. Meis. 2017. "*Candida auris*: A Rapidly Emerging Cause of Hospital-Acquired Multidrug-Resistant Fungal Infections Globally." *PLoS Pathogens* 13 (5). https://doi.org/10.1371/JOURNAL.PPAT.1006290.

Iguchi, S., Y. Itakura, A. Yoshida, K. Kamada, R. Mizushima, Y. Arai, Y. Uzawa, and K. Kikuchi. 2019. "*Candida auris*: A Pathogen Difficult to Identify, Treat, and Eradicate and Its Characteristics in Japanese Strains." *Journal of Infection and Chemotherapy : Official Journal of the Japan Society of Chemotherapy* 25 (10): 743–49. https://doi.org/10.1016/J.JIAC.2019.05.034.

Jackson, Brendan R., Nancy Chow, Kaitlin Forsberg, Anastasia P. Litvintseva, Shawn R. Lockhart, Rory Welsh, Snigdha Vallabhaneni, and Tom Chiller. 2019. "On the Origins of a Species: What Might Explain the Rise of *Candida auris*?" *Journal of Fungi (Basel, Switzerland)* 5 (3). https://doi.org/10.3390/JOF5030058.

Kurtzman, CP, JW Fell, and T Boekhout. 2011. *The Yeasts: A Taxonomic Study*. https://doi.org/10.1016/B978-044481312-1/50096-4.

Lee, Wee Gyo, Jong Hee Shin, Young Uh, Min Gu Kang, Soo Hyun Kim, Kyung Hwa Park, and Hee Chang Jang. 2011. "First Three Reported Cases of Nosocomial Fungemia Caused by *Candida auris*." *Journal of Clinical Microbiology* 49 (9): 3139–42. https://doi.org/10.1128/JCM.00319-11.

Li, Heng. 2013. "Aligning Sequence Reads, Clone Sequences and Assembly Contigs with BWA-MEM," March. http://arxiv.org/abs/1303.3997.

Lockhart, Shawn R., Kizee A. Etienne, Snigdha Vallabhaneni, Joveria Farooqi, Anuradha Chowdhary, Nelesh P. Govender, Arnaldo Lopes Colombo, et al. 2017. "Simultaneous Emergence of Multidrug-Resistant *Candida auris* on 3 Continents Confirmed by Whole-Genome Sequencing and Epidemiological Analyses." *Clinical Infectious Diseases : An Official Publication of the Infectious Diseases Society of America* 64 (2): 134–40. https://doi.org/10.1093/CID/CIW691.

Madden, Anne A., Mary Jane Epps, Tadashi Fukami, Rebecca E. Irwin, John Sheppard, D. Magdalena Sorger, and Robert R. Dunn. 2018. "The Ecology of Insect-Yeast

Relationships and Its Relevance to Human Industry." *Proceedings. Biological Sciences* 285 (1875). https://doi.org/10.1098/RSPB.2017.2733.

McKenna, Aaron, Matthew Hanna, Eric Banks, Andrey Sivachenko, Kristian Cibulskis, Andrew Kernytsky, Kiran Garimella, et al. 2010. "The Genome Analysis Toolkit: A MapReduce Framework for Analyzing Next-Generation DNA Sequencing Data." *Genome Research* 20 (9): 1297–1303. https://doi.org/10.1101/GR.107524.110.

Prakash, A., C. Sharma, A. Singh, P. Kumar Singh, A. Kumar, F. Hagen, N. P. Govender, A. L. Colombo, J. F. Meis, and A. Chowdhary. 2016. "Evidence of Genotypic Diversity among *Candida auris* Isolates by Multilocus Sequence Typing, Matrix-Assisted Laser Desorption Ionization Time-of-Flight Mass Spectrometry and Amplified Fragment Length Polymorphism." *Clinical Microbiology and Infection : The Official Publication of the European Society of Clinical Microbiology and Infectious Diseases* 22 (3): 277.e1-277.e9. https://doi.org/10.1016/J.CMI.2015.10.022.

CLSI. 2008. "Reference Method for Broth Dilution Antifungal Susceptibility Testing of Yeasts : Approved Standard." *Clinical and Laboratory Standards Institute, M27-A3* 28 (14). https://cir.nii.ac.jp/crid/1130282271681047296.

Satoh, Kazuo, Koichi Makimura, Yayoi Hasumi, Yayoi Nishiyama, Katsuhisa Uchida, and Hideyo Yamaguchi. 2009. "*Candida auris* Sp. Nov., a Novel Ascomycetous Yeast Isolated from the External Ear Canal of an Inpatient in a Japanese Hospital." *Microbiology and Immunology* 53 (1): 41–44. https://doi.org/10.1111/J.1348-0421.2008.00083.X.

Sharma, C., N. Kumar, R. Pandey, J. F. Meis, and A. Chowdhary. 2016. "Whole Genome Sequencing of Emerging Multidrug Resistant *Candida auris* Isolates in India Demonstrates Low Genetic Variation." *New Microbes and New Infections* 13 (September): 77–82. https://doi.org/10.1016/J.NMNI.2016.07.003.

Singh, Ashutosh, Aradhana Masih, Juan Monroy-Nieto, Pradeep Kumar Singh, Jolene Bowers, Jason Travis, Ananta Khurana, David M. Engelthaler, Jacques F. Meis, and Anuradha Chowdhary. 2019. "A Unique Multidrug-Resistant Clonal Trichophyton

Population Distinct from Trichophyton Mentagrophytes/Trichophyton Interdigitale Complex Causing an Ongoing Alarming Dermatophytosis Outbreak in India: Genomic Insights and Resistance Profile." *Fungal Genetics and Biology : FG & B* 133 (December). https://doi.org/10.1016/J.FGB.2019.103266.

Sipiczki, Matthias, and Ratna Mohd Tap. 2016. "*Candida vulturna* pro Tempore Sp. Nov., a Dimorphic Yeast Species Related to the *Candida haemulonis* Species Complex Isolated from Flowers and Clinical Sample." *International Journal of Systematic and Evolutionary Microbiology* 66 (10): 4009–15. https://doi.org/10.1099/IJSEM.0.001302.

Solomon, SL, KB Oliver - American family physician, and undefined 2014. n.d. "Antibiotic Resistance Threats in the United States: Stepping Back from the Brink." *Aafp.Org*. Accessed June 24, 2023. https://www.aafp.org/afp/2014/0615/p938.html.

Tedersoo, Leho, Mohammad Bahram, Sergei Põlme, Urmas Kõljalg, Nourou S. Yorou, Ravi Wijesundera, Luis Villarreal Ruiz, et al. 2014. "Fungal Biogeography. Global Diversity and Geography of Soil Fungi." *Science (New York, N.Y.)* 346 (6213). https://doi.org/10.1126/SCIENCE.1256688.

Uden, N. van, and M. C. Kolipinski. 1962. "*Torulopsis Haemulonii* Nov. Spec., a Yeast from the Atlantic Ocean." *Antonie van Leeuwenhoek* 28 (1): 78–80. https://doi.org/10.1007/BF02538724.

Welsh, Rory M., Meghan L. Bentz, Alicia Shams, Hollis Houston, Amanda Lyons, Laura J. Rose, and Anastasia P. Litvintseva. 2017. "Survival, Persistence, and Isolation of the Emerging Multidrug-Resistant Pathogenic Yeast *Candida auris* on a Plastic Health Care Surface." *Journal of Clinical Microbiology* 55 (10): 2996–3005. https://doi.org/10.1128/JCM.00921-17.

Chapter 3

Candida auris on Apples: Diversity and Clinical Significance

Abstract *Candida auris* is a multidrug-resistant nosocomial fungal pathogen. While the marine environment was recently identified as a natural niche for *C. auris*, the environment(s) that might have contributed to the development and spread of antifungal resistance in *C. auris* remains a mystery. Because stored fruits are often treated with fungicides to prevent postharvest spoilage, we hypothesized that stored fruits could serve as a possible selective force for and a transmission reservoir of antifungal-resistant isolates of pathogenic yeasts, including *C. auris*. To test this hypothesis, we screened fruits to study the diversity of pathogenic yeasts and their antifungal susceptibility profiles. Among the 62 screened apples, the surfaces of 8 were positive for *C. auris*, and all were stored apples. Whole-genome sequencing (WGS) showed that *C. auris* strains from apples were genetically diverse and exhibited broad phylogenetic distribution among the subclades within clade I. Interestingly, strains from apples had closely related strains from other sources in India, including from patients, hospitals, and marine environments, and from clinical strains from other parts of the world. A broad range of fungicides, including dimethyl inhibitors (DMIs), were detected in stored apples, and all *C. auris* isolates exhibited reduced sensitivity to DMIs. Interestingly, *C. auris* was not isolated from freshly picked apples. Together, the results suggest a potentially complex ecology for *C. auris* with agriculture fungicide application on stored fruits as a significant selective force for drug resistance in clinics.

Importance In 2019, the U.S. Centers for Disease Control and Prevention classified the multidrug-resistant *Candida auris* as one of five pathogens posing the most urgent threats to public health. At present, the environment(s) that might have contributed to the development and spread of antifungal resistance in *C. auris* is unknown. Here, we tested whether fruits could be a source of multidrug-resistant *C. auris*. We identified genetically

diverse *C. auris* strains with reduced sensitivity to major triazole dimethyl inhibitors fungicides on the surfaces of stored apples. The successful isolation of *C. auris* from apples here calls for additional investigations into plants as a reservoir of *C. auris*. Our findings suggest that *C. auris* in the natural ecosystem may come in contact with agriculture fungicides and that stored fruits could be a significant niche for the selection of azole resistance in *C. auris* and other human fungal pathogens.

For the study in this chapter, I conducted the bioinformatic analyses including whole genome sequencing data analyses and phylogenetic analyses. I am a co-first author of the following paper:
Yadav, A., Jain, K., Wang, Y., Pawar, K., Kaur, H., Sharma, K., Tripathy, V., Singh, A., Xu, J. and Chowdhary, A. 2022. "*Candida auris* on Apples: Diversity and Clinical Significance." mBio 13(2):e00518-22.

3.1 Introduction

Candida auri is a fungal pathogen and a serious threat to global health (CDC. 2019., n.d.). Since 2009, *C. auris* has caused an escalating number of health care-associated outbreaks. This recently emerged pathogen exhibits high rates of drug resistance and high transmissibility within health care facilities, causing a significant challenge for treating infected patients and for eradicating the pathogen from health care settings (Yadav et al., 2021). Since its first identification in 2009 in Japan, *C. auris* has independently emerged and/or spread to all populated continents, with several regions reporting clinical strains belonging to phylogenetically distant clades (Satoh et al., 2009b; Lockhart et al., 2017a; Anuradha Chowdhary et al., 2017). Indeed, genomic analyses have revealed the near-simultaneous emergence of five distinct lineages across six continents, encompassing over 40 countries within the past ~400 years (Lockhart et al., 2017a; Chow et al., 2020). A recent report about the isolation of *C. auris* from the marine environment in India suggested a potential natural niche for *C. auris* (Arora et al., 2021). Specifically, the study reported isolation of *C. auris* from the sandy beach and a tidal swamp in the tropical Andaman

Islands, with several strains showing close genetic relationships to clinical isolates in mainland India. Interestingly, compared to the common feature of multidrug resistance among clinical strains, one *C. auris* strain from the tidal marsh was sensitive to all tested antifungal drugs. They hypothesized that the drug-susceptible *C. auris* strain from an aquatic habitat with no known human activity might represent an ancestral state of the pathogen which subsequently developed drug resistance during its adaptation to anthropogenic environments (Arora et al., 2021; Casadevall et al., 2021). At present, the environments that might have contributed to the development and spread of antifungal resistance in *C. auris* remain a mystery.

In natural environments, yeasts are predominantly saprotrophs and have been found on many types of ecological niches where organic compounds are common, including soil, wood, litter, and the surfaces of leaves and fruits (Samarasinghe et al., 2021). For example, several species of yeasts were isolated from fruits in tropical and subtropical habitats, including opportunistic human pathogens *Candida krusei*, *Candida orthopsilosis*, *Candida parapsilosis*, *Candida pelliculosa*, and *Candida tropicalis* (Opulente et al., 2019; Lo et al., 2017; Youming Shen et al., 2018). Notably, Lo et al. (2017) found fluconazole-resistant *C. tropicalis* on the surface of fruits and with genotypes similar or identical to those infecting humans. Given that stored fruits are often treated with fungicides to prevent postharvest spoilage and to extend their shelf life, the results suggest that in addition to acting as an ecological niche for pathogenic yeasts, fruits could also be a possible selective force for and a transmission reservoir of antifungal-resistant isolates of human-pathogenic yeasts (Jiang et al., 2019). However, so far, no isolate of *C. auris* has been reported from fruits.

In this study, we screened seasonal tropical and temperate fruits to study the ecological diversity of pathogenic yeasts with an emphasis on the isolation of *C. auris*. Colonies of *C. auris* were obtained from the surfaces of stored apples. The antifungal susceptibilities and whole-genome sequences of all *C. auris* isolates were obtained and compared with those of previously reported strains from India and other regions. Our results suggest that

exposure to fungicides used for fruit storage could be a selective force for azole resistance in *C. auris* in clinical settings.

3.2 Results

Yeast diversity on tropical and temperate fruits. This study analyzed fruit samples collected from March 2020 to September 2021. We surveyed a total of 84 fruits representing nine fruit plant species, including seasonal tropical and temperate fruits collected from New Delhi, adjoining National Capital Region (NCR), and other regions of northern India. We focused on investigating yeasts on the fruits' surfaces using the swabbing technique. A total of 144 yeast strains belonging to 22 species were isolated from the surface (epicarp) of fruits of the nine sampled species, with each fruit species containing at least one yeast species (Table 3. 1). Different from the epicarp, no yeast was isolated from the endocarp tissue of any of the 84 fruits that we screened. Among the isolated yeast genera, the genus *Candida* predominated (73%) the surfaces of all the fruits investigated, with C. guilliermondii (20.8%) being the most common, followed by *C. parapsilosis* (15.9%), *C. tropicalis* (13%), and *C. auris* (11%).

Table 3. 1. Distribution of yeast species (n = 22) isolated from nine fruit plant species (tropical and temperate) [a]

S. No.	Species (No. of colonies)	Fruits (Common name)
1	*Candida auris* (n=16)	*Malus domestica*[TEM] (apple)
2	*C. lusitaniae* (n=7)	*M. domestica*
3	*C. parapsilosis* (n=23) [b]	*M. domestica*
4	*Lodderomyces elongisporus* (n=13) [b]	*M. domestica*
5	*C. carpophila* (n=1) *C. blankii* (n=1) *C. magnoliae* (n=1) *C. rugosa* (n=1) *C. albicans* (n=1) *Issatechnika terricolis* (n=1) *Hansempora uvarum (*n=1) *H. vineac* (n=1)	*M. domestica*
6	*C. tropicalis* (n=19) [b]	*M. domestica*, *Cucumis melo*[TRP] (melon), *Mangifera Indica*[TRP] (mango), *Pyrus pyrifolia*[TEM] (pear, kishtabahira, Asian pear), *Punica granatum*[TRP] (Pomegranate), *Citrus sinensis*[TRP] (orange)
7	*C. guilliermondii* (n=30) [b]	*M. domestica*, *M. indica*, *Prunus bokharensis*[TEM] (plum, Bokhara plum)
8	*C. caribbica* (n=2)	*M. domestica*, *C. melo*
9	*Kodamea ohmeri* (n=16) [b]	*M. domestica*, *C. melo*
10	*Trichosporan asahii* (n=1) *C. krusei* (n=1)	*C. melo*
11	*Pichia manshurica* (n=1)	*V. vinifera*[TRP] (grapes)
12	*Merozyma ferinosa* (n=3)	*P. pyrifolia*
13	*C. kefyr* (n=2)	*Ananas comosus*[TRP] (pineapple), *P. granatum*
14	*Aureobasidium pollulans* [c] (n=2)	*M. indica*

[a] TRP; tropical fruit, TEM; temperate fruit.

[b] Two to six colonies per apple surface.

[c] Black yeast.

***C. auris* on apple surfaces.** In this study, due to the broad cultivation of apples around the world and their year-long availability in our local markets, we focused on investigating yeasts from apples, with 62 of the 84 sampled fruits being apples. In addition, we focused

on the two most common varieties of apples in India, Red Delicious and Royal Gala. These apples included both freshly harvested (n = 20) and stored apples (n = 42). The stored apples were purchased from local fruit vendors of Delhi and adjoining NCR between March and April in 2020 and between June and July in 2021. The fresh apples, all Red Delicious variety, were collected during the harvesting season (September 2021) from four apple orchards located in northern India, in the Solan and Kullu districts of Himachal Pradesh and in Srinagar city of Jammu and Kashmir. Two of the four orchards, one in Solan and the other in Kullu, used organic farming. In contrast, the orchard in Srinagar and the other orchard in Solan used nonorganic farming approaches.

Among the 62 apples, 8 (13%) yielded *C. auris*. A total of 16 *C. auris* colonies were recovered from surfaces of these eight apples (Tables 1 and 2). *Candida auris* was isolated from the surfaces of both the Red Delicious (n = 5) and the Royal Gala (n = 3) varieties. Interestingly, all 16 *C. auris* colonies were from stored apples purchased from the local fruit vendors. In contrast, only 1 of the 20 fresh apples collected from the four orchards resulted in a single yeast colony belonging to the species *C. albicans*. Overall, the surfaces of the eight *C. auris*-positive apples yielded 1 to 5 colonies each by surface swabbing. Interestingly, 4 of 8 apples positive for *C. auris* harbored only this yeast species, whereas the remaining 4 apples were co-colonized by *C. parapsilosis*, *C. guilliermondii*, and/or *Kodamaea ohmeri*. In contrast to the low yeast diversity of the 8 stored apples that were positive for *C. auris*, the 34 stored apples from local markets that were negative for *C. auris* had high yeast diversity. In total, these 34 apples harbored 16 species, including 11 spp. of *Candida* and 5 species in five other genera (Tables 1 and 2).

Table 3. 2. Spectrum of yeast species from the surfaces of 62 apples and detection of fungicides.

Slot No. of apples	**Date of collection**	**Apple varieties**	**No. of apples positive for *C. auris*/ total apples screened (No. of *C. auris* colonies)**	**Co-colonising yeast species**	**Fungicides detected (concentration in ppm)**		
					Categories of fungicides	***C. auris* positive apples**	***C. auris* negative apples**

1	16-03-2020	'Red Delicious'	2/5 (n=3)	*C. parapsilosis* *C. guilliermondii*	Not done		
2	15-04-2020	'Royal Gala'	1/9 (n=5)		Not done		
3	04-06-2021	'Royal Gala'	1/3 (n=2)		Triazoles	Flusilazole* (0.02) Sulfentrazone (0.019)	Flusilazole* (0.01-0.02)
					Diazoles	Carbendazim (0.07)	Carbendazim (0.04-0.19)
					Other fungicides	Kresoxim-methyl (0.05)	Kresoxim-methyl (0.05-0.18)
4	26-07-2021	'Royal Gala'	1/5 (n=1)	*C. guilliermondii*	Triazoles	Flusilazole* (0.02)	Flusilazole* (0.02-0.09)
					Diazoles	Carbendazim (0.07)	Carbendazim (0.04-0.19)
					Other fungicides	Kresoxim-methyl (0.05)	Kresoxim-methyl (0.05-0.18)
5	26-07-2021	'Red Delicious'	1/5 (n=2)		Triazoles	Sulfentrazone (0.019)	Sulfentrazone (0.013-0.016)
					Diazoles	Fludioxonil (0.01) Pyroclostrobin (0.02)	Fludioxonil (0.03) Pyroclostrobin (0.01-0.02)
					Other fungicides	Boscalid (0.04) Pyrimethanil (0.91)	Boscalid (0.03-0.03) Pyrimethanil (1.46-1.93) Imidacloprid (0.04)
6	26-07-2021	'Royal Gala'	1/5 (n=2)	*K. ohmeri*	Triazoles	-	-
					Diazoles	-	-
					Other fungicides	Captan (0.12)	Captan (0.04-0.08)
7	26-07-2021	'Red Delicious'	1/5 (n=1)		Triazoles	Sulfentrazone (0.03)	Sulfentrazone (0.01-0.02)
					Diazoles	Fludioxonil (0.02) Thiabendazole (0.03)	Thiabendazole (0.02-0.04) Pyraclostrobin (0.01-0.02)

					Pyraclostrobin (0.04)	
				Other fungicides	Diphenylamine (0.36) Pyrimethanil (0.93)	Diphenylamine (0.26-0.52) Pyrimethanil (0.55-1.16)
8	26-07-2021	'Red Delicious'	0/5		No detection	
9	03-09-2021	'Red Delicious'	0/5	Triazoles	-	Tebuconazole* (0.01-0.03)
				Diazoles	-	-
				Other fungicides	-	Biphenyl (0.01) Hexythiazox (0.01)
10	03-09-2021	'Red Delicious'	0/5	Triazoles	-	Tebuconazole (0.05) Difenoconazole* (0.03)
				Diazoles	-	-
				Other fungicides	-	-
11	07-09-2021	'Red Delicious'	0/5		No detection	
12	21-09-2021	'Red Delicious'	0/5		No detection	

[a] Slot no. 1 to 8 represent apples purchased from local vendors (nonseasonal stored apples), slot no. 9 to 12 represent seasonal apples which were hand-picked from three apple orchards from apple-growing belts of Northern India, slot no. 9 to 10, from orchards used nonorganic farming, and slot no. 11 to 12 used organic farming.

[b] Demethylation inhibitor (DMI) triazoles.

[c] Negative for specific category of fungicide.

Growth characteristics of *C. auris* strains on the surfaces of apples (CasSA). All 16 CasSA showed oval yeast cells without pseudohyphae, similar to that of the *C. auris* reference strain B8441. The growth curve analysis of CasSA showed similar growth patterns, reaching stationary phase within approximately 20 h. Furthermore, all CasSA

grew in the presence of 640 mg/L calcofluor white (CFW) and at 10% sodium chloride concentration.

CasSA exhibit haploid genome. Flow cytometry analysis of two randomly selected CasSA and B8441 showed geometric mean value of growth phase 1 (G1) cells ranging from 39,563 to 45,000 AU (arbitrary units), close to the geometric mean (40,794 AU) of the haploid *C. glabrata* (ATCC 15545) (see supplemental material, Figure 3. S1A to C). This result indicates that our CasSA are haploid.

Presence of fungicides, including triazole DMIs, in apples. The results of gas chromatography-mass spectrometry (GC-MS) and liquid chromatography with tandem mass spectrometry (LC-MS/MS) showed a diversity of fungicides in the analyzed apples (Table 3. 2). Specifically, of the 48 screened apples, 50% showed presence of triazole fungicides, including three 14α-demethylase inhibitors (DMIs), i.e., tebuconazole (TEB), difenoconazole (DEF), and flusilazole (FLU). Furthermore, we also detected different groups of diazole fungicides, such as methyl benzimidazole carbamates (carbendazim and thiabendazole), quinone outside inhibitors (pyraclostrobin), and fludioxonil, a phenolpyrrole. The fungicides were similarly distributed between apples with and without *C. auris* isolation. As expected, no fungicide was detected in freshly picked apples from organically farmed orchards, whereas triazole DMIs (TEB and DEF) were detected in the freshly picked apples from nonorganic orchards.

CasSA show cross-resistance to agriculture triazole fungicides. We compared the antifungal susceptibilities of medical antifungals and agriculture triazole fungicides for the 16 CasSA with clinical and marine environmental strains from India (7, 14). Except one isolate that had a fluconazole (FLC) MIC of 16 mg/L, the remaining 15 CasSA all had high FLC MICs, >128 mg/L. Further, high MICs of voriconazole (VRC; MIC of ≥2 mg/L) and amphotericin B (AMB; MIC ≥2 mg/L) were observed in 50% and 44% of the 16 CasSA, respectively (Table 3. 3). Antifungal susceptibility profiles of other yeast species isolated

from fruits are given in Table 3. 4. For agriculture triazole fungicides, the 16 CasSA also showed an overall low in vitro susceptibility. Specifically, high geometric mean (GM) MIC values were observed for the three triazole fungicides (DMIs): tebuconazole (TEB; GM MIC of 45.25 mg/L), bromuconazole (BRO; GM MIC of 13.45 mg/L), and flusilazole (FLU; GM MIC 6.72 mg/L). Interestingly, among these three DMIs, two (TEB and FLU) were detected in the apples analyzed in the present study. Similarly, the 16 CasSA had a high GM MIC value of 128 mg/L against the diazole fungicide carbendazim, also detected in our analyzed apples. Cross-resistance was also observed for the clinical and environmental strains used here for comparison. For example, the 25 clinical *C. auris* strains resistant to FLC (MIC of >32 mg/L) all exhibited high MICs against agriculture DMIs, with high GM MIC values of 11.47 mg/L for TEB, 8.94 mg/L for FLU, and 3.29 mg/L for BRO (Table 3. 3 and Figure 3. 1). Interestingly, statistically significant (P = 0.0001) 4-fold-higher GM MIC values of TEB and BRO were observed in the CasSA population compared to those in 25 FLC-resistant clinical *C. auris* strains (Table 3. 3 and Figure 3. 1). Similarly, *C. auris* strains from natural marine environment distant from agriculture with no fungicide usage had statistically significant lower (2- to 9-fold; P = 0.0001) GM MICs of triazole fungicides than the CasSA population.

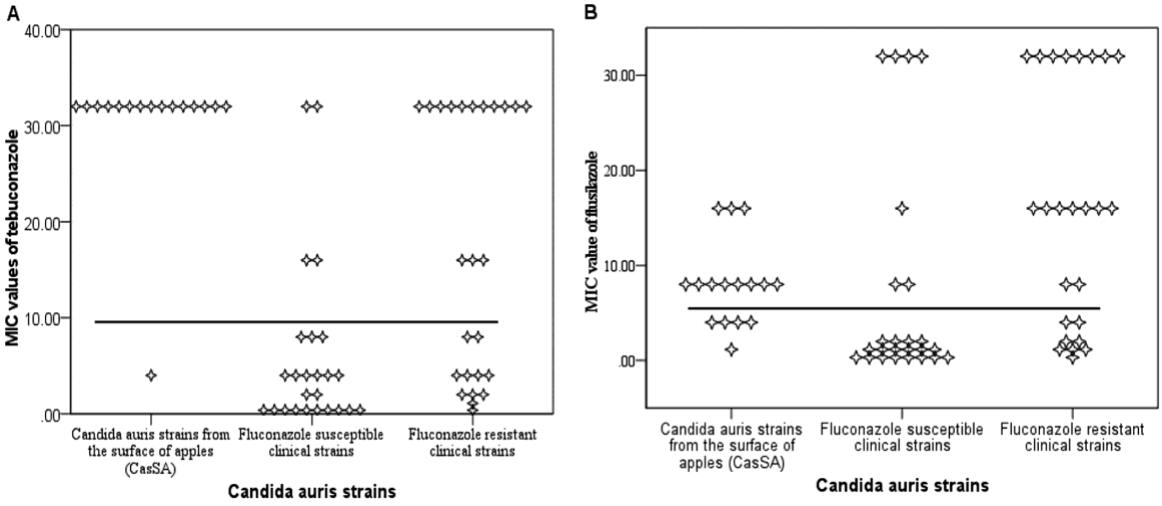

Figure 3. 1. Scatterplot depicting MIC (mg/L) distribution of two DMIs, (A) tebuconazole and (B) flusilazole, against *C. auris* strains from surfaces of apples (CasSA, n = 16), 25 fluconazole-susceptible clinical strains (MIC, <16 mg/L) and 25 fluconazole-resistant clinical strains (MIC >32 mg/L).

Table 3. 3. MIC distribution of medical antifungals and agriculture azoles against 16 *C. auris* strains from surface of apples (CasSA), clinical *C. auris* strains (n=50) and strains from marine environment (n=10, Andaman Islands, India).

***C. auris* (No. of isolates)**	**Parameters**	**MIC distribution of medical antifungals (mg/litre)**							**MIC distribution of agriculture azoles (mg/litre)**						
									DMIs triazoles					**Diazoles**	
		FLC	VRC	ITC	ISA	POS	AMB	5-FC	TEB	BRO	EPX	PCZ	FLU	PCL	CBZ
C. auris strains from surface of apples (n=16)	Range	16-128	1-16	1-32	0.25-4	0.25-2	0.25	0.12-0.25	4-64	1-32	0.25-4	0.25-2	01-16	0.25	128
	[a] GM	112.40	1.04	0.88	0.23	0.08	1.35	0.14	45.25	13.45	1.83	1.19	6.72	0.25	128
	[b] MIC_{50}	128	8	16	2	2	0.25	0.12	64	16	2	2	8	0.25	128
	[c] MIC_{90}	128	16	32	4	2	0.25	0.18	64	32	4	2	16	0.25	128
Marine environmental strains (n=10)	Range	128	0.5-4	01-4	0.03-0.50	0.03-0.25	0.25-4	0.03-64	16-128	1-32	0.25-16	0.25-4	2-32	0.25	128
	GM	105.95	1.20	0.88	0.36	0.22	3.75	28.21	19.32	1.45	0.36	0.32	2.57	0.25	128
	MIC_{50}	128	2	1	0.50	0.25	4	16.03	64	2	1.50	1	2	0.25	128
	MIC_{90}	128	4	4	0.50	0.25	4	64	83.20	15.20	6.2	2.6	20.8	0.25	128
FLC resistant clinical strains (n=25)	Range	32-128	0.06-2	0.03-1	0.01-0.50	0.01-0.25	0.12-8	0.12-64	0.25-64	0.25-16	0.25-8	0.25-8	0.12-64	0.25	128
	GM	84.44	0.47	0.15	0.07	0.06	0.57	1.43	11.47	3.29	0.82	0.87	8.94	0.25	128
	MIC_{50}	128	0.50	0.12	0.06	0.06	0.50	0.50	16	4	1	1	16	0.25	128
	MIC_{90}	128	2	0.5	0.40	0.25	1	64	64	12.80	3.20	3.20	32	0.25	128
FLC susceptible clinical strains	Range	0.25-16	0.03-1	0.03-1	0.01-0.25	0.01-0.5	0.25-4	0.12-64	0.25-32	0.25-8	0.25-2	0.25-4	0.12-64	0.25	128

(n=25)	GM	2	0.08	0.12	0.03	0.05	0.87	0.34	1.89	0.77	0.34	0.37	1.84	0.25	128
	MIC_{50}	2	0.03	0.06	0.03	0.03	0.50	0.12	4	1	0.25	0.25	1	0.25	128
	MIC_{90}	12.8	0.50	0.50	0.25	0.25	2	6.40	16	6.40	0.80	1.60	32	0.25	128

[a] FLC, fluconazole; VRC, voriconazole; ITC, itraconazole; ISA, isavuconazole; POS, posaconazole; AFG, anidulafungin; MFG, micafungin; CAS, caspofungin; AMB, amphotericin B; 5FC, flucytosine.

[b] Geometric mean MICs.

[c] MIC50, MIC at which 50% of tested isolates were inhibited.

[d] MIC90, MIC at which 90% of tested isolates were inhibited.

Table 3. 4. In vitro antifungal susceptibility profile of 12 yeast species (n=112) isolated from nine fruit plant species against ten antifungal drugs using CLSI-BMD method.

S. No.	**Species (no. of strains tested)**	**Parameters**	**MICs (mg/L)**									
			FLC	VRC	ITC	ISA	POSA	AFG	MFG	CFG	AMB	5-FC
1	*C. guilliermondii* (n=27)	Range	0.25-64	0.03-0.12	0.03-0.50	0.01-0.25	0.01-0.25	0.25-4	<0.01-1	0.50-2	0.06-0.50	<0.03-2
		[a]GM	3.61	0.05	0.33	0.09	0.13	1.32	0.43	1.39	0.36	0.21
		[b]MIC_{50}	2	0.06	0.50	0.12	0.25	2	0.50	2	0.50	0.12
		[c]MIC_{90}	16	0.12	0.50	0.25	0.25	4	1	2	0.50	1.20
2	*C. parapsilosis* (n=23)	Range	0.25-2	0.06-0.12	0.03-0.12	0.01	0.01-0.25	0.06-4	0.03-2	0.50-4	0.03-0.50	0.03-0.12
		GM	0.61	0.08	0.07	0.01	0.02	0.48	0.44	1.57	0.13	0.04
		MIC_{50}	0.50	0.09	0.06	0.01	0.01	0.50	0.50	2	0.25	0.03
		MIC_{90}	2	0.12	0.12	0.01	0.02	1	1	2	0.25	0.12
3	*C. tropicalis* (n=19)	Range	0.25-2	0.03-0.06	0.03-0.25	0.01-0.25	0.01-0.25	0.03-0.25	0.01-0.03	0.50-2	0.06-0.50	0.03-0.25
		GM	0.59	0.04	0.09	0.05	0.05	0.07	0.02	1.2	0.16	0.11
		MIC_{50}	0.50	0.03	0.12	0.03	0.06	0.06	0.01	1	0.25	0.12
		MIC_{90}	2	0.06	0.25	0.25	0.25	0.12	0.02	2	0.25	0.25
4		Range	1-8	0.03					0.01-2	1-4		

	Kodamea ohmeri (n=14)				0.03-0.12	0.01-0.03	0.01-0.03	0.03-0.50			0.03-0.12	0.03-0.12
		GM	2	0.03	0.12	0.02	0.01	0.13	0.06	1.70	0.06	0.12
		MIC_{50}	2	0.03	0.12	0.02	0.01	0.12	0.06	1	0.06	0.12
		MIC_{90}	2	0.03	0.12	0.03	0.02	0.42	0.12	4	0.12	0.12
5	*C. lusitaniae* (n=7)	Range	<0.25-8	0.03	<0.03-0.06	<0.01-0.03	<0.01-0.03	0.50-1	0.50-1	0.12-0.50	0.50-1	0.12
6	*Lodderomyces elongisporus* (n=4)	Range	2-4	0.03-0.12	0.25	>0.01	0.06-0.50	0.01	0.01	0.50	0.12	0.12
7	*C. carribica* (n=4)	Range	2-8	0.06-0.12	0.25-1	0.03-0.50	0.06-0.50	0.25-2	0.25-0.50	2	0.50	0.03
8	*C. carpophila* (n=3)	Range	8	0.06	0.25	0.12	0.06	0.50	0.25	2	0.50	0.03-0.06
9	*Merozyma ferinosa* (n=3)	Range	0.25-8	0.03	0.03	<0.01-0.03	0.01	0.50	0.25-0.50	0.12-0.50	1	<0.12
10	*C. rugosa* (n=2)	Range	1	<0.03	<0.03	<0.01	0.01	0.12	0.03	1	0.25	0.50
11	*C. kefyr* (n=2)	Range	0.12	<0.03	<0.03	<0.01	0.03	0.25-0.50	0.06	1	0.25-0.50	0.25-4
12	*C. blankii* (n=1)	MIC	8	0.06	0.12	<0.01	0.06	2	2	1	0.50	0.12
13	*C. krusei* (n=1)	MIC	32	0.12	0.50	<0.01	0.12	0.12	0.25	2	1	8
14	*C. albicans* (n=1)	MIC	4	0.25	0.06	0.01	0.01	1	0.12	1	0.25	0.06
15	*Trichosporon ashaii* (n=1)	MIC	0.25	<0.03	0.06	0.01	0.25	2	2	0.50	0.50	0.12

[a] FLC, fluconazole; VRC, voriconazole; ITC, itraconazole; ISA, isavuconazole; POS, posaconazole; AFG, anidulafungin; MFG, micafungin; CAS, caspofungin; AMB, amphotericin B; 5FC, flucytosine.

[b] Geometric mean MICs.

[c] MIC50, MIC at which 50% of tested isolates were inhibited.

[d] MIC90, MIC at which 90% of tested isolates were inhibited.

A remarkable pattern noted was that clinical *C. auris* strains that were susceptible to FLC (GM MICs of 2 mg/L) also showed low GM MICs (0.34 to 1.89 mg/L) for all agriculture triazole fungicides tested. In fact, 3-fold and 24-fold decreases in GM MICs of TEB and BRO, respectively, were noticed for clinical strains susceptible to FLC compared to those of CasSA ($P \leq 0.0001$). Interestingly, a single strain (VPCI/F1/B/2020) of *C. auris* recovered from apple which was less resistant to FLC (MIC 16 mg/L) also showed low MIC values for all triazole fungicides tested, i.e., BRO (1 mg/L), FLU (1 mg/L), and TEB (4 mg/L).

Genomic analyses of *C. auris*. The whole-genome sequences of the 16 CasSA isolated in this study as well as those of 43 previously reported Indian *C. auris* strains were analyzed and compared using the NASP pipeline (Sahl et al., 2016). *Candida auris* strain B8441 assembly V2 was used as the reference clade I strain. The 43 previously published Indian strains included 25 from patients, 5 from hospital environments, and 13 from the natural marine environment from Andaman Island (Arora et al., 2021; Lockhart et al., 2017; Yadav et al., 2021).

Genetically distinct CasSA belonged to different subclades within clade I. The maximum-likelihood phylogeny clustered all 16 CasSA as belonging to clade I, consistent with the grouping of other *C. auris* strains from India. The 16 CasSA formed five distinct genotype clusters (A to E), with four clusters consisting of more than one CasSA isolate each; cluster D was the exception, which contained a single CasSA, VPCI/F1/B/2020. Out of the 16 CasSA strains, 10 from seven apples (F1, F5, F6, F36, F37, F38, and F39) belonged to three clusters (A, B, and D) with no known closely related genotypes from other sources in India (Figure 3. 2). These apple-specific genotype clusters differed by 28 to 157 single nucleotide polymorphisms (SNPs) with the previously reported clinical, hospital inanimate environment, and natural marine environment strains from India, indicating apple surfaces harboring unique *C. auris* strains. In a broad analysis including 487 global clade I *C. auris* strains with genome sequences deposited in GenBank as of

August 2021, we separated these strains into seven subclades each with at least 75% bootstrap support values. The details of 487 global clade I *C. auris* are given in the supplemental material, Table 3. S1. The 16 CasSA clustered into three of the seven subclades, and their closest genotypes were all Indian clade I strains, with genome-wide SNP differences ranging from 0 to 157 between individual CasSA and their closest genotype from India (Figure 3. 3).

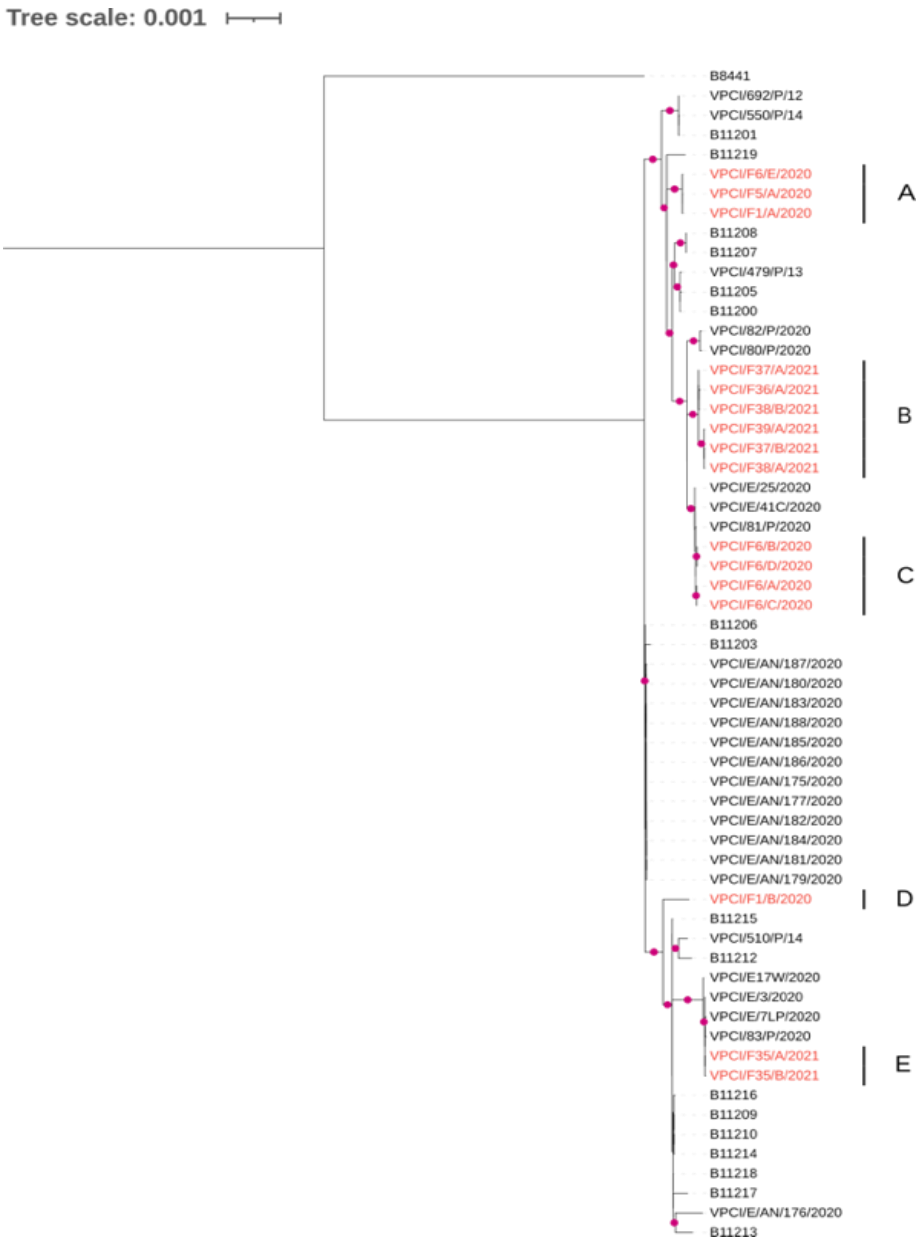

Figure 3. 2. Maximum-likelihood phylogenetic tree of 60 *C. auris* strains was constructed by using RAxML v8.0.25. Included in the tree are 16 *C. auris* strains from surfaces of apples (CasSA), 13 environmental strains from Andaman Islands, India, and 30 Indian clinical strains along with reference strain, B8441. The tree was constructed based on the 1,281 shared SNPs among the 59 strains. Branches with bootstrap support over 75% of 100 bootstrap iterations are labeled with red markers. CasSA were highlighted in red and clustered in 5 subclusters (A to E).

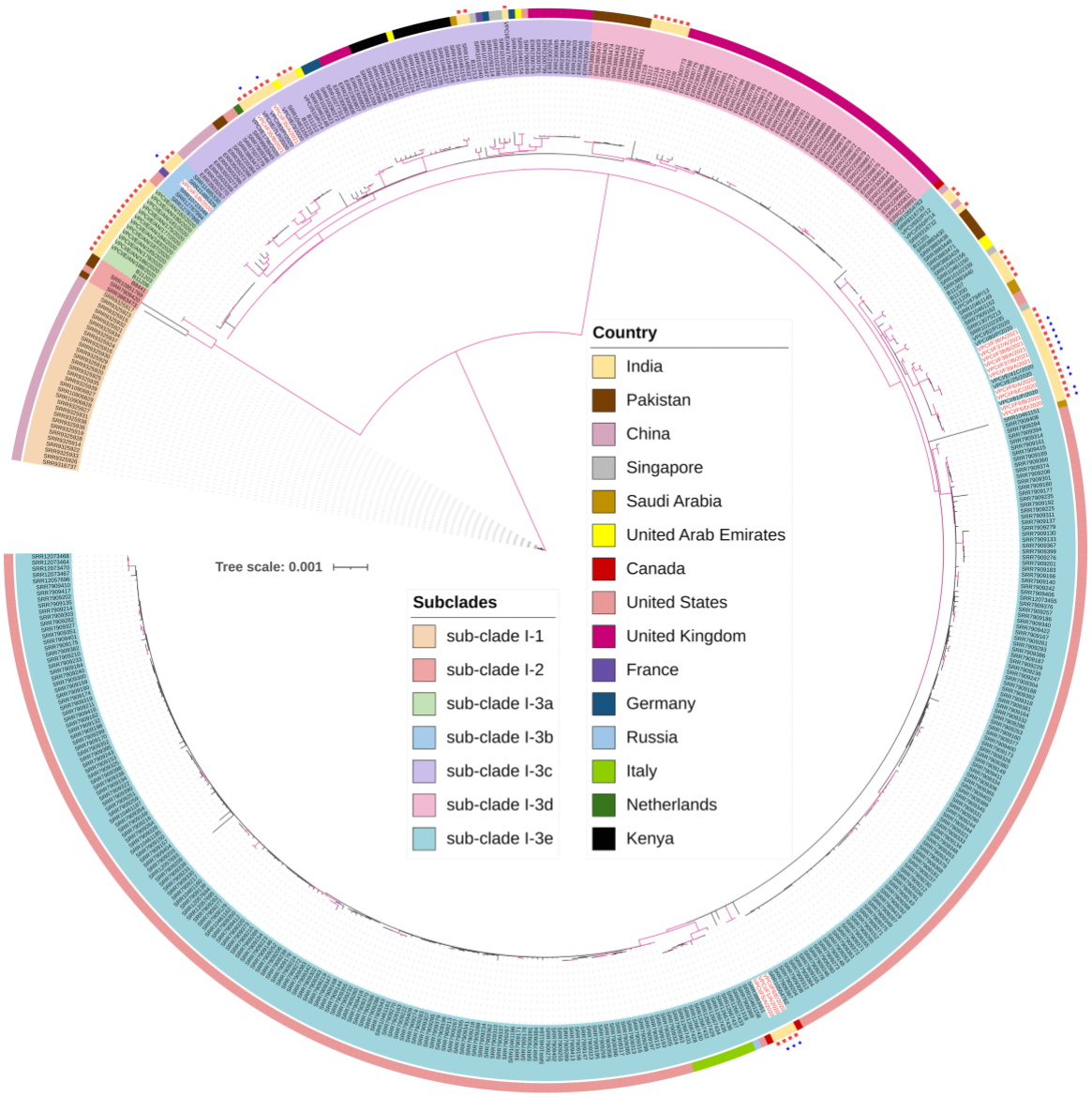

Figure 3. 3. Maximum likelihood phylogenetic tree showing the relationships among 503 clade I *Candida auris* isolates from around the globe. The isolates' relationships were inferred based on their whole-genome single nucleotide polymorphisms. Here, based on their branch lengths and bootstrap support values, the 503 isolates were further classified into 7 sub-clades, including three major sub-clades (sub-clade I-1, sub-clade I-2, and sub-clade I-3), with sub-clade I-3 containing five more recently derived ones (sub-clades I-3a, I-3b, I-3c, I-3d, and I-3e). Isolates within each sub-clade are highlighted with the same background color over the isolate identifications. The color strip outside of the isolate identification indicates the country of origin for each isolate. In addition, isolates from India are highlighted with red squares. Furthermore, the isolates from

apples in India are marked with blue stars, placed adjacent to their red square labels. Branch lengths are proportional to the amount of SNP differences among strains. Branches in magenta have a bootstrap support above 75%.

Genetically similar *C. auris* strains on different varieties of apples procured from various sources. Genetically identical strains (0 SNP) were observed on the surfaces of two groups of three apples each. One group included strains from apples F1, F5, and F6 (genotype cluster A). These three apples contained both varieties of apples tested, i.e., Red Delicious and Royal Gala, and they were procured from two different vendors separated by 30 km. The second group of genetically identical strains included those from apples F37, F38, and F39 (genotype cluster B). In addition, genotype cluster B also included a genetically highly similar strain from apple F36 (2 to 9 SNPs), and together these four apples (F36 to 39) including both apple varieties were procured from three geographically separated vendors. We note that Delhi and NCR vendors purchase fruits from the common National Fruit and Vegetable Market, one of the biggest wholesale fruit and vegetable markets in Asia, located in North Delhi.

Heterogenous population of clade I *C. auris* strains on the surface of individual apples. Interestingly, while several *C. auris* strains from different apples shared identical genotypes, we also observed that several apples contained strains of *C. auris* with different genotypes. Specifically, apple F6 harbored three genotypes belonging to two clusters which differed by as many as 59 SNPs. Similarly, the two strains from apple F1 differed by 107 SNPs. For the three apples (F35, F37, and F38) where two colonies each of *C. auris* were isolated, the pairs of strains differed by 1, 7, and 8 SNPs, respectively, for those from apples F35, F37, and F38. Together, the results here are consistent with the colonization of apples by genetically distinct strains as well as microevolution of the strains after their colonization on individual apples.

***Candida auris* strains on surfaces of apples are related to clinical strains.** Out of 16 CasSA, 6 from two apples (F6 and F35) fell into two genotype clusters, C and E, which included both clinical and fruit strains. In cluster C, four clonal CasSA (0 to 3 SNP difference) recovered from a single apple clustered with three clonal *C. auris* strains

recovered from a single hospitalized patient (VPCI/81/P/2020) and his inanimate hospital environment (0 to 3 SNP differences). Interestingly, both clinical and CasSA strains in cluster C were identical, with 0 to 3 SNP differences, consistent with their recent shared ancestry. Similarly, in genotype cluster E, two clonal CasSA (1 SNP difference) recovered from the surface of apple F35 were found to be highly related (0 to 3 SNP differences) with four clonal *C. auris* strains recovered from the ear of a patient (VPCI/83/P/2020) and his immediate inanimate environment. Together, these observations are consistent with the stored apples serving as a possible reservoir for transmission of *C. auris* strains among people and among ecological niches.

While genetically the closest clinical strains to the 16 CasSA strains were those reported from India, several strains from outside India also showed high similarities to some of the CasSA strains. For example, one strain from France was highly similar to fruit strain VPCI/F1/B/2020. Similarly, two strains from Canada showed high SNP similarities to genetic cluster A of the CasSA, comparable to the closest strain from India (Figure 3. 3).

Divergence time estimation of fruit isolates showed their emergence in the last 2 decades. The divergence time of the 16 CasSA from the other 43 Indian strains was inferred using evolutionary model and Markov Chain Monte Carlo (MCMC) analysis in BEAST v2.6.3 based on the concatenated sequences of only genes containing SNPs (Bouckaert et al., 2019). The specimen collection dates were used as the sampling dates and a strict molecular clock model, and an exponential prior distribution on the clock rate was applied. In addition, we adopted a general time reversible nucleotide substitution and coalescent exponential population model. The emerging dates of the fruit isolates were estimated by calculating time to the most recent common ancestor (TMRCA) of other Indian isolates. All 16 CasSA were grouped into five clusters (Figure 3. 4). Cluster A, consisting of three *C. auris* strains from three different apples with sample B11219, formed an outgroup of the cladogram including clusters B and C, and they diverged from the cladogram in 2005 (12.2 to 18.4, 95% highest posterior density [HPD]). Cluster B is the sister group to cluster C.

They diverged from each other in 2014 (4.7 to 8.4 years ago, 95% HPD). Cluster A and B11219 diverged from each other in 2006 (11.3 to 17.4, 95% HPD). Cluster E, containing two CasSA and 4 Indian clinical samples, recently emerged and formed a bigger cladogram around 2018 (1.8 to 3.4, 95% HPD), which is the outgroup for other 10 Indian clinical samples and one environment sample from Andaman Islands. The estimate divergence time of the 11 samples and the outgroup is around 2005 (12.6 to 19.6, 95% HPD). Cluster D contained a single strain, VPCI/F1/B/2021, and diverged earlier than other fruit isolates, around 2002 (14.9 to 24.2, 95% HPD). The TMRCA frame of 2002 to 2005 overlaps the rise in health care antibiotic consumption in India starting around 2004 to 2006 (Klein et al., 2018).

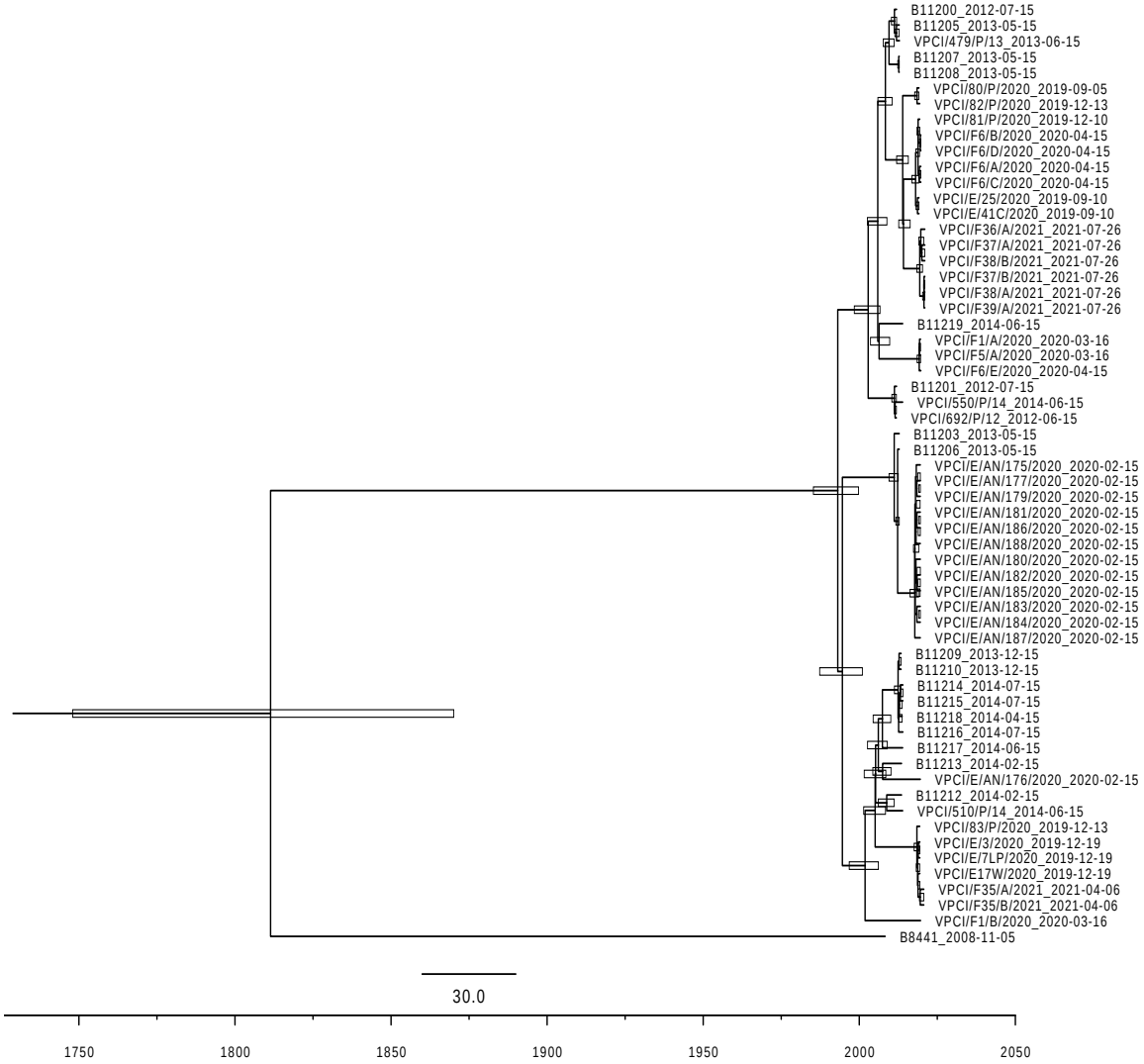

Figure 3. 4. Maximum clade credibility phylogenetic tree of 16 CasSA isolated in the present study, and 43 previously published Indian *C. auris* strains from both clinical and natural marine environment along with clade I reference strain B8441.

Genetic determinants of azole resistance in CasSA. Interestingly, CasSA showed similar genetic determinants of antifungal resistance as previously reported in clinical *C. auris* strains. CasSA strains showed amino acid substitutions K143R (n = 13) or Y132F (n = 3) in the azole target *ERG11* gene along with amino acid substitution V704L (n = 13) or E709D (n = 3) in CDR1 gene (Chowdhary et al., 2018). In the zinc-cluster transcription factor *TAC1B,* amino acid substitution A640V was observed (Rybak et al., 2020). In

addition, two CasSA (VPCI/F35/A/2021, VPCI/F35/B/2021) obtained from the same apple showed an amino acid substitution, G145D, in the *YMC1* gene. These two isolates clustered in the phylogenetic tree (Figure 3. 2) with clinical *C. auris* isolates that also had the same substitution (Yadav et al., 2021). YMCI is associated with several transmembrane transporter activities and is essential in mitochondrial transport as well as important for glutamate metabolism in Baker's yeast *Saccharomyces cerevisiae* (Trotter et al., 2005).

Cuticular wax components of *C. auris*-positive and -negative apples. A total of five apples were investigated by GC-MS for their surface wax components, including two *C. auris*-positive apples and three *C. auris*-negative apples (two freshly picked apples from organic orchards and one stored apple). No specific wax component was present in *C. auris*-colonized versus non-*C. auris*-colonized apples. Further, natural or synthetic wax components could not be differentiated in stored versus freshly picked apples due to the presence of similar components in the natural and artificial wax. Among fatty acids, palmitic acid (C16:0) was detected in all five apples. Overall, a total of 41 aliphatic components were identified in all apples (see supplemental material, Table 3. S2).

Metabarcoding analyses of fungal communities on the surface of apples from nonorganic orchards. As stated above, we were unable to obtain a single *C. auris* colony from 20 freshly picked apples. However, the lack of success in isolating *C. auris* could be due to the low population density and/or low viability of *C. auris* on the surfaces of those freshly picked apples. To investigate this possibility, we directly analyzed the fungal communities on the surfaces of two apples using the culture-independent metagenome barcoding approach based on the internal transcribed spacer 1 (ITS1) sequences (Shen et al., 2018). Overall, the results were consistent with the culture results in that no ITS1 sequence matched that of *C. auris* from either apple. In addition, similar to culture results, several *Candida* species were detected, including *C. orthopsilosis*, *C. albicans*, *C. glabrata*, and *C. krusei* (*Pichia kudriavzevii*). The detailed fungal species distributions obtained from these two apples are given in the supplemental material (Tables S3 and S4).

3.3 Discussion

Our results demonstrate that the surfaces of stored apples represent a novel reservoir of transmission of *C. auris* and show unequivocally that some of the strains from stored apples belong to the same clonal groups as clinical isolates from India. In addition, high levels of antifungal resistance are common among these environmental isolates from apples. The results expand our understanding of the ecology of *C. auris* and should help develop a better strategy to minimize the spread of this multidrug-resistant fungal pathogen. The successful isolation of *C. auris* from apple surfaces is not surprising. Ecologically, yeasts are broadly distributed. *Candida auris* belongs to the *Clavispora* clade of the Metschnikowiaceae family, a group of yeasts isolated principally from nonhuman sources such as plants (both living and dead) and marine environments (Arora et al., 2021; Jackson et al., 2019). Previous studies have shown that several *Metschnikowia* spp., including *Metschnikowia pulcherrima*, *Metschnikowia sinensis*, and *Metschnikowia fructicola*, and *Candida pruni* of the *Clavispora* clade are commonly associated with fruits (Kurtzman and Droby 2001; Zhang et al., 2014). For example, both *M. pulcherrima* and *M. sinensis* have been isolated from apples (Settier-Ramírez et al., 2021). Interestingly, most of these isolations have come from Southeast Asia, in the tropical environments. Specifically, together with results from our previous report on the isolation of *C. auris* from the salt marsh with extensive vegetation, plants in tropical marine wetlands could represent a significant source of *C. auris* as originally proposed by Casadevall et al. (2019; 2021).

The present study further documents the occurrence of *C. auris* isolates with reduced sensitivity to major DMI fungicides on the surface of apples. As expected, a broad range of fungicides were detected in the screened apples, including three triazole DMIs, namely, tebuconazole, difenoconazole, and flusilazole. DMIs share molecular structure characteristics to medical triazoles, and in the agriculture settings, these fungicides have been proposed as a selective force for cross-resistance to medical azoles in human-pathogenic fungi such as *Aspergillus fumigatus* (Bastos et al., 2021). Indeed, previous

studies have shown that cross-resistance to medical triazoles can also be achieved in vitro by exposing yeasts to agriculture azoles. For example, a recent report demonstrated that strains of the *C. parapsilosis* species complex exposed to DMIs (tebuconazole and tetraconazole) for 15 days developed reduced fluconazole susceptibility (Brilhante et al., 2019). Similarly, exposure of *C. parapsilosis* to tetraconazole, an agriculture triazole, led to decreased susceptibility to three medical triazoles, i.e., fluconazole, itraconazole, and voriconazole (Rocha et al., 2016). *Candida auris* strains in the present study exhibited fluconazole resistance as well as high MICs toward voriconazole. We believe that the azole fungicides on the surface of apples have likely contributed to the observed high triazole MICs in these *C. auris* strains. Indeed, large amounts of fungicides are used worldwide in apple cultivation to control fungal diseases on apples, such as apple scab caused by filamentous fungus *Venturia inaequalis*. A recent study reported that a long-term fungicide use led to decreased sensitivity of *V. inaequalis* strains to multiple fungicides, including DMIs, in field conditions (Polat and Bayraktar, 2021). In the present study, all *C. auris* strains excepting one from apples showed resistance to three triazole fungicides (DMIs), i.e., tebuconazole (GM MIC of 45.25 mg/L), bromuconazole (GM MIC of 13.45 mg/L), and flusilazole (GM MIC of 6.72 mg/L). Our findings suggest that *C. auris* in the natural ecosystem may come in contact with agriculture fungicides and fruits may be a potentially significant niche for the development of azole resistance in *C. auris* (Figure 3. 5).

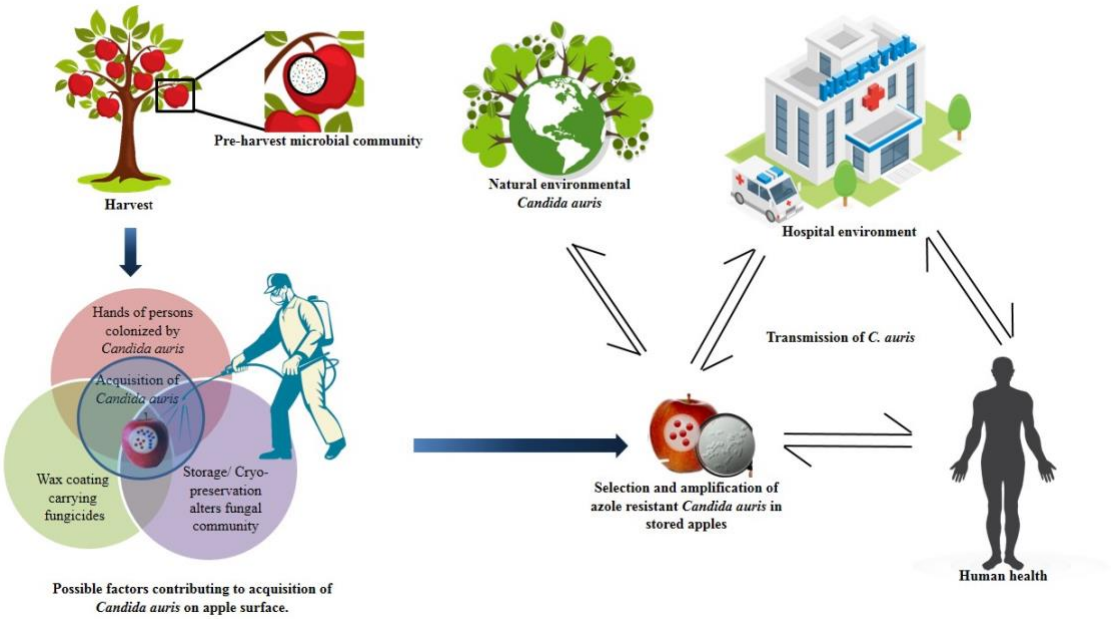

Figure 3. 5. Schematic representation of stored apples as a possible reservoir of selection and transmission of azole resistant *C. auris*.

This study observed that 13% (n = 8/62) of the apples were positive for *C. auris*, yielding a total of 16 *C. auris* strains from surfaces of eight apples. Genomic analyses revealed both genetically distinct strains and closely related clonal clusters, with some of the clonal genotype clusters consisting of strains from different apples, including apples of different varieties and/or from different vendors. The results suggest that either the *C. auris* strains were from the common wholesale fruit market in Delhi and NCR or that long-distance strain dispersal is common for this species in this geographic region. Interestingly, *C. auris* was recovered only from stored apples, and none of the freshly harvested apples collected from conventional and organic farms was positive for *C. auris*. In fact, the metabarcoding (microbiome) analysis of fresh apples showed negative results for *C. auris*. Thus, the most likely hypothesis about the origin of *C. auris* on the surface of stored apples is the contamination of apples by fingers and palms of humans who were colonized with *C. auris* during the postharvest treatment and storage and through the distribution chain. However, the genetic uniqueness of many of the strains suggests that there were likely multiple

sources of *C. auris* contamination on the stored apples. Further, it is important to emphasize that in the stored apples the fungal diversity is likely prone to change over time (Abdelfattah et al., 2016). Indeed, the composition of the postharvest microbiome of apples is known to be affected by bacterial and fungal communities present in packing houses where fruits are processed for market and storage after harvest (Abdelfattah et al., 2016). For example, a high prevalence of medically important yeast genera (*Malassezia*, Candida, and *Trichosporon*) associated with human infections was observed on Red Delicious apples sampled from a local supermarket in West Virginia, United States, but the source of these genera from handling prior to or after arriving at the supermarket could not be determined (Abdelfattah et al., 2016). It should be noted that only a small number of freshly harvested apples were screened in the present study and our understanding of the natural microbiota of our apple cultivars in India is very limited. As a result, it is difficult to interpret if the surface of stored apples represents a significant reservoir of *C. auris*. In addition, we were unable to identify the source of *C. auris* from handling prior to our purchase from the local vendors. It is plausible that multiple practices, like cryopreservation and wax coating with additional fungicides during the storage of apples, may alter the myco-flora of apples' surfaces. Subsequently, *C. auris* could be amplified under the directional selection pressure of fungicides. Interestingly, in four of the eight apples, *C. auris* was the only observed yeast, suggesting a potential competitive dominance of *C. auris* over other yeasts on the surfaces of apples. Indeed, on human skin, commensal Malassezia-dominated communities were replaced by communities dominated by *C. auris* soon after the invasion by *C. auris*, including a significant reduction of other *Candida* species (Proctor et al., 2021).

Common practices used to maintain quality and increase shelf life of stored apples include precooling, washing, sanitizing, and waxing. With these treatments, apples can be stored for 6 to 12 months at low temperatures (1 to 2°C) before distribution. These procedures can affect the natural protective wax layer that covers a fruit's surface (Abdelfattah et al., 2020). Therefore, it is a common practice to apply a thin layer of edible wax, consisting of esters of a higher fatty acid with monohydric alcohols, hydrocarbons, and free fatty acids, to serve

the same function as natural wax, i.e., covering fruit injuries, reducing water loss, and adding a shine/gloss to the fruit surface (Abdelfattah et al., 2020). Interestingly, East Asian, and Iranian clades of *C. auris* are found almost exclusively in the internal ear canal, which also contains natural ear wax (Trotter et al., 2005). *Candida auris* association with natural wax components may explain the presence of this yeast in waxed/stored apples. In fact, linoleic acid, oleic acid, palmitic acid, and stearic acid are the major free fatty acids which are common in both ear wax and apple cuticular wax (Iwasaki et al., 2011; Zhang et al., 2020).

In addition, wax has been used as a carrier of fungicides and no significant change in the amount of fungicide residues was observed during a 40-day storage of waxed apples under ambient conditions (Jiang et al. 2019). In the present study, in stored apples 12 different fungicides were detected, whereas freshly picked nonorganic apples had 4 types of fungicides. The additional classes of fungicides on stored apples were likely added during postharvest treatments of the stored apples. These additional fungicides on stored apples could act as strong selective forces for multidrug-resistant species such as *C. auris*.

CasSA strains showed substantial genetic diversity and broad phylogenetic distribution among the subclades within clade I. Interestingly, these fruit strains had closely related strains from other ecological niches in India, including those from patients, hospital environments, and marine environments. However, strains from other parts of the world that are genetically similar to the Indian fruit strains have also been found, including one from France and two from Canada. Interestingly, the French strain (CNRMA15-337; SRR10723348) was from a patient on Reunion Island in the Indian Ocean and who had travel history to India (Chow et al., 2020; Levy et al., 2020). Similarly, of the two strains from Canada that showed close relationships to three fruit strains (VPCI/F1/A/2020, VPCI/F5/A/2020, and VPCI/F6/E/2020), one (strain CNISP2, i.e., SRR10554762) was from a patient who was previously hospitalized in India (Garcia-Jeldes et al., 2020), while no demographic information is available for the other strain, B13464 (i.e., SRR10461158)

(Chow et al., 2020). Together, these results suggest that stored apples could be a source of transmission of *C. auris* in health care settings. Indeed, more extensive sampling of other stored fruits and from other geographic and ecological niches could reveal additional strains showing close relationships among the ecological niches.

Aside from *C. auris*, this study also revealed other pathogenic *Candida* spp. such as C. guilliermondii (27%), *C. parapsilosis* (23%), and *C. tropicalis* (19%), on the surfaces of fruits. Indeed, among the 22 yeast species isolated from fruits, 12 are known to be capable of causing invasive fungal infections. A recent report showed that *Candida blankii* caused an outbreak of nosocomial fungemia in a neonatal intensive care unit in India (Chowdhary et al., 2020). At present, the source(s) of the pathogen for the outbreak is not known. However, the isolation of *C. blankii* from apple surface suggests that apples could serve as a contact point for transmission of this yeast to patients. Detailed genotypic analyses of strains from diverse sources are needed in order to identify the potential sources for this and other outbreaks.

This study expands our understanding of *C. auris* ecological niches and will serve as a resource for future studies exploring this yeast in natural environments. Our study revealed that the ecology of *C. auris* is likely more complex and diverse than what is known so far. In addition, our study suggested that fungicide application on stored apples and potentially other fruits could be a significant selective force for drug resistance in clinics. Together, the information generated here could guide future epidemiological studies of *C. auris* in other parts of the world and help design better management and control strategies against this important fungal pathogen.

3.4 Materials and Methods

Isolation and identification of yeasts from fruits. A total of 84 fruits were processed within a day of receiving. Briefly, sterile swabs were swept over the epicarp of fruits and

inoculated on Sabouraud dextrose agar with chloramphenicol and gentamicin (SDA-CG) plates, on CHROMagar *Candida* (Becton, Dickinson, Baltimore, MD, USA), and in yeast nitrogen broth (YNB) (Lo et al., 2017; Yadav et al., 2021) and incubated at 37°C. Also, a small piece of flesh without epicarp was cut and homogenized in saline. Four hundred microliters of suspension was inoculated on SDA-CG, on CHROMagar *Candida*, and in YNB (Glushakova, Microbiology, and 2017 2017; Yadav et al., 2021). Identification of yeast colonies was done by matrix-assisted laser desorption ionization-time of flight mass spectrometry (MALDI-TOF MS; Bruker Biotyper OC version 3.1, Daltonics, Bremen, Germany) and internal transcribed spacer region (ITS) sequencing (Yadav et al., 2021).

Detection of fungicides in the apples using GC-MS and LC-MS/MS. Extraction and cleanup of unpeeled whole apples were done as recommended by pesticide residue analysis manual 2007, ICAR (Sharma and others 2007). Briefly, gas chromatograph (Nexis 2030, Shimadzu, Japan) with mass selective triple quadruple detector (GC-MS/MS TQ 8040 NX, M/s Shimadzu, Japan) and liquid chromatography (Aquity UPLC, Waters Corporation, USA) fitted with mass detector (AB 3200, AB Sciex, USA) was used for analysis. For separation of analytes through GC-MS and LC-MS/MS, SH-Rxi-5Sil MS and Chromolith RP-18 columns were used, respectively (Tripathy et al., 2021).

Morphological characterization of *Candida auris*. CasSA and reference B8441 strains were subcultured on SDA, yeast peptone dextrose agar (YPD), and rice Tween agar and incubated at 28°C, 37°C, and 42°C for 5 days. Cells were monitored under optical microscope (Nikon H600L, Japan) at ×40 magnification.

Growth kinetics. For calcofluor white (CFW) susceptibility and salt tolerance testing, all CasSA along with B8441 were grown at 5 mg/L to 2,560 mg/L concentrations of CFW and 10% of sodium chloride (NaCl). Growth turbidity was measured by microplate reader (Infinite 200 Pro, Tecan, Switzerland) at 37°C for 24 has described previously (Arora et al.,

2021). Also, growth at 37°C and 42°C for 48 h was checked as detailed previously (Arora et al., 2021).

Determination of ploidy of *C. auris* strains. Two CasSA strains along with clade I reference strains (B11098 and B8441) and *Candida glabrata* (ATCC 15545) were subjected to fluorescence-activated cell sorting (FACS; FACSAria III, BD Biosciences, USA). Sample preparation and analysis were done as recommended by Todd et al., (2018). Flowjo 7.8 software was used to interpret the FACS results.

Antifungal susceptibility testing against medical antifungals and agriculture azoles. Antifungal susceptibility testing (AFST) was performed using the CLSI broth microdilution method (BMD), following M27-A3 (Rex et al., 2008). AFST for 10 antifungals was performed as described previously (Chowdhary et al., 2018). Agriculture triazole fungicides tested were tebuconazole (TEB), epoxiconazole (EPX) propiconazole (PCZ), bromuconazole (BRO), flusilazole (FLU), and two diazoles, namely, pyraclostrobin (PCL) and carbendazim (CBZ). All agriculture azoles were procured from Sigma (St. Louis, MO, USA), and dilutions for TEB, EPX, PCZ, PCL, BRO, and CBZ were 0.25 to 128 mg/L and 0.125 to 64 mg/L for FLU. *Candida krusei* ATCC 6258 and *Candida parapsilosis* ATCC 22019 were used as quality control strains. All statistical parameters were calculated by using Prism version 6.00 (GraphPad Software).

Genome sequencing. DNA extraction was done by QIAamp DNA minikit as described previously (Arora et al., 2021; Yadav et al., 2021). Whole-genome sequencing (WGS) libraries were prepared using NEBNext ultra II DNA FS kit (New England Biolabs, Ipswich, MA, USA) and sequenced on Illumina HiSeq 4000.

Variant identification and phylogenetic analysis. For phylogenetic analysis, genomes of 42 previously published Indian strains, comprising 24 clinical strains, 5 strains from hospital environments, and 13 marine environmental strains from Andaman Islands, India

(Arora et al., 2021; Lockhart et al., 2017; Yadav et al., 2021), were retrieved for comparison along with B8441, the clade I reference strain. All strains were subjected to NASP pipeline for genome sequencing analysis. First, raw reads with average quality value of 5 bp window lower than 20 or length shorter than 80 were removed using Trimmomatic v.0. Then, the filtered reads were mapped to reference genome B8441 using BWA mem v0.7 and variants were identified using GenomeAnalysisTK v2.7.4 (Arora et al., 2021; Satoh et al., 2009). Afterwards, single nucleotide polymorphisms (SNPs) were filtered out if they were in reference genome duplicated regions, failed the minimum coverage threshold of 10, or had less than 90% of the reads supporting the call. The phylogenetic tree was constructed using RAxML v8.0.25 (Stamatakis 2014) under ASC_GTRCAT nucleotide substitution model and 1,000 bootstrap replicates. After we removed SNP sites that had ambiguous calls in over 0.5% of the samples, 1,281 SNP sites remained among the Indian samples and were concatenated. Additional phylogenetic analysis used B8441 as reference and includes 16 fruit isolates as well as 487 previously reported clade I *C. auris* samples. In this broad analysis, SNP sites with ambiguous calls in over 0.5% of the samples were removed and the remaining SNPs were concatenated for each sample. Maximum-likelihood phylogeny was constructed using RAxML-HPC2 on XSEDE in the CIPRES Science Gateway (Miller et al., n.d.). The tree uses the ASC_GTRCAT nucleotide substitution model and 1,000 bootstrap iterations and was visualized with iTOL (Letunic and Bork 2021).

Divergence time estimation of fruit isolates. The sequences of genes that contain SNPs in any of the 59 samples (43 previously published genomes and 16 CasSA) were concatenated and aligned as one partition. The length of MCMC chain was set to 100 million steps, and samples were recorded every 5,000 steps. Tracer v.1.7.1 was used to investigate MCMC convergence (Yadav et al., 2021). The MCMC chain converged with the effective sample sizes exceeded 700. A maximum clade credibility tree was generated by TreeAnnotator v1.8.4 after discarding 5% as burn-in and visualized in FigTree v1.4.4 (http://tree.bio.ed.ac.uk/software/figtree/). The emerging dates of the fruit isolates were estimated by calculating time to the most recent common ancestor of other Indian isolates.

Detection of cuticular wax components in apples using GC-MS/MS. A total of five apples, including two *C. auris*-positive and three *C. auris*-negative apples representing stored (n = 3) and freshly picked (n = 2) from organic orchards, were screened for wax profiling. Apple peel was removed and grounded and the extraction of organic components was done as described previously (Tripathy et al., 2021). For wax profiling, gas chromatography-tandem mass spectrometry (GC-MS/MS; Agilent 7890A, USA) with an HP-5 column coupled with an Agilent 7000 QQQ MS was used. Analysis of samples was done as recommended by Bhatnagar et al. (2019). Metabolite identification was done by comparing their mass spectra with those obtained from authentic samples and/or the NIST (National Institute of Standards and Technology, USA) mass spectral database using Mass-Hunter software (version B. 05.00).

Metagenomics. Peels were removed and placed in 0.05 M phosphate buffer (pH 6.8) for 30 min with shaking at 200 rpm. Peels were discarded and the solution was stored at −20°C until subsequent analysis. Microbial genomic DNA was extracted by using a column-based method with a QIAamp DNA minikit (Qiagen, Hilden, Germany) and quantified by QUBIT 3 Fluorometer using dS DNA HS dye. Primers ITS1 and ITS2 were used to amplify and sequence the ITS1 region. The processed paired-end reads were mapped using KMA (Clausen, Aarestrup, and Lund 2018). The KMA result file was subjected to metagenomic classification using CCmetagen v.1.2.5 and Kraken2 v.2.1.1, and the report was visualized using krona (CCMetagen-1.2) and Pavian (Breitwieser and Salzberg 2020; Marcelino et al., 2020; Wood and Salzberg 2014).

Data availability

The genome sequences of all 16 *C. auris* strains isolated in the present study from the surfaces of apples are accessible through BioProject number PRJNA809768.

3.5 Acknowledgments

We thank Sayed Shams Yazdani and Girish HR, Microbial Engineering Group, International Centre for Genetic Engineering and Biotechnology (ICGEB), New Delhi, India for providing the GC-MS/MS facilities and Dhiraj Kumar and Aditya Rathee, Cellular Immunology Group (ICGEB), New Delhi for providing assistance in FACS experiments. We thank Gulnaz Bashir, J&K, India and C.L. Dhingra, New Delhi for helping in collection of samples from apple orchards.

A.Y. acknowledges the University Grants Commission (file no. 16-9/2019) and 596/(CSIR-UGC NET JUNE 2019) Government of India (GoI), New Delhi, K.J. acknowledges the Council of Scientific & Industrial Research, GoI [(file no. 08/728(0001)/2019-EMR-I), and K.P. acknowledges the Department of Health and Research, GoI (file no. 12013/36/2020-HR/E) for grant of fellowships. This work was supported in part by a research grant from McMaster University Global Science Initiative (2020-03) to J.X.

All other authors declare no potential conflicts of interest. We alone are responsible for the content and writing of the paper.

A.Y., K.J., and K.P. contributed to sample collection and processing and conducted the experiments. Y.W. performed WGS analysis; K.K.S. and V.T. helped in experiment conduction and reviewed the manuscript; A.C. designed the study, analyzed the data, and drafted the manuscript; J.X. and A.S. analyzed the data and reviewed the manuscript; H.K. reviewed the manuscript. All authors have read and agreed to the final version of the manuscript.

3.6 Supplemental Material

Figure 3. S1 Histograms representing DNA content obtained by FACS. Panels B1 and 2 show haploid *C. auris* reference clade I strains (B11098, B8441). Panels C1 and 2 show

haploid *C. auris* strains on the surfaces of apples (CasSA). Panel A shows a haploid *C. glabrata* strain (ATCC 15545) for comparison, which was also analyzed. The x axis represents nuclear fluorescence, and the y axis represents cell number.
https://journals.asm.org/doi/suppl/10.1128/mbio.00518-22/suppl_file/mbio.00518-22-sf001.docx

Table 3. S1 Details of the 503 global isolates of *C. auris* (specimens, country of origin, and bio-project numbers) included for genomic analysis in the present study.
https://journals.asm.org/doi/suppl/10.1128/mbio.00518-22/suppl_file/mbio.00518-22-st001.xlsx

Table 3. S2 Characterization of aliphatic components in five apples, including two *C. auris*-positive and three *C. auris*-negative apples representing stored (n = 3) and freshly picked (n = 2) from organic orchards.
https://journals.asm.org/doi/suppl/10.1128/mbio.00518-22/suppl_file/mbio.00518-22-st002.docx

Table 3. S3 Taxonomic classification of fungal species detected from the surface of freshly picked apple 1 from organic orchards.
https://journals.asm.org/doi/suppl/10.1128/mbio.00518-22/suppl_file/mbio.00518-22-st003.docx

Table 3. S4
Taxonomic classification of fungal species detected from the surface of freshly picked apple 2 from organic orchards.
https://journals.asm.org/doi/suppl/10.1128/mbio.00518-22/suppl_file/mbio.00518-22-st004.docx

References

Abdelfattah, Ahmed, Susan R Whitehead, Dumitru Macarisin, Jia Liu, Erik Burchard, Shiri Freilich, Christopher Dardick, Samir Droby, and Michael Wisniewski. 2020. "Effect of Washing, Waxing and Low-Temperature Storage on the Postharvest Microbiome of Apple." *Mdpi.Com* 8: 944. https://doi.org/10.3390/microorganisms8060944.

Abdelfattah, Ahmed, Michael Wisniewski, Samir Droby, and Leonardo Schena. 2016. "Spatial and Compositional Variation in the Fungal Communities of Organic and Conventionally Grown Apple Fruit at the Consumer Point-of-Purchase." *Horticulture Research* 3 (October). https://doi.org/10.1038/HORTRES.2016.47.

Arora, Parth, Prerna Singh, Yue Wang, Anamika Yadav, Kalpana Pawar, Ashutosh Singh, Gadi Padmavati, Anuradha Chowdhary, and Jianping Xu. 2021. "Environmental Isolation of *Candida auris* from the Coastal Wetlands of Andaman Islands, India." *MBio* 12 (2): 1–9. https://doi.org/10.1128/MBIO.03181-20/SUPPL_FILE/MBIO.03181-20-ST001.DOC.

Bastos, Rafael W., Luana Rossato, Gustavo H. Goldman, and Daniel A. Santos. 2021. "Fungicide Effects on Human Fungal Pathogens: Cross-Resistance to Medical Drugs and Beyond." *PLoS Pathogens* 17 (12). https://doi.org/10.1371/JOURNAL.PPAT.1010073.

Bhatnagar, Vipul Swarup, Prasun Bandyopadhyay, Girish H. Rajacharya, Sharanya Sarkar, Krishna Mohan Poluri, and Shashi Kumar. 2019. "Amelioration of Biomass and Lipid in Marine Alga by an Endophytic Fungus *Piriformospora Indica*." *Biotechnology for Biofuels* 12 (1). https://doi.org/10.1186/S13068-019-1516-6.

Bouckaert, Remco, Timothy G. Vaughan, Joëlle Barido-Sottani, Sebastián Duchêne, Mathieu Fourment, Alexandra Gavryushkina, Joseph Heled, et al. 2019. "BEAST 2.5: An Advanced Software Platform for Bayesian Evolutionary Analysis." *PLoS Computational Biology* 15 (4). https://doi.org/10.1371/JOURNAL.PCBI.1006650.

Breitwieser, Florian P., and Steven L. Salzberg. 2020. "Pavian: Interactive Analysis of Metagenomics Data for Microbiome Studies and Pathogen Identification."

Bioinformatics (Oxford, England) 36 (4): 1303–4. https://doi.org/10.1093/BIOINFORMATICS/BTZ715.

Brilhante, Raimunda Sâmia Nogueira, Lucas Pereira de Alencar, Silviane Praciano Bandeira, Jamille Alencar Sales, Antônio José de Jesus Evangelista, Rosana Serpa, Rossana de Aguiar Cordeiro, et al. 2019. "Exposure of *Candida parapsilosis* Complex to Agricultural Azoles: An Overview of the Role of Environmental Determinants for the Development of Resistance." *The Science of the Total Environment* 650 (Pt 1): 1231–38. https://doi.org/10.1016/J.SCITOTENV.2018.09.096.

Casadevall, Arturo, Dimitrios P. Kontoyiannis, and Vincent Robert. 2019. "On the Emergence of *Candida auris*: Climate Change, Azoles, Swamps, and Birds." *MBio* 10 (4). https://doi.org/10.1128/MBIO.01397-19.

Casadevall, Arturo, Dimitrios P. Kontoyiannis, and Vincent Robert. 2021. "Environmental *Candida auris* and the Global Warming Emergence Hypothesis." *MBio* 12 (2): 1–3. https://doi.org/10.1128/MBIO.00360-21.

CDC. 2019. n.d. "Antibiotic Resistance Threats in the United States. CDC, U.S. Department of Health and Human Services, Atlanta, GA. U.S. Department of Health and Human Services, Atlanta, Georgia."

Chow, Nancy A., José F. Muñoz, Lalitha Gade, Elizabeth L. Berkow, Xiao Li, Rory M. Welsh, Kaitlin Forsberg, et al. 2020. "Tracing the Evolutionary History and Global Expansion of *Candida auris* Using Population Genomic Analyses." *MBio* 11 (2). https://doi.org/10.1128/MBIO.03364-19.

Chowdhary, A., J. B. Stielow, G. Upadhyaya, P. K. Singh, A. Singh, and J. F. Meis. 2020. "*Candida blankii*: An Emerging Yeast in an Outbreak of Fungaemia in Neonates in Delhi, India." *Clinical Microbiology and Infection : The Official Publication of the European Society of Clinical Microbiology and Infectious Diseases* 26 (5): 648.e5-648.e8. https://doi.org/10.1016/J.CMI.2020.01.001.

Chowdhary, Anuradha, Anupam Prakash, Cheshta Sharma, Milena Kordalewska, Anil Kumar, Smita Sarma, Bansidhar Tarai, et al. 2018. "A Multicentre Study of Antifungal Susceptibility Patterns among 350 *Candida auris* Isolates (2009-17) in India: Role of

the ERG11 and FKS1 Genes in Azole and Echinocandin Resistance." *The Journal of Antimicrobial Chemotherapy* 73 (4): 891–99. https://doi.org/10.1093/JAC/DKX480.

Chowdhary, Anuradha, Cheshta Sharma, and Jacques F. Meis. 2017. "*Candida auris*: A Rapidly Emerging Cause of Hospital-Acquired Multidrug-Resistant Fungal Infections Globally." *PLoS Pathogens* 13 (5). https://doi.org/10.1371/JOURNAL.PPAT.1006290.

Clausen, Philip T.L.C., Frank M. Aarestrup, and Ole Lund. 2018. "Rapid and Precise Alignment of Raw Reads against Redundant Databases with KMA." *BMC Bioinformatics* 19 (1). https://doi.org/10.1186/S12859-018-2336-6.

Garcia-Jeldes, Hector Felipe, Robyn Mitchell, Allison McGeer, Wallis Rudnick, Kanchana Amaratunga, Snigdha Vallabhaneni, Shawn R. Lockhart, et al. 2020. "Prevalence of *Candida auris* in Canadian Acute Care Hospitals among at-Risk Patients, 2018." *Antimicrobial Resistance and Infection Control* 9 (1). https://doi.org/10.1186/S13756-020-00752-3.

Iwasaki, S, H Suzuki, H Moteki, Y Takumi, and S Usami. 2011. "Analysis of Fatty Acids from Wet and Dry Ear Wax Samples." *Jibi to Rinsho* 57: 35–41.

Jackson, Brendan R, Nancy Chow, Kaitlin Forsberg, Anastasia P Litvintseva, Shawn R Lockhart, Rory Welsh, Snigdha Vallabhaneni, and Tom Chiller. 2019. "On the Origins of a Species: What Might Explain the Rise of *Candida auris*?" *Mdpi.Com*. https://doi.org/10.3390/jof5030058.

Jiang, Wenqing, Xiaochu Chen, Fengmao Liu, and Canping Pan. 2019. "Residue Distribution, Dissipation Behavior, and Removal of Four Fungicide Residues on Harvested Apple after Waxing Treatment." *Journal of Agricultural and Food Chemistry* 67 (8): 2307–12. https://doi.org/10.1021/ACS.JAFC.8B06254.

Klein, Eili Y., Thomas P. Van Boeckel, Elena M. Martinez, Suraj Pant, Sumanth Gandra, Simon A. Levin, Herman Goossens, and Ramanan Laxminarayan. 2018. "Global Increase and Geographic Convergence in Antibiotic Consumption between 2000 and 2015." *Proceedings of the National Academy of Sciences of the United States of America* 115 (15): E3463–70. https://doi.org/10.1073/PNAS.1717295115.

Kurtzman, Cletus P., and Samir Droby. 2001. "Metschnikowia Fructicola, a New Ascosporic Yeast with Potential for Biocontrol of Postharvest Fruit Rots." *Systematic and Applied Microbiology* 24 (3): 395–99. https://doi.org/10.1078/0723-2020-00045.

Letunic, Ivica, and Peer Bork. 2021. "Interactive Tree Of Life (ITOL) v5: An Online Tool for Phylogenetic Tree Display and Annotation." *Nucleic Acids Research* 49 (W1): W293–96. https://doi.org/10.1093/NAR/GKAB301.

Levy, Yaël, Guillaume Miltgen, Alexandra Rousseau, Nathalie Lugagne, Laura Teysseyre, Nicolas Traversier, Marie Desnos-Ollivier, Nicolas Allou, and Jérôme Allyn. 2020. "Case Report: Emergence of *Candida auris* in the Indian Ocean Region." *The American Journal of Tropical Medicine and Hygiene* 104 (2): 739–43. https://doi.org/10.4269/AJTMH.20-0758.

Lo, Hsiu Jung, Sheng Hua Tsai, Wen Li Chu, Yin Zhi Chen, Zi Li Zhou, Hong Fu Chen, Ching Fu Lee, and Yun Liang Yang. 2017. "Fruits as the Vehicle of Drug Resistant Pathogenic Yeasts." *The Journal of Infection* 75 (3): 254–62. https://doi.org/10.1016/J.JINF.2017.06.005.

Lockhart, Shawn R., Kizee A. Etienne, Snigdha Vallabhaneni, Joveria Farooqi, Anuradha Chowdhary, Nelesh P. Govender, Arnaldo Lopes Colombo, et al. 2017. "Simultaneous Emergence of Multidrug-Resistant *Candida auris* on 3 Continents Confirmed by Whole-Genome Sequencing and Epidemiological Analyses." *Clinical Infectious Diseases : An Official Publication of the Infectious Diseases Society of America* 64 (2): 134–40. https://doi.org/10.1093/CID/CIW691.

Marcelino, Vanessa R., Philip T.L.C. Clausen, Jan P. Buchmann, Michelle Wille, Jonathan R. Iredell, Wieland Meyer, Ole Lund, Tania C. Sorrell, and Edward C. Holmes. 2020. "CCMetagen: Comprehensive and Accurate Identification of Eukaryotes and Prokaryotes in Metagenomic Data." *Genome Biology* 21 (1). https://doi.org/10.1186/S13059-020-02014-2.

Miller, MA, W Pfeiffer, T Schwartz - 2010 gateway computing, and undefined 2010. n.d. "Creating the CIPRES Science Gateway for Inference of Large Phylogenetic Trees."

Ieeexplore.Ieee.Org. Accessed June 24, 2023. https://ieeexplore.ieee.org/abstract/document/5676129/.

Opulente, Dana A., Quinn K. Langdon, Kelly V. Buh, Max A.B. Haase, Kayla Sylvester, Ryan V. Moriarty, Martin Jarzyna, Samantha L. Considine, Rachel M. Schneider, and Chris Todd Hittinger. 2019. "Pathogenic Budding Yeasts Isolated Outside of Clinical Settings." *FEMS Yeast Research* 19 (3). https://doi.org/10.1093/FEMSYR/FOZ032.

Polat, Z, H Bayraktar - Journal of Phytopathology, and undefined 2021. 2021. "Resistance of *Venturia Inaequalis* to Multiple Fungicides in Turkish Apple Orchards." *Wiley Online Library* 169 (6): 360–68. https://doi.org/10.1111/jph.12990.

Proctor, Diana M., Thelma Dangana, D. Joseph Sexton, Christine Fukuda, Rachel D. Yelin, Mary Stanley, Pamela B. Bell, et al. 2021. "Integrated Genomic, Epidemiologic Investigation of *Candida auris* Skin Colonization in a Skilled Nursing Facility." *Nature Medicine* 27 (8): 1401–9. https://doi.org/10.1038/S41591-021-01383-W.

Rex, John H., xxx, xx xx, xx xx, and xx xx. 2008. "Reference Method for Broth Dilution Antifungal Susceptibility Testing of Yeasts : Approved Standard." *Clinical and Laboratory Standards Institute, M27-A3* 28 (14). https://cir.nii.ac.jp/crid/1130282271681047296.

Rocha, Marcos Fábio Gadelha, L. P. Alencar, M. A.N. Paiva, Luciana Magalhães Melo, Silviane Praciano Bandeira, Y. B. Ponte, Jamille Alencar Sales, et al. 2016. "Cross-Resistance to Fluconazole Induced by Exposure to the Agricultural Azole Tetraconazole: An Environmental Resistance School?" *Mycoses* 59 (5): 281–90. https://doi.org/10.1111/MYC.12457.

Rybak, Jeffrey M., José F. Muñoz, Katherine S. Barker, Josie E. Parker, Brooke D. Esquivel, Elizabeth L. Berkow, Shawn R. Lockhart, et al. 2020. "Mutations in TAC1B: A Novel Genetic Determinant of Clinical Fluconazole Resistance in *Candida auris*." *MBio* 11 (3). https://doi.org/10.1128/MBIO.00365-20.

Sahl, Jason W., Darrin Lemmer, Jason Travis, James M. Schupp, John D. Gillece, Maliha Aziz, Elizabeth M. Driebe, et al. 2016. "NASP: An Accurate, Rapid Method for the Identification of SNPs in WGS Datasets That Supports Flexible Input and Output

Formats." *Microbial Genomics* 2 (8): e000074. https://doi.org/10.1099/MGEN.0.000074.

Samarasinghe, Himeshi, Yi Lu, Renad Aljohani, Ahmad Al-Amad, Heather Yoell, and Jianping Xu. 2021. "Global Patterns in Culturable Soil Yeast Diversity." *IScience* 24 (10). https://doi.org/10.1016/J.ISCI.2021.103098.

Satoh, Kazuo, Koichi Makimura, Yayoi Hasumi, Yayoi Nishiyama, Katsuhisa Uchida, and Hideyo Yamaguchi. 2009. "*Candida auris* Sp. Nov., a Novel Ascomycetous Yeast Isolated from the External Ear Canal of an Inpatient in a Japanese Hospital." *Microbiology and Immunology* 53 (1): 41–44. https://doi.org/10.1111/J.1348-0421.2008.00083.X.

Settier-Ramírez, Laura, Gracia López-Carballo, Pilar Hernández-Muñoz, Angélique Fontana, Caroline Strub, and Sabine Schorr-Galindo. 2021. "New Isolated *Metschnikowia Pulcherrima* Strains from Apples for Postharvest Biocontrol of Penicillium Expansum and Patulin Accumulation." *Toxins* 13 (6). https://doi.org/10.3390/TOXINS13060397.

Sharma, Krishan Kumar, and others. 2007. "Pesticide Residue Analysis Manual." *Directorate of Information and Publications of Agriculture, New Delhi, Inida*. https://agris.fao.org/agris-search/search.do?recordID=US201300127990.

Shen, Youming, Jiyun Nie, Zhixia Li, Haifei Li, Yonglong Wu, Yafeng Dong, and Jianyi Zhang. 2018. "Differentiated Surface Fungal Communities at Point of Harvest on Apple Fruits from Rural and Peri-Urban Orchards." *Scientific Reports* 8 (1). https://doi.org/10.1038/S41598-017-17436-5.

Stamatakis, Alexandros. 2014. "RAxML Version 8: A Tool for Phylogenetic Analysis and Post-Analysis of Large Phylogenies." *Bioinformatics (Oxford, England)* 30 (9): 1312–13. https://doi.org/10.1093/BIOINFORMATICS/BTU033.

Todd, Robert T., Ann L. Braverman, and Anna Selmecki. 2018. "Flow Cytometry Analysis of Fungal Ploidy." *Current Protocols in Microbiology* 50 (1). https://doi.org/10.1002/CPMC.58.

Tripathy, Vandana, Krishan Kumar Sharma, Thomas George, Chidanand Shiveshankar Patil, Yogesh Subhash Saindane, Soudamini Mohapatra, Lekha Siddamallaiah, et al. 2021. "Dissipation Kinetics and Risk Assessment of Iprovalicarb + Propineb Fungicide in Tomato under Different Agroclimates." *Environmental Science and Pollution Research International* 28 (24): 31909–19. https://doi.org/10.1007/S11356-021-12919-5.

Trotter, Pamela J., Amy L. Adamson, Angela C. Ghrist, Lindsay Rowe, Lori R. Scott, Matthew P. Sherman, Nicole C. Stites, et al. 2005. "Mitochondrial Transporters Involved in Oleic Acid Utilization and Glutamate Metabolism in Yeast." *Archives of Biochemistry and Biophysics* 442 (1): 21–32. https://doi.org/10.1016/J.ABB.2005.07.016.

Wood, Derrick E., and Steven L. Salzberg. 2014. "Kraken: Ultrafast Metagenomic Sequence Classification Using Exact Alignments." *Genome Biology* 15 (3). https://doi.org/10.1186/GB-2014-15-3-R46.

Yadav, Anamika, Anubhav Singh, Yue Wang, Merlijn Hi Van Haren, Ashutosh Singh, Theun De Groot, Jacques F. Meis, Jianping Xu, and Anuradha Chowdhary. 2021. "Colonisation and Transmission Dynamics of *Candida auris* among Chronic Respiratory Diseases Patients Hospitalised in a Chest Hospital, Delhi, India: A Comparative Analysis of Whole Genome Sequencing and Microsatellite Typing." *Journal of Fungi* 7 (2): 81. https://doi.org/10.3390/JOF7020081.

Zhang, Dian Peng, Cai Ge Lu, Tao Tao Zhang, Davide Spadaro, De Wen Liu, and Wei Cheng Liu. 2014. "*Candida pruni* Sp. Nov. Is a New Yeast Species with Antagonistic Potential against Brown Rot of Peaches." *Archives of Microbiology* 196 (7): 525–30. https://doi.org/10.1007/S00203-014-0999-6.

Zhang, Ya Li, Chun Xiang You, Yuan Yuan Li, and Yu Jin Hao. 2020. "Advances in Biosynthesis, Regulation, and Function of Apple Cuticular Wax." *Frontiers in Plant Science* 11 (August). https://doi.org/10.3389/FPLS.2020.01165.

Chapter 4

Candida auris in Dog Ears

Abstract: *Candida auris* is an emerging global public health threat and is resistant to most anti-fungal agents. Though fungi are significant pathogens for animals, the role of *C. auris* in animal health remains unexplored. Here, we analysed the microbial cultures of skin and ear swabs of 87 dogs in Delhi and performed fungal meta-barcode sequencing of ear and skin samples of 7 dogs with confirmed otitis externa (OE). Overall, 4.5% of dogs (4/87) with chronic skin infections contained evidence of *C. auris* in their ear canal (n = 3) and on their skin surface (n = 1). Of the three OE dogs with *C. auris* infection, a diversity of fungi was observed, and their meta-barcode ITS sequence reads for *C. auris* ranged from 0.06% to 0.67%. Whole-genome sequencing of six *C. auris* strains obtained from two dogs showed relatedness with Clade I clinical strains. The report highlights the isolation of *C. auris* from an animal source; however, the routes of transmission of this yeast to dogs and the clinical significance of transmission between dogs and humans remain to be investigated.

For the study in this chapter, I conducted the bioinformatic analyses including whole genome sequencing data analyses and metabarcoding data analyses. I am a co-first author of the following publication:
Yadav, A., Wang, Y., Jain, K., Panwar, V., Kaur, H., Kasana, V., Xu, J. and Chowdhary, A. 2023. "*Candida auris* in dog ears". Journal of Fungi 9(7), 720.

4.1 Introduction

Candida auris is a newly emerged human pathogenic yeast and is resistant to most antifungal agents. It has caused a diversity of infections and outbreaks in hospitals and presents a huge treatment challenge for clinicians and public health authorities. First

reported in Japan in 2009, *C. auris* has spread rapidly worldwide (Satoh et al., 2009b; Du et al., 2020; Yue Wang et al., 2022) and caused the World Health Organisation to declare it as one of the four 'critical priority' fungal pathogens (Parums, 2022). Outside the hospital settings, *C. auris* has been isolated from surface of stored apples, tidal marshes, hypersaline environments, and recently from wastewater suggesting that this yeast can survive in harsh conditions (Arora et al., 2021; Escandón, 2022; Yadav et al., 2022; Rossi et al., 2023). Interestingly, trace sequences identical or highly similar to that of *C. auris* at the fungal barcode locus i.e., the internal transcribed spacer (ITS) region were found in metabarcoding data on an ear sample from a Spanish dog with otitis externa (OE) and from the skin of newts in the United Kingdom (Irinyi et al., 2022). Though fungi are significant pathogens for animals, no live culture of *C. auris* has been isolated from animals and its role in animal health remains to be explored (Seyedmousavi et al., 2018). We hereby report the isolation of *C. auris* from ear samples of two dogs. Additionally, culture-independent assessment of mycobiome analysis (DNA metabarcoding data) showed the presence of *C. auris*-specific ITS reads from the ear and skin of dogs with chronic skin infections.

4.2 Material and Methods

Swab collection and processing: In this study, we analysed the microbial communities of skin and ear swab samples in culture from a heterogeneous cohort of 87 dogs from a public referral hospital cum shelter in Delhi, India. The skin and ear swabs were collected and processed for bacterial and fungal cultures using the routine diagnostic protocol for suspected skin and ear infections. An ethics review was not requested by the Animal Care Centre because it was considered as a clinical observation study. The ear canal was sampled using sterile swabs (HIMEDIA, Mumbai, India) by rubbing the skin between the vertical-horizontal junctions. The skin swabs were obtained from the presenting lesions covering the dorsal-ventral skin, paws, and groin region. For microbiologic culture, the swabs were streaked directly on standard bacterial culture media, i.e., sheep blood agar (SBA) and MacConkey agar at 37 °C for 24 h. For fungal growth, Sabouraud dextrose agar (SDA) and CHROMagar (Becton, Dickinson, Baltimore, MD, USA) media were used and incubated

at 37 °C for 24 h and 48 h, respectively. Additionally, for isolation of *Candida auris*, each swab was inoculated into yeast nitrogen base (YNB) broth with 10% NaCl at 37 °C for 4 days followed by streaking onto the SDA plates (Yadav et al., 2021; 2022). All microbial colonies, including bacteria and yeasts on blood agar, MacConkey agar, SDA, and CHROMagar, were identified by matrix-assisted laser desorption ionization-time of flight mass spectrometry (MALDI-TOF MS; Bruker Biotyper OC version 3.1, Daltonics, Bremen, Germany) with a score ≥2. *C. auris* colonies obtained in culture were further confirmed by sequencing of internal transcribed spacer region (ITS) within the ribosomal RNA gene cluster (Kathuria et al., 2015).

Fungal DNA extraction and ITS amplicon sequencing (Metagenomics): In addition to samples for microbiological cultures, ITS meta-barcode sequencing was conducted for swab samples (skin, n = 2; ear swabs, n = 7) from seven dogs to study the fungal communities in these dogs with OE. Swabs were collected and placed in 0.05 M phosphate buffer for 30 min with a continuous shaking at 200 rpm. Swabs were discarded, and the solution was stored at −20 °C until subsequent analyses (Yadav et al., 2022). Microbial genomic DNA was extracted from each sample using a column-based QIAamp DNA minikit (Qiagen, Hilden, Germany) and quantified by QUBIT 4 fluorometer (ThermoFisher, USA) using DNA HS assay kit (ThermoFisher). Primers ITS-1, 5′-TCCGTAGGTGAACCTTGCGG-3′, ITS2, 5′-GCTGCGTTCTTCATCGATGA-3′, ITS3, 5′-GCATCGATGAAGAACGCAGC-3′, and ITS4, 5′-TCCTCCGCTTATTGATATGC-3 were used for amplifying the ITS1 and ITS2 regions, respectively. Illumina sequencing platform (NOVASEQ 6000, PIPITS v2.7) was used to perform ITS fungal sequencing, and PIPITS v2.7 was used for analysis (Gweon et al., 2015). Magic-BLAST was used to map the raw metabarcoding sequences of each sample against the fungal ITS database containing 15,695 fungal species (Boratyn et al., 2019). The reference ITS sequences can be downloaded at https://ftp.ncbi.nlm.nih.gov/refseq/TargetedLoci/Fungi/. To calculate the relative read abundance at the species level in each sample, the read counts of each species were divided by the total reads mapping to the fungal ITS database. Then, the read

abundance was pooled into the genera level, and the average read abundance of the samples for each genus was used to select the taxa for the heatmap. A total of 28 genera with average read abundance over 0.11% were included, and the 28 genera covered an average of 98% reads that were mapped to the database. A heatmap was generated using matplotlib and seaborn (Hunter, 2007; Waskom, 2021). Additionally, in each sample, we specifically searched for ITS sequences of *C. auris*. For samples that contained *C. auris* ITS sequences (>94% sequence identity over the cleaned and filtered ITS reads), the relative frequencies of *C. auris* ITS sequences in each sample were calculated. To better reveal the differences among samples, the read abundance for each genus was standardized. The standardization was carried out for each taxon by subtracting the minimum and dividing each by its maximum.

Antifungal susceptibility testing: The susceptibility testing of yeasts was performed using the CLSI broth microdilution method, following M27-A3 (CLSI, n.d.). The antifungals tested were fluconazole (FLU, Sigma, St Louis, MO, USA), itraconazole (ITC, Lee Pharma, Hyderabad, India), voriconazole (VRC, Pfizer, Groton, CT, USA), posaconazole (POS, Merck, Whitehouse Station, NJ, USA), isavuconazole (ISA, Basilea Pharmaceutical, Basel, Switzerland), 5-flucytosine (5-FC, Sigma), micafungin (MFG, Astellas, Toyama, Japan), anidulafungin (AFG, Pfizer), and amphotericin B (AMB, Sigma). The drugs were tested for 10 (two-fold) dilutions, and the drug concentration ranges were as follows: FLU, 0.25 ->128 mg/L; ITC, VRC, and AMB, 0.03-16 mg/L; POS, ISA, AFG, MFG, 0.015-8 mg/L; 5-FC, 0.125-64 mg/L (Chowdhary et al., 2018). *Candida krusei* strain ATCC6258 and *C. parapsilosis* strain ATCC22019 were used as quality controls. All statistical parameters were calculated using Prism version 6.00 (GraphPad Software).

Antibiotic susceptibility testing was conducted for all bacterial isolates using disk diffusion method following CLSI M100, Ed-32. For Gram-positive bacteria, including *Staphylococcus pseudointermedius*, *S. intermedius*, *S. simulans*, and *S. schleiferi*, eight drugs were tested, namely penicillin, ampicillin, clindamycin, vancomycin, azithromycin,

linezolid, cefoxitin, and cotrimoxazole. For Gram-negative bacteria, i.e., *Acinetobacter baumanii*, and *Pseudomonas aeruginosa*, ciprofloxacin, levofloxacin, gentamicin, amikacin, meropenem, cefepime, ceftazidime, ceftazidime-clavulanate, piperacillin, and piperacillin-tazobactam were tested. The inhibitory zone diameters obtained around the anti-biotic discs were measured after incubation for 24 h at 37 °C and evaluated (CLSI, n.d.).

Whole Genome Sequencing (WGS): Genomic DNA of all *C. auris* isolates (n = 6 obtained from ear swabs of two dogs with OE) were extracted using a column-based QIAamp DNA minikit (Qiagen, Hilden, Germany) and quantified by a QUBIT 3 Fluorometer using dS DNA HS Dye. WGS libraries were prepared using NEBNext ultra II DNA FS kit (New England Biolabs, Ipswich, MA, USA), as described previously, and sequenced on Illumina HiSeq 4000 (Arora et al., 2021; Yadav et al., 2021). For phylogenetic analysis to identify the clade affinity of our strains, one reference genome from each of the four major clades was included for comparison, including strains B8441 (clade I), B11220 (clade II), B11221 (clade III), and B11245 (clade IV). All strains were subjected to NASP pipeline for genome sequencing analysis, as described previously (Yadav et al., 2022). The phylogenetic tree was constructed using RAxML v8.0.25 under ASC_GTRCAT nucleotide substitution model and 1000 bootstrap replicates (Stamatakis, 2014). A maximum-likelihood tree was constructed based on SNPs present in at least one sample. This analysis revealed that all of our strains belonged to clade I (see Results below). We then proceeded to conduct an additional phylogenetic analysis using B8441 as reference and including 569 previously reported clade I *C. auris* samples from different countries, including Indian clinical strains (Sharma et al., 2016), strains recovered from apples (Yadav et al., 2022), and strains from the marine environment of the Andaman Islands (Arora et al., 2021). In this broad clade I-specific analysis, SNP sites with ambiguous calls in over 0.5% of the samples were removed, and the remaining SNPs were concatenated for each sample. Maximum-likelihood phylogeny was constructed using RAxML-HPC2 on XSEDE in the CIPRES Science Gateway (Miller et al., n.d.). The tree

uses the ASC_GTRCAT nucleotide substitution model and 1000 bootstrap iterations and was visualized with iTOL (Letunic et al., 2021).

4.3 Results

Population description: Among 87 dogs, 52 (60%) were stray dogs who were admitted in the ICU with severe skin lesions due to chronic skin diseases (group I). In group I dogs with skin infections, eight had otitis externa with clinical signs of ear infection, i.e., erythema, oedema, erosion, and exudate in the affected ear. These dogs are labelled as group IA (Table 4. 1). The remaining 35 dogs (40%) were pet dogs (group II) who were attending the outpatient services for minor ailments of the gastrointestinal and urinary tracts.

Fungal and bacterial culture: Overall, the ear swabs of all 52 dogs (group I and IA cohort) yielded microbial growth. On the contrary, the skin samples of only 31% (n = 16) of the dogs had microbial growth, including the isolation of bacteria (n = 8) and yeast (n = 8) in eight dogs each. Furthermore, ear samples and skin samples of 14% (n = 7) and 4% (n = 2) of dogs contained both living yeasts and living bacteria. In the group I and IA cohorts, *Candida tropicalis* (n = 3) and *Malassezia pachydermatis* (n = 3) were the predominant fungi on the skin (6% each), followed by *Candida glabrata* in a single dog. Also, in two (4%) dogs, *Acinetobacter baumanii* and *Staphylococcus pseudointermedius* were detected on the skin. In ear samples, *M. pachydermatis* was the predominant fungal species (n = 11, 21% dogs), followed by *C. tropicalis* (n = 8) in 15% cases (Table 4. 1).

Table 4. 1. Distribution of yeasts and bacteria on the skin and in the ear of 87 dogs collected from North Delhi, India.

Disease Categories in Dogs (Numbers)	Period of Sampling	Yeasts		Bacterial Isolation (Body Site, no. of Dogs Positive for the Given Species)
		Culture (Body Site, no. of Dogs Positive for the Given Species)	Amplicon Sequencing (ITS Reads for *C. auris*/total Reads Matched to Fungal ITS; Percentage of ITS Reads)	

Group I Chronic skin disease with otitis externa (*n* = 8),	27-09-22 to 17-04-23	*C. auris* (E *, *n* = 1) (D1) @ *C. rugosa* (E, *n* = 2), *C. krusei* (E, *n* = 3) (D2) @ *C. lusitaniae* (E, *n* = 1) *C. glabrata* (S #, *n* = 1) (D3) @	*C. auris* from ear swab of D1 dog (34394/27920633; 0.12%) *C. auris* from ear swab of D2 dog (39577/59853350; 0.06%) *C. auris* from skin swab of D3 dog (3231/479708; 0.67%)	*A. baumanii* (E, *n* = 1) *S. pseudointermedius* (S, *n* = 1)
Group IA Chronic skin disease (*n* = 44),	14-08-22 to 17-04-23	*C. auris* (E, *n* = 1) (D4) @ *M. pachydermatis* (E, *n* = 11; S, *n* = 3) *C. tropicalis* (E, *n* = 8; S, *n* = 3), *T. asahii* (E, *n* = 7), *C. glabrata* (E, *n* = 6, S; *n* = 1), *C. rugosa* (E, *n* =1), *C. albicans* (E, *n* = 1),	ND	*A. baumanii* (E, *n* =15; S, *n* = 2) *S. pseudointermedius* (E, *n* = 9; S, *n* = 2) *S. intermedius*, (E, *n* = 1; S, *n* = 1) *K. pneumoniae* (E, *n* = 1) *S. simulans* (S, *n* = 1) *S. schleiferi* (S, *n* = 1) *P. aeruginosa* (E, *n* = 1)
Group II Negative for skin and ear infections (*n* = 35),	11-05-22 to 02-09-22	*C. tropicalis* (E, *n* = 3; S, *n* = 3) *M. pachydermatis* (E, *n* = 3; S, *n* = 1) *C. krusei* (E, *n* = 2) *C. lusitaniae* (S, *n* = 2) *C. parapsilosis* (E, *n* = 1)	ND	*A. baumanii* (E, *n* = 1; S, *n* = 2), *S. pseudointermedius* (E, *n* = 6), *P. aeruginosa* (E, *n* = 3; S, *n* = 1) *S. schleiferi* (E, *n* = 1; S, *n* = 1) *S. intermedius* (S, *n* = 2), *K. pneumoniae* (S, *n* = 1), *E. faecalis* (S, *n* = 1), *B. cereus* (E, *n* = 1)

* ear, @ dogs positive for *C. auris* either by culture or ITS amplicon sequencing, # skin. *tropicalis* (n = 8) in 15% cases (Table 4. 1).

In group IA, all cases had confirmed ear infections, and the ear swabs yielded yeasts as the sole etiologic agent in four of eight cases. The ear swabs of the remaining four dogs had both yeasts and bacterial colonies in culture. Notably, a single dog with OE (D1 dog) showed colonisation with multiple yeasts in the ear skin, including *C. auris* (645-V-22), *Candida lusitaniae*, and *Candida rugosa*, along with *Acinetobacter baumanii*. The *C. auris*-positive dog (D1) was admitted with chronic skin infection and OE in the hospital for more than a month before our sampling, and the dog was on topical treatment with miconazole, mupirocin, and ofloxacin. A repeat sampling of the ear canal of this dog after

four weeks again yielded *C. auris* (645-V-22_2). Interestingly, the ear swab obtained from another dog (D4) in group 1 (with only skin infection) who had no symptoms of otitis was also positive for *C. auris*, yielding five colonies of *C. auris* (D_953_1 to D_953_5) in culture.

Interestingly, 63% (n = 22) of the group II cohort (n = 35) with no skin or ear infections showed microbial growth from ear and/or skin swabs, but none of the colonies were *C. auris*. Also, a high rate of skin colonisation (43%, n = 15) was noted in these otherwise healthy dogs, whereas ear samples of only seven dogs showed microbial growth. Of these seven dogs, both *Candida tropicalis* (n = 3) and *M. pachydermatis* (n = 3) were observed to be equally distributed in the ear samples, followed by *Candida krusei* (n = 2) and *Candida parapsilosis* (n = 1). The skin surface was predominately colonised by *C. tropicalis* (n = 3, 14%) and *C. lusitaniae* (n = 2, 9%), and bacterial colonisation was due to *A. baumanii* (n = 2, 5.7%) and *S. intermedius* (n = 2, 5.7%).

We investigated healthcare workers' (HCW, n = 6) hand swabs for microbial growth. The ICU board of the Animal Facility guided the collection of hand swab cultures from healthcare workers (n = 6) handling the dogs and the environmental sampling of the ICU for microbial cultures. Also, the hand swab of a single HCW in the ICU was analysed for fungal diversity using metabarcoding. Hand colonisation by microbes was noted in five of the six HCWs. Overall, a varied spectrum of yeasts, including *C. krusei*, *C. parapsilosis*, *C. tropicalis*, *Trichosporan asahii*, and *A. baumanii*, was observed on the skin surfaces of the hands of HCWs. Additionally, the doors, benches, and floor of the ICU were found to be colonised by *C. tropicalis* and *C. krusei*.

Metagenomics analysis: According to metabarcoding data, evidence of *C. auris* was found in the ear skin samples of two dogs (both with OE) and on the skin of a single dog in the group IA cohort. A total of 248,515,598 ITS reads were obtained from ten samples (nine samples from dogs and one HCW's hands), with an average of 24,851,560 reads per

sample. After sequence alignment, 151,552,302 ITS reads were matched to a fungal ITS database with an average of 15,155,230 reads per sample. The length of the high-quality reads was 152 base pairs. The meta-barcode data from the ear of the dog with a positive culture for *C. auris* (D1) were also found positive for 34,394 ITS reads (0.12%) for *C. auris*. In addition, two dogs with negative culture for *C. auris* also showed the presence of 39,577 (0.06%) and 3231 (0.6%) ITS reads for *C. auris* from the ear (D2) and skin (D3), respectively. The heatmap shows the percentage of ITS read abundance of fungi in the 10 samples (Figure 4. 1). The percent ITS reads for all fungal species are given in Table 4. S1.

Interestingly, among the three dogs containing ITS sequences for *C. auris*, there seemed to be a negative correlation between the ITS read abundance for *Malassezia* species and that of C. auris (Table 4. S1). In addition, a single ear sample with the highest percentage (52.2%) of ITS reads for *Malassezia* did not have traces of *C. auris*. However, there was a big variation in the frequencies of *Malassezia* ITS sequences (0-52.2%) among *C. auris*-negative dogs. Aside from *C. auris*, other *Candida* species were frequently recovered. Of the seven dogs with OE whose ear swabs were subjected to ITS amplicon sequencing, there was an average of 15,155,230 ITS reads per samples for *Candida* species. In addition, the presence of *C. tropicalis*, *C. krusei*, *C. parapsilosis*, *T. asahii*, and *A. baumanii* in the microbial cultures of the hand swab of an HCW showed correlation with the presence of ITS reads (3.2%) of *Candida* species.

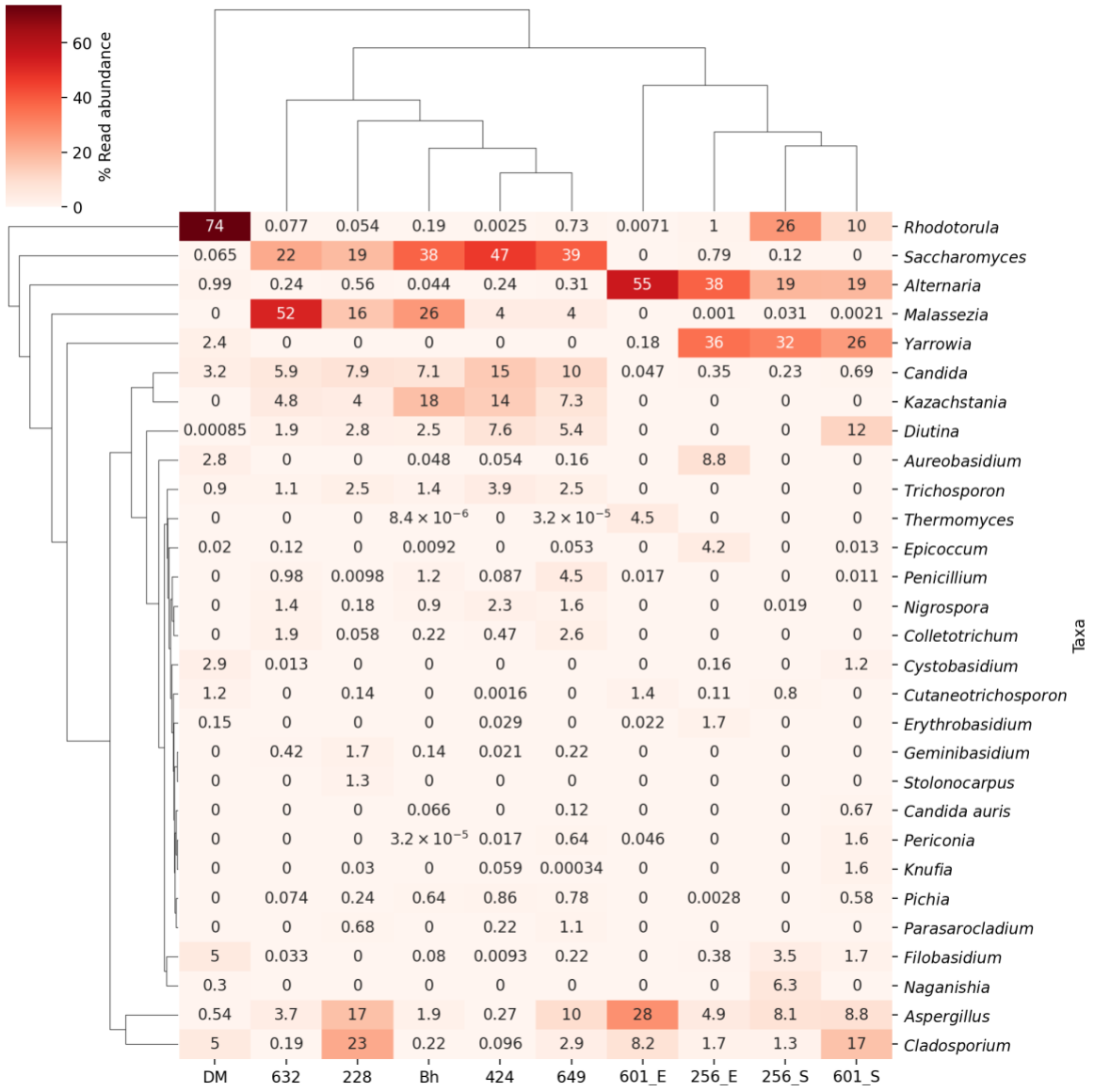

Figure 4. 1. Heat map showing distribution of 28 most common fungal genera in ear and skin samples from seven dogs and one healthcare worker. Different intensities of colours represent the percent read abundance of a genus in each sample. The dendrogram on the left is to indicate the similarity between different genera based on their read abundance profiles. Genera that are closer together on the dendrogram share more similar abundance patterns in our samples. The dendrogram on the top represents the clustering and relationships between the different samples based on their read abundance profiles of listed genera. Samples that are closer together on the dendrogram share more similar read abundance profiles.

Antifungal susceptibility testing (AFST): The MIC data of the antifungals tested are summarised in Table S2. The two *C. auris* strains (645-V-22, 645-V-22_2) from the D1 dog, were found to be resistant to fluconazole (FLU) (MIC >128 mg/L), while all of the other five strains isolated from the D4 case showed 2-4-fold fewer MICs for FLU (32-64 mg/L). All *C. auris* strains were susceptible to the other tested drugs (Table 4. S2).

All of tested isolates of *Staphylococcus*, *Pseudomonas*, and *Acinetobacter* genera were susceptible to all drugs except *S. pseudointermedius*, which was found to be resistant to clindamycin and azithromycin.

Whole genome sequencing: WGS analysis revealed that two *C. auris* strains (645-V-22, 645-V-22_2) obtained from the D1 dog four weeks apart differed by four SNPs from each other, suggesting that the same strain persisted during the four weeks in the colonised ear. In the D4 dog, four of the five isolates were sequenced, and clonal clustering of all four strains of *C. auris* was observed with a 2-6 SNPs difference among the strains. Notably, these four strains (D_953_1, D_953_2, D_953_3, and D_953_5) showed a difference of 955-965 SNPs from *C. auris* strains isolated from the D1 dog, suggesting the circulation of genetically distinct *C. auris* strains. All four *C. auris* strains from the D4 dog clustered with B8441, a clade I reference strain (Pakistan). Interestingly, the *C. auris* strains from the D4 dog showed close genetic relatedness (8-11 SNPs difference) with the Pakistan clade I reference strain. Phylogenetic analysis of 569 global clade I *C. auris* strains grouped the two D1 strains with two *C. auris* strains causing candidemia (7-14 SNPs) in Delhi, India (Figure 4. 2) (Wang et al., 2022; Sharma et al., 2016). These two strains from the D1 dog showed K143R amino acid substitution in the *ERG11* gene and A640V amino acid substitution in the *TAC1B* gene. Notably, four *C. auris* strains from the D4 dog showed the absence of mutation in azole-resistance-related genes, i.e., *ERG11* and *TAC1B.*

Figure 4. 2. Genetic relationships of *C. auris* isolates from dog ears and clade I strains from other countries inferred based on concatenated genome-wide SNPs. Branches with bootstrap support over 0.95 are highlighted in purple. Indian strains were labelled with triangles in various colours to indicate their isolation sources. The inner colour strips specify the geographic location of the isolates.

4.4 Discussion

Our report documents for the first time the isolation of live *C. auris* culture from an animal source. Overall, 4 of the 87 dogs (4.5%) contained evidence of *C. auris* infection or colonisation in their ear and on the surface of their skin. Notably, three of the four *C. auris*-positive dogs, either by culture (n = 2) or by ITS meta-barcode sequencing (n = 2),

harboured this yeast in the ear canal. Furthermore, among the eight dogs in the OE cohort, two had *C. auris*, suggesting an association of *C. auris* with external ear canal infections.

Candida auris has been previously isolated from ear infections in humans from Korea, Japan, and Iran (Abastabar et al., 2019; Jung et al., 2020; Satoh et al., 2009) but those strains mainly belonged to Clade II and Clade V (Jung et al., 2020; Wang et al., 2022). In a recent study from Spain investigating the bacterial and fungal microbiota in the ear canals of dogs with OE, 12 (0.01%) *C. auris*-specific ITS reads out of a total of 81,213 ITS reads were found in a single dog (Irinyi et al., 2022; Puigdemont et al., 2021). In contrast, in the present study, an ample number of *C. auris* reads accounting for 0.06% and 0.12% was observed in the ear samples, much higher than that in the ear sample of the Spanish dog. In addition, the skin of a single dog was also found to be colonised by *C. auris*, with 3231 (0.67%) ITS reads. The genomic data of *C. auris* strains from the ears of two dogs showed that genetically distinct strains of Clade I were infecting or colonising the dogs. A close association of *C. auris* strains from a single dog (D4) with the Pakistan clade I reference strain suggested a clonal transmission of this yeast in the Indian subcontinent. Interestingly, this strain with a low MIC of fluconazole (32 mg/L) had no known mutations in genes related to azole resistance, i.e., in the *ERG11* and *TAC1B* genes. In contrast, *C. auris* strains from the D1 dog showed similarity with the Indian clinical strains and exhibited previously known K143R amino acid substitution in the *ERG11* gene and A640V amino acid substitution in the *TAC1B* gene, likely contributing to the high MIC of fluconazole (MIC > 128 mg/L).

It is important to emphasise that in the present study, *C. auris* was not detected on the healthy intact skin of pet dogs using the culture method. However, the ITS amplicon sequencing was not performed on the skin and ear swabs of otherwise healthy dogs. *C. auris* colonised the breached skin of the ears of dogs with chronic skin conditions admitted to the ICU, but colonisation of the fomites samples in the ICU was not observed. This scenario is unlike the colonisation by *C. auris* in humans, where the close inanimate

environment is readily contaminated with this yeast due to shedding of skin scales. The fact that, in the present study, the skin of the ears of dogs was found to be colonised by *C. auris* rather than the exposed (ventral and dorsal) skin probably contributed to reduced shedding in the environment. It worth emphasising the circulation of closely related *C. auris* clade I strains in humans and dogs. However, the prevalence of *C. auris* transmissions between humans and domesticated animals warrants further investigations. Finally, the association of *C. auris* with ears in humans and dogs hints toward the ear canal possibly being an important reservoir of this yeast.

Supplemental Materials

Table 4. S1. Distribution of the 28 most common fungal genera in the ten samples (9 samples from dogs and one HCW hands). Individual sheets list the percent ITS reads data for all fungal genera from ten samples.

Taxa	**Sample (# of reads matched to fungal ITS database; # of total sequencing reads)**									
	228 (33273658; 60203466)	**424 (67983199; 16430174)**	**632 (22310865; 32662380)**	**256_E (389857; 32160886)**	**256_S (63806; 3748614)**	**601_E (226429; 32531543)**	**601_S (479708; 43517646)**	**649 (27920633; 39062956)**	**Bh (59853350; 82710348)**	**DM (235677; 2876654)**
Candida auris (count)	0	0	0	0	0	0	0.673534734 (3231)	0.123184886 (34394)	0.066123283 (39577)	0
Saccharomyces	18.57483178	46.85034639	22.29686299	0.786442208	0.122245557	0	0	39.17927291	38.16666068	0.06491936
Alternaria	0.564455522	0.24353079	0.239986213	38.3266172	19.35084475	55.02696209	19.2598414	0.310988651	0.043949086	0.990338472
Rhodotorula	0.053787293	0.002471199	0.077222465	1.015500555	26.48810457	0.007066233	10.03485454	0.730907498	0.193280744	73.65716638
Malassezia	15.77151812	4.003180786	52.23173552	0.001026017	0.031345015	0	0.002084601	3.969286799	26.294119406	0
Yarrowia	0	0	0	35.562778328	31.586377119	0.180630573	25.624122968	0	0	2.388438414
Aspergillus	17.02662809	0.273670594	3.677853817	4.861526149	8.118358775	28.18631889	8.769918367	9.969773966	1.933266893	0.542691905
Cladosporium	22.57838318	0.0959649	0.185376049	1.703701614	1.322759615	8.175189574	16.79876091	2.885525554	0.215550174	4.980969717
Candida	7.947632328	14.7918331	5.862090062	0.351410902	0.233520359	0.047255431	0.686459263	10.38731822	7.091497803	3.208204449
Kazachstania	4.007843081	14.028011192	4.76289467	0	0	0	0	7.338590783	17.519844475	0
Diutina	2.794405713	7.592877004	1.948436334	0	0	0	12.093119002	5.352790533	2.54425358	0.000848619
Trichosporon	2.460796465	3.864823054	1.076565162	0	0	0	0	2.488854748	1.387122024	0.897838992
Aureobasidium	0	0.053542648	0	8.786298566	0	0	0	0.156629687	0.048286353	2.794078336

Filobasidium	0	0.009252287	0.032732931	0.377061333	3.520045137	0	1.670391155	0.215331794	0.079612921	4.966967502
Penicillium	0.009764481	0.087242155	0.977729909	0	0	0.017223942	0.010631467	4.535917936	1.157276911	0
Naganishia	0	0	0	0	6.322289944	0	0	0	0	0.295319441
Nigrospora	0.178195015	2.283711606	1.447653419	0	0.018807009	0	0	1.586636664	0.897415099	0
Colletotrichum	0.05838252	0.466512383	1.909087792	0	0	0	0	2.588293754	0.216238523	0
Thermomyces	0	0	0	0	0	4.479549881	0	3.22342E-05	8.35375E-06	0
Epicoccum	0	0	0.116938541	4.177942169	0	0	0.012716069	0.053422858	0.009249273	0.019518239
Cystobasidium	0	0	0.013231222	0.16134121	0	0	1.192808959	0	0	2.876818697
Cutaneotrichosporon	0.136898083	0.001588628	0	0.106705792	0.797730621	1.426495723	0	0	0	1.180429147
Pichia	0.244677036	0.864860858	0.074353908	0.002821547	0	0	0.578685367	0.776579815	0.635804011	0
Geminibasidium	1.73831203	0.020872807	0.417576817	0	0	0	0	0.219343165	0.142403057	0
Periconia	0	0.016886527	0	0	0	0.045930512	1.555529614	0.642041318	3.17443E-05	0
Parasarocladium	0.677148271	0.218392223	0	0	0	0	0	1.079928954	0	0
Erythrobasidium	0	0.029139556	0	1.683694278	0	0.021640338	0	0	0	0.146386792
Knufia	0.030264181	0.058543884	0	0	0	0	1.629532966	0.00034025	0	0
Stolonocarpus	1.279961464	0	0	0	0	0	0	0	0	0

*Matched % : # of reads matched to each taxa * 100 / # of reads matched to the fungi ITS database.

Table 4. S2. In vitro antifungal susceptibility profile of 10 yeast species isolated from dogs (n = 87) against ten antifungal drugs using CLSI-BMD method.

Isolate ID	**Species**	**FLU**	**ITC**	**VRC**	**ISA**	**POSA**	**AMB**	**MFG**	**AFG**	**5-FC**
645_V_22	*C. auris*	128	1	0.5	0.25	0.5	0.5	0.5	0.015	0.5
645_V_22_2	*C. auris*	128	0.5	0.5	0.125	0.25	0.25	0.25	0.015	0.25
D_953_1	*C. auris*	32	0.06	0.03	0.125	0.015	0.5	1	0.06	0.125
D_953_2	*C. auris*	32	0.06	0.03	0.125	0.015	0.5	1	0.03	0.125
D_953_3	*C. auris*	64	0.06	0.03	0.125	0.015	0.5	0.5	0.06	0.125
D_953_4	*C. auris*	32	0.06	0.03	0.125	0.015	0.25	0.5	0.03	0.125
D_953_5	*C. auris*	64	0.06	0.03	0.125	0.015	0.5	1	0.03	0.125

Data availability

Genomic and meta-barcode data of the present study are submitted under bioproject number PRJNA917187.

References

Abastabar, Mahdi, Iman Haghani, Fatemeh Ahangarkani, Mohammad Sadegh Rezai, Mojtaba Taghizadeh Armaki, Somayeh Roodgari, Keyvan Kiakojuri, Abdullah M.S. Al-Hatmi, Jacques F. Meis, and Hamid Badali. 2019. "*Candida auris* Otomycosis in Iran and Review of Recent Literature." *Mycoses* 62 (2): 101–5. https://doi.org/10.1111/MYC.12886.

Arora, Parth, Prerna Singh, Yue Wang, Anamika Yadav, Kalpana Pawar, Ashutosh Singh, Gadi Padmavati, Jianping Xu, and Anuradha Chowdhary. 2021. "Environmental Isolation of *Candida auris* from the Coastal Wetlands of Andaman Islands, India." Edited by Leah E. Cowen. *MBio* 12 (2): 1–9. https://doi.org/10.1128/mBio.03181-20.

Boratyn, Grzegorz M., Jean Thierry-Mieg, Danielle Thierry-Mieg, Ben Busby, and Thomas L. Madden. 2019. "Magic-BLAST, an Accurate RNA-Seq Aligner for Long and Short Reads." *BMC Bioinformatics* 20 (1): 1–19. https://doi.org/10.1186/S12859-019-2996-X/FIGURES/11.

Chow, Nancy A., Theun De Groot, Hamid Badali, Mahdi Abastabar, Tom M. Chiller, and Jacques F. Meis. 2019. "Potential Fifth Clade of *Candida auris*, Iran, 2018." *Emerging Infectious Diseases* 25 (9): 1780–81. https://doi.org/10.3201/eid2509.190686.

Chowdhary, Anuradha, Anupam Prakash, Cheshta Sharma, Milena Kordalewska, Anil Kumar, Smita Sarma, Bansidhar Tarai, et al. 2018. "A Multicentre Study of Antifungal Susceptibility Patterns among 350 *Candida auris* Isolates (2009-17) in India: Role of the ERG11 and FKS1 Genes in Azole and Echinocandin Resistance." *The Journal of Antimicrobial Chemotherapy* 73 (4): 891–99. https://doi.org/10.1093/JAC/DKX480.

M100; "Performance Standards for Antimicrobial Disk Susceptibility Testing. 32nd Ed" *Clinical and Laboratory Standards Institute, Pennsylvania, USA.2022.*

M27-A3; "Reference Method for Broth Dilution Antifungal Susceptibility Testing of Yeasts, 3rd Ed M27-A3." *Clinical and Laboratory Standards Institute, Wayne, PA. 2008*.

Du, Han, Jian Bing, Tianren Hu, Craig L. Ennis, Clarissa J. Nobile, and Guanghua Huang. 2020. "*Candida auris*: Epidemiology, Biology, Antifungal Resistance, and Virulence." *PLoS Pathogens* 16 (10). https://doi.org/10.1371/JOURNAL.PPAT.1008921.

Escandón, Patricia. 2022. "Novel Environmental Niches for *Candida auris*: Isolation from a Coastal Habitat in Colombia." *Journal of Fungi (Basel, Switzerland)* 8 (7). https://doi.org/10.3390/JOF8070748.

Gweon, Hyun S., Anna Oliver, Joanne Taylor, Tim Booth, Melanie Gibbs, Daniel S. Read, Robert I. Griffiths, and Karsten Schonrogge. 2015. "PIPITS: An Automated Pipeline for Analyses of Fungal Internal Transcribed Spacer Sequences from the Illumina Sequencing Platform." *Methods in Ecology and Evolution* 6 (8): 973–80. https://doi.org/10.1111/2041-210X.12399.

Hunter, John D. 2007. "Matplotlib: A 2D Graphics Environment." *Computing in Science & Engineering* 9 (03): 90–95. https://doi.org/10.1109/MCSE.2007.55.

Irinyi, Laszlo, Michael Roper, Richard Malik, and Wieland Meyer. 2022. "Finding a Needle in a Haystack - In Silico Search for Environmental Traces of *Candida auris*." *Japanese Journal of Infectious Diseases* 75 (5): 490–95. https://doi.org/10.7883/YOKEN.JJID.2022.068.

Kathuria, Shallu, Pradeep K. Singh, Cheshta Sharma, Anupam Prakash, Aradhana Masih, Anil Kumar, Jacques F. Meis, and Anuradha Chowdhary. 2015. "Multidrug-Resistant *Candida auris* Misidentified as *Candida haemulonii*: Characterization by Matrix-Assisted Laser Desorption Ionization-Time of Flight Mass Spectrometry and DNA Sequencing and Its Antifungal Susceptibility Profile Variability by Vitek 2, CLSI Broth Microdilution, and Etest Method." *Journal of Clinical Microbiology* 53 (6): 1823–30. https://doi.org/10.1128/JCM.00367-15/ASSET/DE9AD252-4BA1-41A1-82B2-90A66E0811F5/ASSETS/GRAPHIC/ZJM9990942730002.JPEG.

Letunic, Ivica, and Peer Bork. 2021. “Interactive Tree Of Life (ITOL) v5: An Online Tool for Phylogenetic Tree Display and Annotation.” *Nucleic Acids Research* 49 (W1): W293–96. https://doi.org/10.1093/NAR/GKAB301.

Miller, MA, W Pfeiffer, T Schwartz - 2010 gateway computing, and undefined 2010. n.d. “Creating the CIPRES Science Gateway for Inference of Large Phylogenetic Trees.” *Ieeexplore.Ieee.Org*. Accessed June 24, 2023. https://ieeexplore.ieee.org/abstract/document/5676129/.

Parums, Dinah V. 2022. “Editorial: The World Health Organization (WHO) Fungal Priority Pathogens List in Response to Emerging Fungal Pathogens During the COVID-19 Pandemic.” *Medical Science Monitor: International Medical Journal of Experimental and Clinical Research* 28: e939088-1. https://doi.org/10.12659/MSM.939088.

Puigdemont, Anna, Sara D’Andreano, Laura Ramió-Lluch, Anna Cuscó, Olga Francino, and Pilar Brazis. 2021. “Effect of an Anti-Inflammatory Pomegranate Otic Treatment on the Clinical Evolution and Microbiota Profile of Dogs with Otitis Externa.” *Veterinary Dermatology* 32 (2): 158-e37. https://doi.org/10.1111/VDE.12930.

Rossi, Alessandro, Jorge Chavez, Thomas Iverson, John Hergert, Kelly Oakeson, Nathan LaCross, Chidinma Njoku, Andrew Gorzalski, and Daniel Gerrity. 2023. “*Candida auris* Discovery through Community Wastewater Surveillance during Healthcare Outbreak, Nevada, USA, 2022.” *Emerging Infectious Diseases* 29 (2): 422–25. https://doi.org/10.3201/EID2902.221523.

Satoh, Kazuo, Koichi Makimura, Yayoi Hasumi, Yayoi Nishiyama, Katsuhisa Uchida, and Hideyo Yamaguchi. 2009. “*Candida auris* Sp. Nov., a Novel Ascomycetous Yeast Isolated from the External Ear Canal of an Inpatient in a Japanese Hospital.” *Microbiology and Immunology* 53 (1): 41–44. https://doi.org/10.1111/J.1348-0421.2008.00083.X.

Seyedmousavi, Seyedmojtaba, Sandra Bosco, Sybren De Hoog, Frank Ebel, Daniel Elad, Renata R. Gomes, Ilse D. Jacobsen, et al. 2018. “Fungal Infections in Animals: A Patchwork of Different Situations.” *Medical Mycology* 56 (suppl_1): S165–87. https://doi.org/10.1093/MMY/MYX104.

Sharma, C., N. Kumar, R. Pandey, J. F. Meis, and A. Chowdhary. 2016. “Whole Genome Sequencing of Emerging Multidrug Resistant *Candida auris* Isolates in India Demonstrates Low Genetic Variation.” *New Microbes and New Infections* 13 (September): 77–82. https://doi.org/10.1016/J.NMNI.2016.07.003.

Spruijtenburg, Bram, Hamid Badali, Mahdi Abastabar, Hossein Mirhendi, Sadegh Khodavaisy, Joobin Sharifisooraki, Mojtaba Taghizadeh Armaki, Theun de Groot, and Jacques F. Meis. 2022. “Confirmation of Fifth *Candida auris* Clade by Whole Genome Sequencing.” *Emerging Microbes & Infections* 11 (1): 2405–11. https://doi.org/10.1080/22221751.2022.2125349.

Stamatakis, Alexandros. 2014. “RAxML Version 8: A Tool for Phylogenetic Analysis and Post-Analysis of Large Phylogenies.” *Bioinformatics (Oxford, England)* 30 (9): 1312–13. https://doi.org/10.1093/BIOINFORMATICS/BTU033.

Wang, Yue, and Jianping Xu. 2022. “Population Genomic Analyses Reveal Evidence for Limited Recombination in the Superbug *Candida auris* in Nature.” *Computational and Structural Biotechnology Journal* 20 (January): 3030–40. https://doi.org/10.1016/J.CSBJ.2022.06.030.

Waskom, Michael L. 2021. “Seaborn: Statistical Data Visualization.” *Journal of Open Source Software* 6 (60): 3021. https://doi.org/10.21105/joss.03021.

Yadav, Anamika, Kusum Jain, Yue Wang, Kalpana Pawar, Hardeep Kaur, Krishan Kumar Sharma, Vandana Tripathy, Ashutosh Singh, Jianping Xu, and Anuradha Chowdhary. 2022. “*Candida auris* on Apples: Diversity and Clinical Significance.” Edited by Leah E. Cowen. *MBio* 13 (2). https://doi.org/10.1128/MBIO.00518-22.

Yadav, Anamika, Anubhav Singh, Yue Wang, Merlijn Hi Van Haren, Ashutosh Singh, Theun De Groot, Jacques F. Meis, Jianping Xu, and Anuradha Chowdhary. 2021. “Colonisation and Transmission Dynamics of *Candida auris* among Chronic Respiratory Diseases Patients Hospitalised in a Chest Hospital, Delhi, India: A Comparative Analysis of Whole Genome Sequencing and Microsatellite Typing.” *Journal of Fungi* 7 (2): 81. https://doi.org/10.3390/JOF7020081.

Chapter 5

Population Genomic Analyses Reveal Evidence for Limited Recombination in the Superbug *Candida auris* in Nature

Candida auris is a recently emerged, multidrug-resistant pathogenic yeast capable of causing a diversity of human infections worldwide. Genetic analyses based on whole-genome sequences have clustered strains in this species into five divergent clades, with each clade containing limited genetic variation and one of two mating types, MTLa or MTLα. The patterns of genetic variations suggest simultaneous emergence and clonal expansion of multiple clades of this pathogen across the world. At present, it is unclear whether recombination has played any role during the evolution of *C. auris*. In this study, we analyzed patterns of associations among single nucleotide polymorphisms in both the nuclear and the mitochondrial genomes of 1,285 strains to investigate potential signatures of recombination in natural *C. auris* populations. Overall, we found that polymorphisms in the nuclear and mitochondrial genomes clustered the strains similarly into the five clades, consistent with a lack of evidence for recombination among the clades after their divergence. However, variable percentages of SNP pairs showed evidence of phylogenetic incompatibility and linkage equilibrium among samples in both the nuclear and the mitochondrial genomes, with the percentages higher in the total population than those within individual clades. Our results are consistent with limited but greater frequency of recombination before the divergence of the clades than afterwards. SNPs at loci related to antifungal resistance showed frequencies of recombination similar to or lower than those observed for SNPs in other parts of the genome. Together, though very limited, evidence for the observed recombination for both before and after the divergence of the clades suggests the possibility for continuous genetic exchange in natural populations of this important yeast pathogen.

For the study in this chapter, the following paper has been published:
Wang, Y. and Xu, J. 2022. "Population genomic analyses reveal evidence for limited recombination in the superbug *Candida auris* in nature". Computational and Structural Biotechnology Journal 20: 3030-3040.

5.1 Introduction

Candida auris is a recently emerged yeast pathogen. Since the first report in 2009, *C. auris* has been reported to cause a large number of hospital-related infection outbreaks in many countries, with a high mortality rate (Satoh et al., 2009; Sharp et al., 2021; Sathyapalan et al., 2021; Nobrega de Almeida et al., 2021; Salah et al., 2021; Berrio et al., 2021; Alshamrani et al., 2021; Du et al., 2022; Armaki et al., 2021; Villanueva-Lozano et al., 2021; Prestel et al., 2021) Morphologically and diagnostically, *C. auris* is similar to several other species in the genus *Candida* (Oh et al., 2010; Borman et al., 2016; Yue et al., 2018). However, different from most other pathogenic yeast species, *C. auris* can grow at a high temperature (42 °C) and high salinity conditions, and most strains are resistant to at least one class of antifungal drugs (Arora et al., 2021; Chowdhary et al., 2017). Other traits of medical importance in *C. auris* include the ability to form biofilm and to persist in hospital environments including medical devices (Oh et al., 2010). These unique traits of *C. auris* and its rapid spread have alarmed the World Health Organization and many national public health agencies (n.d.).

Whole-genome sequence analyses have revealed that the global *C. auris* strains belonged to five distinct clades, Clades I to V. While multiple strains have been reported for each of the five clades, only four of the five clades, Clades I to IV, have whole-genome sequences available from multiple strains each. In contrast, the whole-genome sequence of only one Clade V strain is available. The five clades differ from each other by 20,000 to over 200,000 nuclear genome SNPs. In contrast, within each clade, most strains were genetically very similar to each other, with pairwise SNP differences between them ranging from 0 to ~3,800 SNPs (Chow et al., 2020; 2019; Muñoz et al., 2018; Lockhart et al., 2017). Such

observations suggest that the current global strains were recently derived from a few divergent founder strains, with each underwent rapid clonal expansion and dispersal to result in their current distributions.

So far, no evidence for mating and sexual reproduction have been reported in *C. auris*. Among all strains of *C. auris* analyzed so far, those from Clades I and IV have the MTLa mating type while those in Clades II and III have the alternative MTLα mating type. The lack of alternative mating types within individual clades is consistent with clonal divergence among clades and asexual reproduction within clades in *C. auris*. In addition, within Clade I, all strains sequenced so far contain a deletion of two nucleotides at positions 3,309 and 3,310 at the STE6 gene. STE6 is a pheromone transporter, essential for mating in yeasts. The deletion of these two nucleotides makes STE6 non-functional and consequently the strains in Clade I most likely sterile (Wasi et al., 2019). Furthermore, several meiosis-specific genes that might have influence on mating and recombination such as DMC1, RAD55, RAD57, and MSH4/5 were not detected in the reference strains of Clades I-IV (Muñoz et al., 2018). Interestingly, RAD57 was found in the draft genome of a different strain (Bravo Ruiz et al., 2020), indicating polymorphisms among strains in the distributions of mating and meiosis-specific genes in *C. auris*. Nevertheless, as it has been observed in a related yeast *Candida lusitaniae* (Reedy et al., 2009; Sherwood et al., 2014), the absence of certain mating and meiosis-specific genes should not preclude the possibility that *C. auris* may be capable of mating and sexual reproduction in nature.

Earlier reports of *C. auris* identified geographic clustering among strains of the five clades. Specifically, strains of Clade I were isolated predominantly from South Asia, Clade II predominantly from East Asia, Clade III predominantly from Africa, Clade IV predominantly from the Americas, and several strains of Clade V from Iran in central Asia (Safari et al., 2022; Lockhart et al., 2017; Armaki et al., 2021). However, recent reports showed increasingly broad geographic distributions of clades I, II, III, and IV around the world, with most continents and several countries containing strains belonging to two or

more clades. Indeed, strains of different clades have been detected in the same hospitals (Hamprecht et al., 2019; Borman et al., 2017). Thus, it has been hypothesized that the increasingly mixed distributions of strains with different mating types may create possibilities for mating and recombination among strains of *C. auris* from different clades to generate genetically diverse hybrid offspring (Ross et al., 2020).

In this study, we analyze the genome-wide allelic associations based on data from over 1,200 strains of *C. auris* to investigate the potential signatures of recombination of this species in nature. The strains were from diverse geographic regions across the world and all known ecological niches such as different body sites in humans, hospital settings, and natural environments. Both the nuclear and mitochondrial genomes were analyzed. Different from the nuclear genome, inheritance of the mitochondrial genome in sexual crosses typically do not follow Mendelian laws, and with both uniparental and biparental inheritance having been observed in ascomycetes (Yan et al., 2007; Hewitt et al., 2020; C. W. Birky et al., 1978; Jr Birky, 2003; Xu et al., 2015). If mating occurred in *C. auris*, the different inheritance mechanisms between the nuclear and mitochondrial genomes will result in cytonuclear genome recombination within and between *C. auris* clades. To investigate the cytonuclear genome recombination, we compared the nuclear and mitochondrial phylogenies. Here, since *C. auris* is a haploid species, associations between alleles at the same SNP site (i.e., the Hardy-Weinberg equilibrium test) cannot be analyzed. Instead, we focus on analyzing associations between alleles at different single nucleotide polymorphism (SNP) sites. Following traditional tests of recombination, pairs of SNP sites that show evidence for phylogenetic incompatibility (PI) are considered as putative evidence for recombination. SNP pairs showing PI are further tested to determine if the relative proportions of the respective genotypes deviate from random association (i.e., in linkage equilibrium, LE). Here, SNP sites from both the nuclear and mitochondrial genomes are identified and analyzed. In addition, we separately analyze SNPs that are shared among clades from those that are found only within individual clades. The details

of the population samples, the two tests of recombination, the results and implications of our analyses are described below.

5.2 Materials and Methods

5.2.1 Data collection

Whole-genome sequence data for 1,286 *C. auris* strains were downloaded from the National Center for Biotechnology Information (NCBI) Sequence Read Archive. These strains were from five continents, including 673 from the Americas, 141 from Europe, 179 from Africa, 281 from Asia, 10 from Oceania, and two whose location information is unknown. In total, these samples were distributed among 27 countries and were collected from various sources from 1997 up to May 2022. The datasets were from 40 BioProjects that have been linked to 29 studies (Salah et al., 2021; Arora et al., 2021; Chow et al., 2020; Muñoz et al., 2018; Lockhart et al., 2017; Vogelzang et al., 2019; Cheshta Sharma et al., 2015; Yadav et al., 2022; Maphanga et al., 2022; Proctor et al., 2021; Chatterjee et al., 2015; Heath et al., 2019; Sekizuka et al., 2019; Rhodes et al., 2018; Tse et al., 2021; Woodworth et al., 2019; Hamprecht et al., 2019; Pchelin et al., 2020; C. Sharma et al., 2016; Tan et al., 2019; De Luca et al., 2022; Tian et al., 2021; Eyre et al., 2018; Escandón et al., 2019; Yadav et al., 2021; Chow et al., 2018; Travis K. Price et al., 2021; Pilato et al., 2021; Biswas et al., 2020). Among these 40 BioProjects, eight (including PRJEB21518, PRJNA638416, PRJNA640677, PRJNA657990, PRJNA722434, PRJNA732280, PRJNA772662, and PRJNA796037) currently have no related publications. The details of these strains, including their collection dates, isolation sources, sampling countries, clade affiliations, and reference publications are presented in Table 4. S1.

5.2.2 Genome sequence analysis

To analyze signature of recombination, we first obtained the biallelic SNPs in the genomes of all strains. Here, the completely assembled genome of a commonly used *C. auris*

reference strain B8441 (of Clade I) was chosen as the reference to derive the whole-genome SNP dataset for the whole population. The whole-genome SNP dataset was also used to confirm the clade affiliation of each strain. After clade confirmation, strains within each clade were then compared to their corresponding reference strain from the same clade to derive the SNPs for each clade. Specifically, the following four strains were used as references for Clades I-IV respectively, B8441 (GCA_002759435.2; Clade I), B11220 (GCA_003013715.2; Clade II), B11221 (GCF_002775015.1; Clade III), and B11245 (GCA_008275145.1; Clade IV). These four strains were chosen because of their completeness in the genome assemblies and annotations (Muñoz et al., 2018). Because only one Clade V strain has been sequenced at the whole-genome level, the Clade V strain is not included for downstream analyses of recombination and subsequent analyses included the remaining 1,285 strains. SNPs for both the nuclear and mitochondrial genomes were similarly identified using the same four reference strains. However, to date for mitochondrial genome (mitogenome), the NCBI nucleotide database contained only five assembled mitogenomes of *C. auris*, including three circular mitogenomes of Clade I strains (including that of Clade I reference strain B8441 with its mitogenome assembled as MT849287.1), one circular mitogenome of a Clade II strain, and one linear mitogenome of a Clade III strain which likely represents an incomplete mitogenome assembly. Thus, to generate the mitogenome references for Clades II, III and IV, we used raw sequencing reads from strains B11220, B11221, and B11245 and assembled their mitogenomes into circular molecules using NOVOPlasty4.2 (Dierckxsens et al., 2017). These assembled mitogenome sequences were then used as references to identify mitogenome SNPs among strains within each of the four clades.

For SNP identification, we used the NASP pipeline (Sahl et al., 2016). Specifically, the following steps were applied to all the strains within each analyzed sample. The adapter sequences and low-quality reads in the raw SRA files were trimmed with Trimmomatic v 0-2.39 (Bolger et al., 2014). Trimmed reads were then aligned against the selected reference genomes using BWA-MEM v 0.7.17 (Li, 2013). SNPs were identified with GATKv2.7

(McKenna et al., 2010). Finally, for quality insurance, SNP sites were filtered out from specific strains if: (i) they were in repetitive regions of the genomes, (ii) they had read depth lower than 10x, and/or (iii) they had less than 90% of the base calls at the position within the strain.

5.2.3 Phylogenetic analysis

To investigate whether there is evidence for mitochondrial and nuclear genome phylogenetic incongruence at the clade level, we compared the phylogenetic relationships among strains separately derived based on nuclear and mitochondrial genome SNPs. Incongruent relationships among clades between nuclear and mitochondrial genome phylogenies would be consistent with recombination/hybridization among clades. In this analysis, we used strain B8441 as the reference, SNPs of all strains were determined for the nuclear genome. Strains were clustered into representative clades based on nuclear SNPs. Similarly, the mitochondrial SNPs of each strain were determined based on comparison with the mitochondrial genome of strain B8441. Samples with ambiguous calls at over 10% of the SNP sites were removed from the dataset. Then, SNP sites with ambiguous calls of less than 5% of the remaining samples were concatenated. The phylogeny was inferred using FastTree with the GTR+CAT model (Morgan N. Price et al., 2010), and visualized with iTOL (https://itol.embl.de/).

5.2.4 PI and LE tests

To investigate evidence for potential recombination between SNPs, we used two approaches that had different null hypotheses (Xu, 2021). In the first, we determined the prevalence of SNP pairs with PI in the population. In the PI test, the null hypothesis is strict clonality and assumes the absence of parallel mutation. Consequently, in strictly asexual organisms, PI should be absent, and all SNP pairs should be phylogenetically compatible. Specifically, in haploid organisms such as *C. auris*, a pair of SNP sites with two alternative bases each is considered phylogenetically compatible if ≤3 possible genotype combinations

are observed in the population. For example, one SNP site has two alternative nucleotides A and G in the population and another SNP site has two alternative nucleotides C and T in the population, if three or fewer of the four possible SNP combinations (AC, AT, GC, and GT) are found in the population, these two SNP sites are considered phylogenetically compatible and be consistent with asexual reproduction in the population. In contrast, if all four possible SNP combinations are found in the population, the two SNPs are considered PI and consistent with recombination between the two SNP sites. [An alternative explanation is parallel mutation at the two SNP sites.] PI is determined using the four-gamete test (FGT). For pairs of SNPs that are PI, we further test whether the observed frequencies of the four genotypes deviate significantly from those expected under random recombination, following the LE test protocol commonly used for haploid organisms (Xu 2006). Different from that of the PI test, the null hypothesis for LE test is random allelic association between SNP sites.

For both tests, we examined the following five datasets. The first dataset contains SNPs in the whole population of 1,285 strains. Here, every SNP site is included if the site has an alternative base in at least one of the 1,285 strains. The SNPs in this dataset are determined based on the alignments of their sequence reads to the genome assembly of strain B8441, the Clade I reference for both the nuclear and mitochondrial genomes. The second dataset consists of four sub-datasets, one for each of four clades and includes nuclear genome SNPs. The third dataset also consists of four sub-datasets, one for each of four clades and includes only the mitogenome SNPs. The fourth dataset again consists of four sub-datasets, one for each of the four clades but included both the nuclear and mitochondrial SNPs where each nuclear SNP was compared with each mitochondrial SNP within each of the four clades in the tests of recombination. The fifth dataset contains only SNPs that are shared among all four clades. In the fifth dataset, each SNP must be polymorphic within each of the four clades.

For each of the above datasets, we first used the FGT to identify pairs of SNP sites that show evidence for PI. The identified PI SNP pairs were then tested for their LE. These tests were performed using in-house scripts written in R3.5 (R Core Team, 2020). The P-values were adjusted to minimize false discovery rate (FDR) for multiple testing (Benjamini et al., 1995). Circular plot with linked SNPs showing PI was generated using circos-0.69-9 for each of the four individual clades (Krzywinski et al., 2009).

5.2.5 SNP annotation

As described above, SNP pairs showing evidence of PI and recombination could have been derived due to convergent/parallel mutations among different strains. In general, convergent mutations are more likely to happen to genes under strong selection pressure. To examine this possibility, we annotated the SNPs showing the strongest evidence of recombination to determine whether they are located on genes known to be associated with stress response. We also extracted SNPs from known or putative drug-resistance genes in *C. auris* from the analyzed genomes, using SnpEff5.0 (Cingolani et al., 2012). Both the FGT and LE tests were conducted for the SNPs in these known or putative drug-resistance genes. In addition, the SNPs in these known or putative drug-resistance genes were compared to the SNPs that showed evidence of PI.

5.3 Results

5.3.1 SNP distributions

The whole nuclear genome analysis classified the 1,286 *C. auris* isolates into five clades. This result is consistent with those reported previously (Table 5. S1). Among the 1,286 isolates, 537 isolates belonged to Clade I, 24 belonged to Clade II, 513 belonged to Clade III, 210 belonged to Clade IV, and one belonged to Clade V. The total number of biallelic SNP sites in the nuclear genome for Clades I to V when compared to the Clade I reference strain B8441 were 4,775, 68,248, 48,825, 173,958, and 250,369 respectively. Because there is only one whole-genome sequenced Clade V strain reported so far in the database and this

strain is the most divergent among all the strains, we deleted this Clade V strain from subsequent recombination analyses. Interestingly, 13 SNPs were found to be polymorphic within all four clades. Within the four individual clades, the numbers of nuclear SNP sites were 4,775 for Clade I, 3,456 for Clade II, 3,038 for Clade III, and 1,427 for Clade IV (Table 5. 1).

Table 5. 1. Numbers of SNP loci for the nuclear and mitochondrial genomes within individual clades and between each of the clades and the Clade I reference strain B8441.

Reference	Feature	**Clade-specific**	**Comparison with Clade I strain B8441**
Clade I	Nuclear	4,775	4,775
	Mitochondrial	46	46
Clade II	Nuclear	3,456	68,248
	Mitochondrial	0	12
Clade III	Nuclear	3,038	48,825
	Mitochondrial	19	21
Clade IV	Nuclear	1,427	173,958
	Mitochondrial	0	28
Clade V	Nuclear	N/A	250,369
	Mitochondrial	N/A	60

For SNPs in the "Clade-specific" column, different clades used different reference genomes for SNP calling, as described in the text.

For the mitochondrial genome, we found a total of 46 SNP sites between B8441 and other strains within Clade I; 12 SNP sites between strain B8441 and those in Clade II; 24 SNP sites between B8441 and those in Clade III; 26 SNP sites between B8441 and those in Clade IV; and 60 SNP sites between B8441 and strain NG-19339 IFRC2087 in Clade V. Different from the nuclear SNPs, none of the mitochondrial SNPs were found to be polymorphic within all four clades. Within individual clades, 46 SNP sites were found in Clade I, 19 SNP sites were detected in Clade III, and no SNP site was found within either Clade II or Clade IV (Table 5. 1).

The mean SNP differences between pairs of strains within each clade for both the mitochondrial and nuclear genomes are summarized in Table 5. 2. To standardize the

comparisons between the nuclear and mitochondrial genomes, the mean pairwise SNP frequencies were divided by the reference nuclear and mitochondrial genome sizes (kb) respectively. The mean nuclear SNP differences between pairs of strains within Clades I - IV are 2.45%, 7.71%, 2.36%, and 1.43% respectively. Interestingly, the mitogenomes showed very different patterns from those of the nuclear genomes. In Clades I and III, there was a higher SNP frequency in the mitogenome than in the nuclear genome. However, in Clades II and IV, despite their comparable or higher nuclear SNP frequencies than Clades I and III, no SNP was found in the mitogenomes of either Clade II or Clade IV (Table 5. 2).

Table 5. 2. Nuclear and mitochondrial average SNP difference rates within each of Clades I-IV.

	Clade I	Clade II	Clade III	Clade IV
Reference genome size (nuclear; mitochondrial, ×10^6 bp)	12.37; 0.028212	12.25 vs. 0.027071	12.74 vs. 0.028214	12.43 vs. 0.028239
Sample size	537	24	514	210
Nuclear average SNP difference rates	2.45%	7.71%	2.36%	1.43%
Mitochondrial average SNP difference rates	15.96%	0	21.24%	0

5.3.2 Phylogenetic tree

Based on mitogenome SNPs, Misas et al. (2020) clustered 130 *C. auris* strains into four clades, consistent with the clade affiliations based on nuclear SNPs. In their analyses, Clade III and Clade IV samples contained no SNP in their mitogenomes (Misas et al., 2020). Furthermore, only one Clade II strain was included in their study, thus precluding the assessment of mitogenome variation within Clade II. Here, we included all *C. auris* strains with whole-genome sequences deposited in NCBI up to May 2022 in our analyses to determine whether including extra strains will reveal a cytonuclear phylogenetic pattern and a mitogenome variation pattern different from those reported by Misas et al (Misas et al., 2020). Our phylogenetic analysis revealed that the mitochondrial and nuclear genomes showed a congruent clustering pattern at the clade level (Figure 5. 1), largely consistent

with that observed in the previous study. Overall, this result suggests that at the clade level, there was no evidence for cytonuclear genome recombination among the four clades. However, there were several notable features. First, when using the Clade I strain B8441 mitogenome as the reference, several Clade IV strains had ambiguous nucleotide calls at several SNP loci, causing these strains having different branch lengths compared to other Clade IV strains on the phylogenetic tree. Second, all 24 Clade II strains analyzed here had the same mitogenome SNP pattern. Third, there were mitogenome SNPs within Clade III.

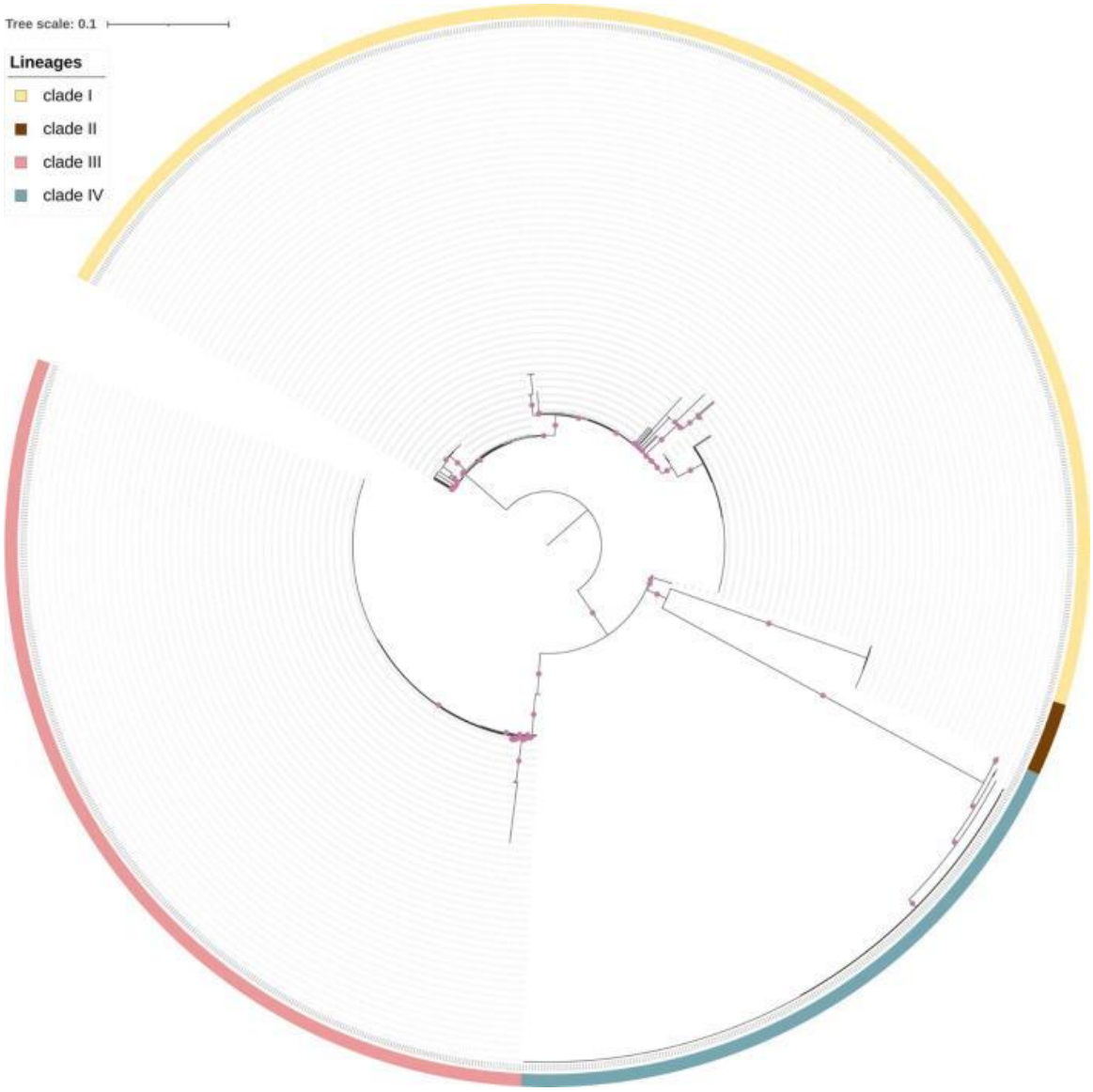

Figure 5. 1. Neighbour-joining tree based on mitochondrial genomes showing relationships among 1,070 isolates. The color strips around the periphery indicate the clade affiliation of the strains based on their nuclear genome SNPs. Nodes with local support value over 0.75 were marked with a purple dot.

5.3.3 PI and LE analyses

The PI and LE analyses were conducted for each of the five datasets described in the Materials and Methods section. Below are brief summaries of the test results.

Total sample: For the total sample of 1,285 strains, 3.56% nuclear SNP pairs showed evidence of PI. Among these PI SNP pairs, 8.27% did not deviate significantly from random association. While the percentage of mitogenome SNP pairs being PI (3.29%) was similar to that of the nuclear genome, a much higher percentage of those mitochondrial SNP pairs (38.76%) were in LE than those nuclear SNP pairs (8.27%; Table 5. 3). Together, the results suggest that in the total population of *C. auris*, both the nuclear and mitochondrial genomes showed low but unambiguous signatures of recombination with the mitogenome showed more frequent recombination than the nuclear genome.

Table 5. 3. Nuclear and mitochondrial genome SNPs and signatures of recombination in the total population of *C. auris*.

	Nuclear genome	Mitochondrial genome
Reference genome size (×10^6 bp)	12.37	0.028212
Sample size	1,285	1,285
Number of SNP sites	232,179	89
Total number of analyzed SNP pairs	26,953,427,931	3,916
SNP pairs in PI (% of total pairs)	959,299,294 (3.56%)	129 (3.29%)
SNP pairs in PI that fail to reject LE (% of total pairs that are in PI)	79,294,977 (8.27%)	50 (38.76%)

Clade-specific nuclear genome analyses: For the clade-specific nuclear SNPs, the percentages of SNP pairs being PI were 0.83%, 0.33%, 0.097%, and 1.36% for Clades I, II, III, and IV respectively (Table 5. 4). These percentages were all lower than that in the

total population shown in Table 5. 3. Among the nuclear SNP pairs being PI, the percentages in LE were 77.95% (Clade I), 100% (Clade II), 88.10% (Clade III), and 81.11% (Clade IV) (Table 5. 4), all higher than in the total population. Overall, the results are consistent with limited but unambiguous signatures of recombination within each of the four clades.

Table 5. 4. Nuclear genome SNPs and signatures of recombination within each of the four clades of *C. auris*.

	Clade I	**Clade II**	**Clade III**	**Clade IV**
Reference nuclear genome size (×10^6 bp)	12.37	12.25	12.74	12.43
Sample size	537	24	514	210
Number of SNP sites	4,775	3,456	3,038	1,427
Total number of analyzed SNP pairs	11,397,925	5,970,240	4,613,203	1,017,451
SNP pairs in PI (% of total pairs)	94,327 (0.83%)	19,836 (0.33%)	4,496 (0.097%)	13,853 (1.36%)
SNP pairs in PI that fail to reject LE (% of total pairs that are in PI)	73,529 (77.95%)	19,836 (100%)	3,961 (88.10%)	11,237 (81.11%)

Clade-specific mitogenome analyses: We conducted similar tests to those described above for the mitogenome SNPs within the four individual clades. However, as described above, no unambiguous mitogenome variant was detected among strains within either Clade II or Clade IV. Thus, the PI and LE tests were conducted for only Clade I and Clade III samples. Among the 46 mitogenome SNP sites within Clade I, 0.68% (7/1,035) of all SNP pairs were in PI and two of the seven incompatible pairs were in LE (Table 5. 5). However, no SNP pair was in PI among the 19 mitochondrial SNPs within Clade III (Table 5. 5). Together, the results suggest evidence for mitogenome recombination among strains within Clade I but absent in other clades.

Table 5. 5. Mitochondrial genome SNPs and signatures of recombination within Clades I and III. No SNP was found in the mitochondrial genomes of Clades II and IV.

	Clade I	**Clade III**
Reference mitochondrial genome size (×10^6 bp)	0.028212	0.028214
Sample size	537	514
Number of SNP sites	46	19
Total number of analyzed SNP pairs	1,035	171

SNP pairs in PI (% of total pairs)	7 (0.68%)	0
SNP pairs in PI that fail to reject linkage equilibrium (% of total pairs that are in PI)	2 (28.57%)	NA

Clade-specific nuclear-mitochondrial SNP comparisons: We further compared the nuclear SNPs with mitochondrial SNPs between each other within each clade. Here, three population samples were analyzed: the total sample, the Clade I sample, and the Clade III sample. Due to the lack of unambiguous mitochondrial SNPs within Clades II and IV, these two clades were not individually analyzed. For Clade I, we found that 1.0% of cytonuclear SNP pairs were in PI, among which 61.16% were in LE (Table 5. 6). For Clade III, the percentage of cytonuclear SNP pairs in PI was 0.58%, among which 28.27% were in LE (Table 5. 6). However, when the 232,179 nuclear SNPs were compared with all the 89 mitochondrial genome SNPs in the total sample, a much higher percentage (4.11%) of cytonuclear SNP pairs was in PI, and with 38.16% of them in LE (Table 5. 6). Together, the results indicate that even though the mitochondrial and nuclear genomes showed overall congruent phylogeny at the clade level, at the individual SNP pair level, there was evidence of cytonuclear recombination/hybridization in both the total sample as well as in Clades I and III.

Table 5. 6. Signatures of recombination based on mitochondrial and nuclear SNP comparisons.

	Clade I	**Clade III**	**All four clades**
Reference genome size (nuclear; mitochondrial, ×10^6 bp)	12.37; 0.028212	12.74; 0.028214	12.37; 0.028212
Sample size	537	514	1,285
Nuclear SNPs; mitochondrial SNPs	4,775; 46	3,038; 19	232,179; 89
Total number of analyzed SNP pairs	219,650	57,722	20,663,931
SNP pairs in PI (% of total pairs)	2,186 (1.0%)	336 (0.58%)	848,648 (4.11%)
SNP pairs in PI that fail to reject LE (% of total pairs that are in PI)	1,337 (61.16%)	95 (28.27%)	323,863 (38.16%)

5.3.4 Potential recombinogenic loci

Our analyses above revealed relatively low percentages of SNP pairs being PI in the nuclear genome, in the mitochondrial genome, and between the nuclear-mitochondrial genomes in

individual clades. Here we are interested in identifying the top SNPs showing PI. In this analysis, we used a threshold of 20% as the cut-off to identify SNPs as high-frequency recombinant SNPs (i.e., the recombinogenic SNPs). Specifically, if a SNP was in PI with over 20% of the total SNPs in the population, the SNP is considered as putative recombinogenic SNP. Our search found that 20, 8, 0, and 23 SNP sites were recombinogenic in Clades I, II, III, and IV respectively. Overall, Clades II and III, the two MTLα clades, showed fewer recombinogenic SNPs than the two MTLa Clades I and IV (Figure 5. 2). Annotation of these SNP sites indicated that all the recombinogenic SNP sites are present in intergenic regions except one located in an intron. Comparison of the recombinogenic SNP sites among Clades I, II and IV identified two regions shared by all three clades. These are the intergenic regions between B9J08_000508 and B9J08_000509; and between B9J08_002254 and B9J08_002255. The GO annotations of the SNP flanking genes were extracted from the Candida Genome Database (Skrzypek et al., 2017) and presented in Table 5. S3.

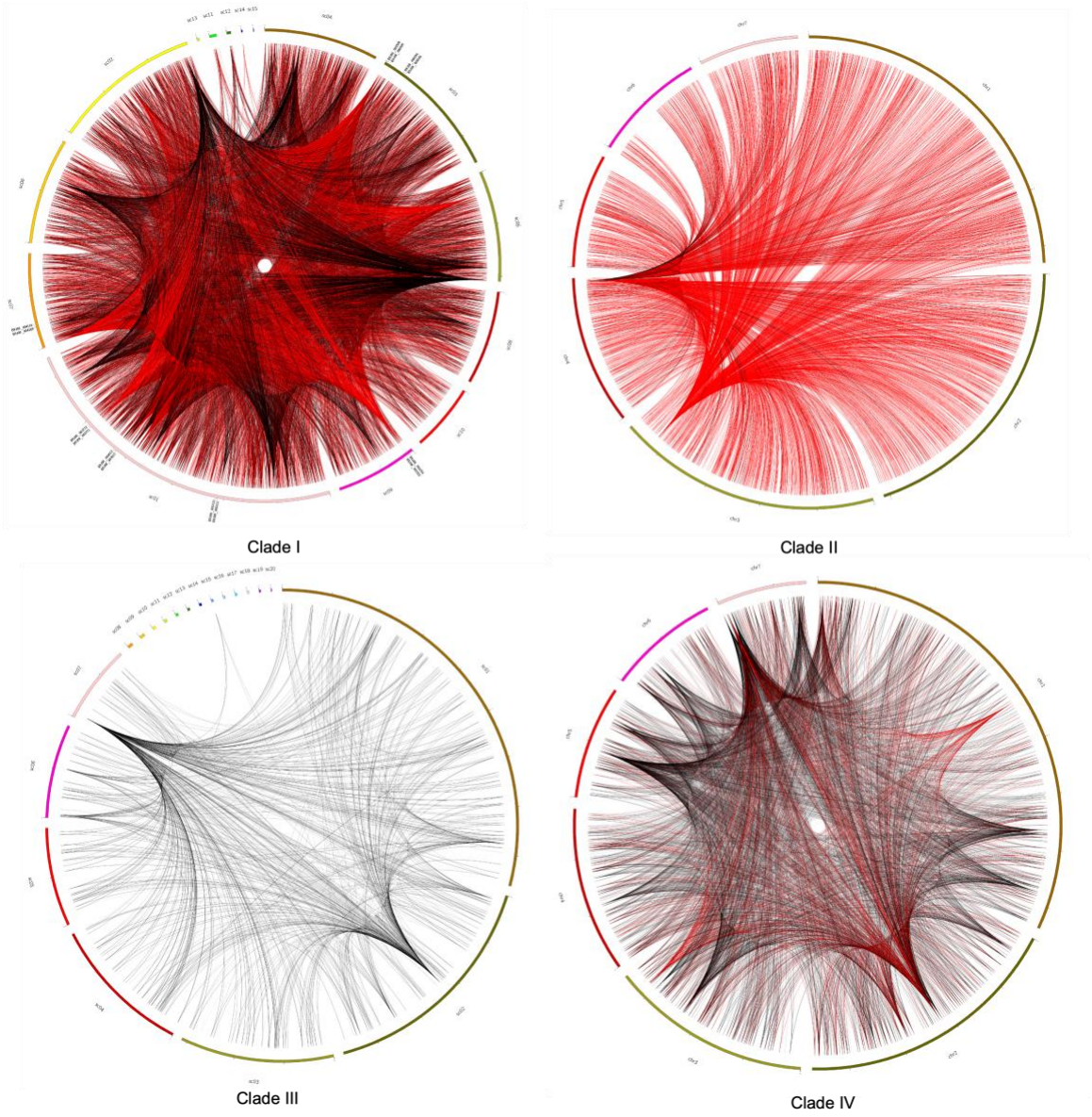

Figure 5. 2. Circular plot showing genomic locations and links of SNP pairs that are phylogenetically incompatible in each of the four clades. Highlighted in red are the phylogenetically incompatible SNP pairs involving recombinogenic SNPs.

5.3.5 Clade-shared SNP region

Among the 232,179 nuclear genome SNPs, 13 were polymorphic within each of the four clades. These 13 SNPs were located in three genomic regions and all three regions were

intergenic (Table 5. 7). Two of the three clade-shared SNP regions were the same as the "recombinogenic" regions identified above. The upstream gene of one region (region #2 in Table 5. 7) has no known function while its downstream gene as well as both the upstream and downstream genes for the two remaining regions (regions #1 and #3) contain domains of genes known to be involved in multiple biological processes (Table 5. 7). Two of the three regions (region 1 and region 2) overlapped with the recombinogenic regions identified above. However, excluding SNPs in these three regions from PI and LE testing had a minor impact on the total number and frequency of SNPs showing evidence for recombination. FGT of the 13 SNPs for each of the five datasets revealed relatively high levels of PI within Clade I (67/78 = 85.90%), Clade II (2/78 = 2.56%), Clade III (48/78 = 61.54%), Clade IV (33/78 = 42.31%), and the total sample (67/78 = 85.90%) and a very low level in Clade II (2/78 = 2.56%). We found that 12 of 67 PI SNP pairs in Clade I were in LE. For Clades II and III and the total samples, all PI SNP pairs were in linkage disequilibrium. In Clade IV, 15.15% of the PI SNP pairs were in LE.

Table 5. 7. Details of the 13 clade-shared SNPs and the genes located around them.

	SNP loci	**Ref**	**Alt**	**Upstream gene**	**Annotation**	**Downstream gene**	**Annotation**
Clade-shared SNP region 1 (PEKT02000002.1)	9130 9137 9157 9175	G C T G	A T A A	B9J08_000509: 12915 - 10831	Has domain(s) with predicted hydrolase activity	B9J08_000508: 8454 - 6094	Ortholog(s) have role in negative regulation of *TORC1* signaling and cytoplasm localization
Clade-shared SNP region 2 (PEKT02000006.1)	48506 48561 48573 48580 48583 48586	T G G G G G	A A A A A A	B9J08_002255: 49410 - 49006	Protein of unknown function	B9J08_002254: 47801 - 47169	Has domain(s) with predicted FMN binding, oxidoreductase activity
Clade-shared SNP region 3 (PEKT02000007.1)	2433109 2433112 2433123	G C A	A T C	B9J08_003771: 2429975 - 2431693	Ortholog(s) have unfolded protein binding activity, role in protein folding and	B9J08_003772: 2436486 - 2436992	Has domain(s) with predicted DNA-binding transcription factor activity, RNA polymerase II-specific, zinc ion

	chaperonin-containing T-complex localization	binding activity, role in regulation of transcription, DNA-templated and nucleus localization

Antifungal resistance related mutations

PI could be caused by parallel mutation or recombination. Parallel mutation is more likely to be selected and maintained in the population if they confer selective advantages. To investigate whether parallel mutations contribute to the observed PI, we selected genes previously identified or suspected as related to antifungal resistance and analyzed the associations among their SNPs. Specifically, the following genes were included in our analyses: *FUR*, *TAC1B*, *ERG3*, *ERG5*, *CDR1*, *PMS1*, *HOG1*, *ERG7*, *ERG11*, *STE6*, *YMC1*, *PDR1*, and *MSH2*. Here we hypothesize that if parallel mutations were responsible for the observed PI, we would see a significantly higher percentages of SNPs in these drug resistance related genes being PI than those in other parts of the genome. A total of 801 SNPs were identified among 1,285 strains in these 13 genes. Interestingly, among the 801 SNPs, 10,029 SNP pairs (out of 320,400 total pairs; 3.13%) showed PI. This rate is similar to that found between all SNPs in the nuclear genome (3.56%, Table 5. 3). Of the 10,029 SNP pairs in PI, only 631 (6.29%) did not deviate significantly from random association, a percentage lower than that found for all SNPs in the nuclear genome (8.27%, Table 5. 3). The results here suggest no evidence of higher frequency of parallel mutation at the antifungal resistance-associated genes in *C. auris*.

We further investigated whether similar rates of PI were also present among SNPs in these drug-resistance related genes for each of the four clades. After removing the fixed SNPs within each clade from the total SNPs identified above, 36, 23, 16, and 36 SNPs were identified in the 13 genes for Clades I, II, III, and IV respectively. Details about these mutations are listed in Supplementary Table 5. S2. Only 3 pairs of antifungal related SNPs showed PI in Clade I, and with all three pairs in linkage disequilibrium. No evidence for PI between antifungal related SNPs was found for Clades II and III. For Clade IV, 75 of the

630 SNP pairs (11.90%) showed evidence for PI and with 71 of the 75 SNP pairs (94.67%) did not deviate significantly from LE. In addition, the exclusion of these SNPs from each of the clades had limited impact on the frequencies of SNP pairs that are in PI.

Together, our analyses indicate the possibility of antifungal pressure (and potentially other stresses) to select for parallel mutations across the clades to account for the observed PI, especially for Clade IV. However, such selection cannot explain most of the observed PI across the clades. In addition, none of the SNPs in the drug resistance-related genes, including those in Clade IV, belonged to the recombinogenic SNPs nor were they shared among all four clades.

5.4 Discussions

In this study, we analyzed the whole genome SNPs of 1,286 *C. auris* strains collected from across the world over the past 20+ years to investigate the potential signatures of recombination in this species. SNPs in both the nuclear and mitochondrial genomes were analyzed, both in the total sample as well as for each of the four clades where multiple strains have been sequenced. Our analyses revealed signatures of infrequent recombination in both the total sample as well as within each of the four individual clades. In addition, specific groups of SNPs, including those in genes involved in antifungal drug resistance as well as those that are shared among all four clades, were separately analyzed to help identify the potential contributors to the observed signatures of recombination. Different patterns of allelic associations were found among the sample types and between the nuclear and mitochondrial genomes. Below we discuss the main findings of our analyses and the major implications of our results.

5.4.1 Comparison between nuclear and mitochondrial genomes

The 1,285 genomes analyzed here represented all the strains of *C. auris* that have been sequenced and deposited in GenBank by researchers, up to May 2022. Multiple studies

have analyzed variable numbers of strains, with the largest number of strains analyzed by Muñoz et al. (2018) where 304 strains from many geographic regions were included. Most studies have focused on nuclear genomes. Analyses of nuclear genomes in those studies revealed that the global population of *C. auris* could be grouped into five distinct clades, with Clades I to IV represented by multiple strains in each while Clade V was represented by only one whole-genome sequenced strain (so far). However, one previous study analyzed mitogenome variations. Based on mitogenome SNPs of 130 *C. auris* strains, Misas et al. (2020) showed that the mitogenome and nuclear genome SNPs clustered the strains into four similar clades. However, their analyses included only one Clade II strain and their results based on 10 Clade III strains from South Africa revealed no mitogenome sequence variation within Clade III. Our analyses here significantly expanded the sample sizes of all four clades with a total of 1,285 strains. While a similar pattern of sequence divergence within *C. auris* into five clades for both the nuclear genome and the mitochondrial genome was observed as previously reported (20,70), our analyses also revealed several notable features. Specifically, first, despite having more than twice as many strains as the earlier study (210 vs 86), we found no unambiguous SNP within the mitogenome of Clade IV, similar to that found by Misas et al. (2020). Second, the inclusion of 23 additional Clade II strains (versis one strain in the Misas et al. study) revealed no mitogenome SNP within Clade II. Third, the inclusion of 504 additional strains from more diverse geographic sources in Clade III (i.e., 514 in this study vs 10 in the Misas et al study) revealed abundant mitogenome SNPs within Clade III. Together, these analyses revealed that the amounts of sequence variations between the nuclear and mitochondrial genomes differed at both the whole species as well as within individual clades. At the whole species level, the SNP frequency in the nuclear genome was 1.876% (232,179/12.37×106), about six times of that of the mitochondrial genome (0.315%; 89/28212).

The lower observed genetic variation in the mitochondrial genome than in the nuclear genome has been reported in several other fungal species, including the human pathogen *Cryptococcus gattii* species complex and the ectomycorrhizal mushroom *Tricholoma*

matsutake species complex (Xu et al., 2009; Sandor et al., 2018; 2020). However, within individual clades, while two clades (Clades II and IV) showed limited to no mitochondrial SNPs (consistent with the overall pattern within the species), the remaining two clades (Clades I and III) showed greater mitochondrial SNP frequencies than their respective nuclear genomes. At present, the mechanisms for the different amounts of sequence diversity between the two genomes among the clades are unknown. The small sample size and limited ecological niches (mostly from ear discharges) might have contributed to no mitochondrial sequence variation in Clade II. However, this explanation cannot hold for Clade IV where 210 strains from four continents and a variety of human body sites were examined, similar to those of Clades I and III strains in this study (Table 5. S1). Geographically, strains of Clades II and IV are predominantly found in East Asia and the Americas respectively while Clades I and III are predominantly from South Asia and Africa respectively. It is possible that the higher temperature and other potential environmental factors in South Asia and Africa may have contributed to the higher mutation rates in mitochondrial genomes than in nuclear genomes in Clades I and III. The mechanisms for the observed divergent mitochondrial vs nuclear genetic variations among the four clades within *C. auris* remain to be elucidated.

5.4.2 Evidence of recombination

At both the species and individual clade levels, though the frequencies were generally low, evidence for PI was observed in both the nuclear and the mitochondrial genomes, with a significant proportion of those PI SNP pairs also in linkage equilibrium. However, the frequencies of PI SNP pairs differed among the samples. Overall, the frequency of nuclear PI SNP pairs at the species level was from twice to over 30 times of those within individual clades (Table 5. 3, Table 5. 4). A similar pattern was also observed for the mitochondrial genome SNPs. Together, these results suggested that there was more frequent recombination before the divergence of the clades than after individual clades were established. Specifically, though signatures of recombination were also detected within

each of the four clades after their respective divergence, clonal reproduction and expansion seemed more dominant in natural populations of *C. auris* after the divergence of clades than before their divergence. Our observed pattern is largely consistent with the expectations of each clade having only one mating type and therefore less likely to mate and recombine among strains of the same clade.

Relative to the frequent reports of recombination in the nuclear genomes of fungal populations, reports of mitochondrial genome recombination are still rare. However, the list of fungal species and populations showing evidence of mitogenome recombination is growing. For example, since 1998, mitochondrial DNA recombination has been reported for the honey mushroom *Armillaria gallica* (Saville et al., 1998), the commercial button mushroom *Agaricus bisporus* (Xu et al., 2013), the wild ectomycorrhizal mushroom *Russula virescens* species complex (Cao et al., 2013), and the opportunistic human fungal pathogen *Cryptococcus gattii* species complex (Xu et al., 2009). In the commercial mushroom *A. bisporus*, the observed frequency of mitochondrial loci with PI was correlated with the life cycles of two varieties within the species, with the outcrossing heterothallic population showing more evidence of mitochondrial genome recombination than the secondarily homothallic populations (Xu et al., 2013).

Because the ancestral population of *C. auris* contained strains of both mating types, evidence for recombination in the total sample was expected. The higher rate of SNP pairs that showed evidence for PI than those within individual clades is consistent with sexual recombination in the ancient population of this species. The absence of incongruent relationships among clades between nuclear and mitochondrial genome phylogenies is consistent with the absence of mating and recombination among the four clades after their divergence from each other. However, the observed PIs among SNP pairs within individual clades after their divergence are puzzling. Specifically, each clade is known to contain strains of only one mating type, MTLa for Clades I and IV, and MTLα for Clades II and III. In addition, we found limited evidence of parallel mutations in the genes that are most

likely under parallel selective pressure, the antifungal drug resistance-related genes. While we cannot completely exclude the possibility that convergent mutations might have contributed to some of the observed PIs, our analyses revealed that even if they existed, such an effect would likely be minimal. However, evidence for recombination have been found in natural fungal populations known to contain only a single mating type. For example, same-sex mating has been reported in the human fungal pathogen *Cryptococcus neoformans* species complex and such mating can generate genetic recombinants, similar to what have been reported for opposite-sex mating and to natural populations containing strains of both mating types (Fu et al., 2015). It is possible that low-frequency same-sex mating could have similarly happened to the individual *C. auris* clades to generate the observed PIs and linkage equilibrium. Alternatively, low frequency strains of the alternative mating type may exist within each of the four clades in nature and mating between strains of opposite mating types could have generated the observed signatures of recombination. Indeed, these two possibilities are not mutually exclusive, and both could have contributed to the observed signatures of recombination. Broader and more intensive sampling as well as experimental investigations of genetic crosses are needed in order to test these two possibilities.

5.4.3 Genes adjacent to clade-shared SNPs

Our analyses revealed three clade-shared SNP regions, with SNPs in two of these regions showing high frequency of PI with other SNPs in the genome. Interestingly, all three clade-shared SNP regions are in intergenic regions between genes coding for hydrolases, oxidoreductases, and transcription factors with potential impacts on cell growth and lifespan (Table 5. 7). For example, the ortholog of B9J08_000508, the downstream gene of clade-shared SNP region 1, is known to regulate the target of rapamycin complex 1 (*TORC1*) signaling. *TORC1* is a multiprotein signaling complex functions as the organizer that incorporate internal and external cues to regulate cell growth and cell cycle progression (Loewith et al., 2011). A recent study demonstrated that *TORC1* signaling plays an

important role in controlling NaCl resistance through Sir2 in *Saccharomyces cerevisiae* (Devare et al., 2020). The clade-shared SNPs within the upstream region of *TORC1* gene may be involved in regulating the expression levels of *TORC1*.

Interestingly, the downstream gene of clade-shared SNP region 2, B9J08_002254, codes for a protein containing a putative FMN-binding domain which is known to be most frequently found in bacteria. It has been hypothesized that proteins containing such a domain in fungi may have been horizontally transferred from bacterial to fungal genomes (Shelest, 2008). Indeed, multiple independent transfers of such genes and the associated upstream sequences from bacteria to strains of *C. auris* in different clades could have contributed to the observed distributions of clade-shared polymorphisms and PIs. Our BLAST searches revealed that based on the amino acid sequence, the closest match to B9J08_002254 was in the bacterial genus *Achromobacter*, with a 99% query coverage and an E value of 1e-54.

The two genes located upstream and downstream of the clade-shared SNP region #3 were B9J08_003771 and B9J08_003772. Gene B9J08_003771 has a predicted unfolded protein-binding activity, while B9J08_003772 has a predicted DNA-binding transcription factor activity, zinc ion binding activity, and transcriptional regulation activity. The unfolded protein response is known to help human fungal pathogens survive in the host through balancing the load of proteins entering the endoplasmic reticulum and the protein-folding capacity of the organelle (Krishnan et al., 2014). For example, in *C. albicans*, the zinc finger protein CZF1 is one of the DNA-binding proteins of the Cys6Zn2 class of transcriptional regulators with a multitude of functions such as biofilm induction, hyphal growth regulation, white-opaque switch, and yeast cell adherence (Finkel et al., 2012; Brown et al., 1999; Nobile et al., 2012; Whiteway et al., 1992; Zordan et al., 2007). While functionally likely important, how the polymorphisms in the intergenic regions of these two genes contribute to strain and population fitness remains to be investigated.

5.4.4 Conclusions and perspectives

This study identified limited but unambiguous evidence of recombination in both the total sample and within individual clades. In addition, evidence of recombination was found in both the nuclear and mitochondrial genomes, as well as between the nuclear and mitochondrial genomes. Overall, signatures of recombination were more prominent in the total sample than within individual clades, consistent with greater frequencies of recombination before the divergence of the four clades than after their divergence. At present, while several possibilities were suggested, the mechanism(s) for the observed recombination is not known. Nevertheless, the signatures of recombination identified here suggested a number of avenues from which further investigations could be conducted, including more extensive sampling for alternative mating types within each clade, laboratory attempts of both same-sex and opposite-sex mating, and identifying the adaptive significance of clade-shared SNPs. Such investigations should allow us to better understand the genetic architecture of virulence and drug resistance evolution within and among the divergent clades of this pathogen in natural and clinical environments.

Supplementary Data

https://doi.org/10.1016/j.csbj.2022.06.030

References

Alshamrani, Majid M., Aiman El-Saed, Azzam Mohammed, Majed F. Alghoribi, Sameera M. Al Johani, Harold Cabanalan, and Hanan H. Balkhy. 2021. “Management of *Candida auris* Outbreak in a Tertiary-Care Setting in Saudi Arabia.” *Infection Control and Hospital Epidemiology* 42 (2): 149–55. https://doi.org/10.1017/ICE.2020.414.

Armaki, Mojtaba Taghizadeh, Saeid Mahdavi Omran, Keyvan Kiakojuri, Shaghayegh Khojasteh, Jalal Jafarzadeh, Mahin Tavakoli, Hamid Badali, et al. 2021. “First Fluconazole-Resistant *Candida auris* Isolated from Fungal Otitis in Iran.” *Current Medical Mycology* 7 (1): 51. https://doi.org/10.18502/CMM.7.1.6243.

Arora, Parth, Prerna Singh, Yue Wang, Anamika Yadav, Kalpana Pawar, Ashutosh Singh, Gadi Padmavati, Anuradha Chowdhary, and Jianping Xu. 2021. "Environmental Isolation of *Candida auris* from the Coastal Wetlands of Andaman Islands, India." *MBio* 12 (2): 1–9. https://doi.org/10.1128/MBIO.03181-20/SUPPL_FILE/MBIO.03181-20-ST001.DOC.

Benjamini, Yoav, and Yosef Hochberg. 1995. "Controlling the False Discovery Rate: A Practical and Powerful Approach to Multiple Testing." *Journal of the Royal Statistical Society: Series B (Methodological)* 57 (1): 289–300. https://doi.org/10.1111/J.2517-6161.1995.TB02031.X.

Berrio, Indira, Diego H. Caceres, Wilfrido Coronell R, Soraya Salcedo, Laura Mora, Adriana Marin, Carmen Varón, et al. 2021. "Bloodstream Infections with *Candida auris* among Children in Colombia: Clinical Characteristics and Outcomes of 34 Cases." *Journal of the Pediatric Infectious Diseases Society* 10 (2): 151–54. https://doi.org/10.1093/JPIDS/PIAA038.

Birky, C. W., C. A. Demko, P. S. Perlmann, and R. Strausberg. 1978. "Uniparental Inheritance of Mitochondrial Genes in Yeast: Dependence on Input Bias of Mitochondrial DNA and Preliminary Investigations of the Mechanism." *Genetics* 89 (4): 615. https://doi.org/10.1093/GENETICS/89.4.615.

Birky, Jr. 2003. "The Inheritance of Genes in Mitochondria and Chloroplasts: Laws, Mechanisms, and Models." *Annual Review of Genetics* 35 (November): 125–48. https://doi.org/10.1146/ANNUREV.GENET.35.102401.090231.

Biswas, Chayanika, Qinning Wang, Sebastiaan J. Van Hal, David W. Eyre, Bernard Hudson, Catriona L. Halliday, Krystyna Mazsewska, et al. 2020. "Genetic Heterogeneity of Australian *Candida auris* Isolates: Insights from a Nonoutbreak Setting Using Whole-Genome Sequencing." *Open Forum Infectious Diseases* 7 (5). https://doi.org/10.1093/OFID/OFAA158.

Bolger, Anthony M., Marc Lohse, and Bjoern Usadel. 2014. "Trimmomatic: A Flexible Trimmer for Illumina Sequence Data." *Bioinformatics (Oxford, England)* 30 (15): 2114–20. https://doi.org/10.1093/BIOINFORMATICS/BTU170.

Borman, Andrew M., Adrien Szekely, and Elizabeth M. Johnson. 2016. "Comparative Pathogenicity of United Kingdom Isolates of the Emerging Pathogen *Candida auris* and Other Key Pathogenic *Candida* Species." *MSphere* 1 (4). https://doi.org/10.1128/MSPHERE.00189-16.

Borman, Andrew M., Adrien Szekely, and Elizabeth M. Johnson. 2017. "Isolates of the Emerging Pathogen *Candida auris* Present in the UK Have Several Geographic Origins." *Medical Mycology* 55 (5): 563–67. https://doi.org/10.1093/MMY/MYW147.

Bravo Ruiz, Gustavo, Zoe K. Ross, Neil A. R. Gow, and Alexander Lorenz. 2020. "Pseudohyphal Growth of the Emerging Pathogen *Candida auris* Is Triggered by Genotoxic Stress through the S Phase Checkpoint." *MSphere* 5 (2). https://doi.org/10.1128/MSPHERE.00151-20.

Brown, Douglas H., Angela D. Giusani, Xi Chen, and Carol A. Kumamoto. 1999. "Filamentous Growth of *Candida albicans* in Response to Physical Environmental Cues and Its Regulation by the Unique *CZF1* Gene." *Molecular Microbiology* 34 (4): 651–62. https://doi.org/10.1046/J.1365-2958.1999.01619.X.

Cao, Yang, Ying Zhang, Zefen Yu, Fei Mi, Chunli Liu, Xiaozhao Tang, Yunxian Long, Xiaoxia He, Pengfei Wang, and Jianping Xu. 2013. "Structure, Gene Flow, and Recombination among Geographic Populations of a *Russula Virescens* Ally from Southwestern China." *PLoS ONE* 8 (9): 73174. https://doi.org/10.1371/JOURNAL.PONE.0073174.

Chatterjee, Sharanya, Shuba Varshini Alampalli, Rishi Kumar Nageshan, Sivarajan T. Chettiar, Sangeeta Joshi, and Utpal S. Tatu. 2015. "Draft Genome of a Commonly Misdiagnosed Multidrug Resistant Pathogen *Candida auris*." *BMC Genomics* 16 (1): 1–16. https://doi.org/10.1186/S12864-015-1863-Z.

Chow, Nancy A., Lalitha Gade, Sharon V. Tsay, Kaitlin Forsberg, Jane A. Greenko, Karen L. Southwick, Patricia M. Barrett, et al. 2018. "Multiple Introductions and Subsequent Transmission of Multidrug-Resistant *Candida auris* in the USA: A Molecular

Epidemiological Survey." *The Lancet Infectious Diseases* 18 (12): 1377–84. https://doi.org/10.1016/S1473-3099(18)30597-8.

Chow, Nancy A., Theun De Groot, Hamid Badali, Mahdi Abastabar, Tom M. Chiller, and Jacques F. Meis. 2019. "Potential Fifth Clade of *Candida auris*, Iran, 2018." *Emerging Infectious Diseases* 25 (9): 1780–81. https://doi.org/10.3201/eid2509.190686.

Chow, Nancy A., José F. Muñoz, Lalitha Gade, Elizabeth L. Berkow, Xiao Li, Rory M. Welsh, Kaitlin Forsberg, et al. 2020. "Tracing the Evolutionary History and Global Expansion of *Candida auris* Using Population Genomic Analyses." *MBio* 11 (2). https://doi.org/10.1128/MBIO.03364-19.

Chowdhary, Anuradha, Cheshta Sharma, and Jacques F. Meis. 2017. "*Candida auris*: A Rapidly Emerging Cause of Hospital-Acquired Multidrug-Resistant Fungal Infections Globally." *PLoS Pathogens* 13 (5). https://doi.org/10.1371/JOURNAL.PPAT.1006290.

Cingolani, Pablo, Adrian Platts, Le Lily Wang, Melissa Coon, Tung Nguyen, Luan Wang, Susan J. Land, Xiangyi Lu, and Douglas M. Ruden. 2012. "A Program for Annotating and Predicting the Effects of Single Nucleotide Polymorphisms, SnpEff: SNPs in the Genome of *Drosophila Melanogaster* Strain W1118; Iso-2; Iso-3." *Fly* 6 (2): 80–92. https://doi.org/10.4161/fly.19695.

Devare, Mayur Nimbadas, Yeong Hyeock Kim, Joohye Jung, Woo Kyu Kang, Ki Sun Kwon, and Jeong Yoon Kim. 2020. "*TORC1* Signaling Regulates Cytoplasmic PH through Sir2 in Yeast." *Aging Cell* 19 (6): e13151. https://doi.org/10.1111/ACEL.13151.

Dierckxsens, Nicolas, Patrick Mardulyn, and Guillaume Smits. 2017. "NOVOPlasty: De Novo Assembly of Organelle Genomes from Whole Genome Data." *Nucleic Acids Research* 45 (4): e18. https://doi.org/10.1093/NAR/GKW955.

Du, Han, Jian Bing, Clarissa J. Nobile, and Guanghua Huang. 2022. "*Candida auris* Infections in China." *Virulence* 13 (1): 589–91. https://doi.org/10.1080/21505594.2022.2054120.

"Epidemiological Alert: *Candida auris* Outbreaks in Health Care Services in the Context of the COVID-19 Pandemic - 6 February 2021 - PAHO/WHO | Pan American Health Organization." n.d. Accessed June 24, 2023. https://www.paho.org/en/documents/epidemiological-alert-candida-auris-outbreaks-health-care-services-context-covid-19.

Escandón, Patricia, Nancy A. Chow, Diego H. Caceres, Lalitha Gade, Elizabeth L. Berkow, Paige Armstrong, Sandra Rivera, et al. 2019. "Molecular Epidemiology of *Candida auris* in Colombia Reveals a Highly Related, Countrywide Colonization with Regional Patterns in Amphotericin B Resistance." *Clinical Infectious Diseases* 68 (1): 15–21. https://doi.org/10.1093/CID/CIY411.

Eyre, David W., Anna E. Sheppard, Hilary Madder, Ian Moir, Ruth Moroney, T. Phuong Quan, David Griffiths, et al. 2018. "A *Candida auris* Outbreak and Its Control in an Intensive Care Setting." *New England Journal of Medicine* 379 (14): 1322–31. https://doi.org/10.1056/NEJMOA1714373.

Finkel, Jonathan S., Wenjie Xu, David Huang, Elizabeth M. Hill, Jigar V. Desai, Carol A. Woolford, Jeniel E. Nett, et al. 2012. "Portrait of *Candida albicans* Adherence Regulators." *PLOS Pathogens* 8 (2): e1002525. https://doi.org/10.1371/JOURNAL.PPAT.1002525.

Fu, Ci, Sheng Sun, R. B. Billmyre, Kevin C. Roach, and Joseph Heitman. 2015. "Unisexual versus Bisexual Mating in *Cryptococcus Neoformans*: Consequences and Biological Impacts." *Fungal Genetics and Biology* 78 (May): 65–75. https://doi.org/10.1016/J.FGB.2014.08.008.

Hamprecht, Axel, Amelia E. Barber, Sibylle C. Mellinghoff, Philipp Thelen, Grit Walther, Yanying Yu, Priya Neurgaonkar, et al. 2019. "*Candida auris* in Germany and Previous Exposure to Foreign Healthcare." *Emerging Infectious Diseases* 25 (9): 1763–65. https://doi.org/10.3201/EID2509.190262.

Heath, Christopher H, John R Dyer, Stanley Pang, Geoffrey W Coombs, Dianne J Gardam, Author affiliations, Royal Perth Hospital, et al. 2019. "*Candida auris* Sternal

Osteomyelitis in a Man from Kenya Visiting Australia." *Emerging Infectious Diseases* 25 (1): 192–94. https://doi.org/10.3201/EID2501.181321.

Hewitt, Sarah K., Kobchai Duangrattanalert, Tim Burgis, Leo A.H. Zeef, Samina Naseeb, and Daniela Delneri. 2020. "Plasticity of Mitochondrial DNA Inheritance and Its Impact on Nuclear Gene Transcription in Yeast Hybrids." *Microorganisms* 8 (4). https://doi.org/10.3390/MICROORGANISMS8040494.

Krishnan, Karthik, and David S. Askew. 2014. "Endoplasmic Reticulum Stress and Fungal Pathogenesis." *Fungal Biology Reviews* 28 (2–3): 29. https://doi.org/10.1016/J.FBR.2014.07.001.

Krzywinski, Martin, Jacqueline Schein, Inanç Birol, Joseph Connors, Randy Gascoyne, Doug Horsman, Steven J. Jones, and Marco A. Marra. 2009. "Circos: An Information Aesthetic for Comparative Genomics." *Genome Research* 19 (9): 1639–45. https://doi.org/10.1101/GR.092759.109.

Li, Heng. 2013. "Aligning Sequence Reads, Clone Sequences and Assembly Contigs with BWA-MEM." *ArXiv*. arxiv.org/abs/1303.3997.

Lockhart, Shawn R., Kizee A. Etienne, Snigdha Vallabhaneni, Joveria Farooqi, Anuradha Chowdhary, Nelesh P. Govender, Arnaldo Lopes Colombo, et al. 2017. "Simultaneous Emergence of Multidrug-Resistant *Candida auris* on 3 Continents Confirmed by Whole-Genome Sequencing and Epidemiological Analyses." *Clinical Infectious Diseases : An Official Publication of the Infectious Diseases Society of America* 64 (2): 134–40. https://doi.org/10.1093/CID/CIW691.

Loewith, Robbie, and Michael N. Hall. 2011. "Target of Rapamycin (TOR) in Nutrient Signaling and Growth Control." *Genetics* 189 (4): 1177–1201. https://doi.org/10.1534/GENETICS.111.133363.

Luca, Domenica G. De, David C. Alexander, Tanis C. Dingle, Philippe J. Dufresne, Linda M. Hoang, Julianne V. Kus, Ilan S. Schwartz, Michael R. Mulvey, and Amrita Bharat. 2022. "Four Genomic Clades of *Candida auris* Identified in Canada, 2012–2019." *Medical Mycology* 60 (1). https://doi.org/10.1093/MMY/MYAB079.

Maphanga, Tsidiso G., Ruth S. Mpembe, Serisha D. Naicker, Nelesh P. Govender, and for GERMS-SA. 2022. "In Vitro Antifungal Activity of Manogepix and Other Antifungal Agents against South African *Candida auris* Isolates from Bloodstream Infections." *Microbiology Spectrum* 10 (1). https://doi.org/10.1128/SPECTRUM.01717-21.

McKenna, Aaron, Matthew Hanna, Eric Banks, Andrey Sivachenko, Kristian Cibulskis, Andrew Kernytsky, Kiran Garimella, et al. 2010. "The Genome Analysis Toolkit: A MapReduce Framework for Analyzing Next-Generation DNA Sequencing Data." *Genome Research* 20 (9): 1297–1303. https://doi.org/10.1101/GR.107524.110.

Misas, Elizabeth, Nancy A. Chow, Oscar M. Gómez, José F. Muñoz, Juan G. McEwen, Anastasia P. Litvintseva, and Oliver K. Clay. 2020. "Mitochondrial Genome Sequences of the Emerging Fungal Pathogen *Candida auris*." *Frontiers in Microbiology* 11 (October): 2628. https://doi.org/10.3389/FMICB.2020.560332.

Muñoz, José F., Lalitha Gade, Nancy A. Chow, Vladimir N. Loparev, Phalasy Juieng, Elizabeth L. Berkow, Rhys A. Farrer, Anastasia P. Litvintseva, and Christina A. Cuomo. 2018. "Genomic Insights into Multidrug-Resistance, Mating and Virulence in *Candida auris* and Related Emerging Species." *Nature Communications 2018 9:1* 9 (1): 1–13. https://doi.org/10.1038/s41467-018-07779-6.

Nobile, Clarissa J., Emily P. Fox, Jeniel E. Nett, Trevor R. Sorrells, Quinn M. Mitrovich, Aaron D. Hernday, Brian B. Tuch, David R. Andes, and Alexander D. Johnson. 2012. "A Recently Evolved Transcriptional Network Controls Biofilm Development in *Candida albicans*." *Cell* 148 (1–2): 126–38. https://doi.org/10.1016/J.CELL.2011.10.048.

Nobrega de Almeida, João, Igor B. Brandão, Elaine C. Francisco, Silvio Luis R. de Almeida, Patrícia de Oliveira Dias, Felicidade M. Pereira, Fábio Santos Ferreira, et al. 2021. "Axillary Digital Thermometers Uplifted a Multidrug-Susceptible *Candida auris* Outbreak among COVID-19 Patients in Brazil." *Mycoses* 64 (9): 1062–72. https://doi.org/10.1111/MYC.13320.

Oh, Bong Joon, Jong Hee Shin, Mi Na Kim, Heungsup Sung, Kyungwon Lee, Min Young Joo, Myung Geun Shin, Soon Pal Suh, and Dong Wook Ryang. 2010. "Biofilm

Formation and Genotyping of *Candida haemulonii*, *Candida pseudohaemulonii*, and a Proposed New Species (*Candida auris*) Isolates from Korea." *Medical Mycology* 49 (1): 98–102. https://doi.org/10.3109/13693786.2010.493563.

Pchelin, Ivan M., Daniil V. Azarov, Maria A. Churina, Igor A. Ryabinin, Irina V. Vibornova, Svetlana V. Apalko, Alexander N. Kruglov, Andrey M. Sarana, Anastasia E. Taraskina, and Natalya V. Vasilyeva. 2020. "Whole Genome Sequence of First *Candida auris* Strain, Isolated in Russia." *Medical Mycology* 58 (3): 414–16. https://doi.org/10.1093/MMY/MYZ078.

Pilato, Vincenzo Di, Giulia Codda, Lorenzo Ball, Daniele Roberto Giacobbe, Edward Willison, Malgorzata Mikulska, Laura Magnasco, et al. 2021. "Molecular Epidemiological Investigation of a Nosocomial Cluster of *Candida auris*: Evidence of Recent Emergence in Italy and Ease of Transmission during the COVID-19 Pandemic." *J. Fungi* 7: 140. https://doi.org/10.3390/jof7020140.

Prestel, Christopher, Erica Anderson, Kaitlin Forsberg, Meghan Lyman, Marie A. de Perio, David Kuhar, Kendra Edwards, et al. 2021. "*Candida auris* Outbreak in a COVID-19 Specialty Care Unit — Florida, July–August 2020." *Morbidity and Mortality Weekly Report* 70 (2): 56. https://doi.org/10.15585/MMWR.MM7002E3.

Price, Morgan N., Paramvir S. Dehal, and Adam P. Arkin. 2010. "FastTree 2 - Approximately Maximum-Likelihood Trees for Large Alignments." *PLOS ONE* 5 (3): e9490. https://doi.org/10.1371/JOURNAL.PONE.0009490.

Price, Travis K., Ruel Mirasol, Kevin W. Ward, Ayrton J. Dayo, Evann E. Hilt, Sukantha Chandrasekaran, Omai B. Garner, Annabelle de St Maurice, and Shangxin Yang. 2021. "Genomic Characterizations of Clade III Lineage of *Candida auris*, California, USA." *Emerging Infectious Diseases* 27 (4): 1223–27. https://doi.org/10.3201/EID2704.204361.

Proctor, Diana M., Thelma Dangana, D. Joseph Sexton, Christine Fukuda, Rachel D. Yelin, Mary Stanley, Pamela B. Bell, et al. 2021. "Integrated Genomic, Epidemiologic Investigation of *Candida auris* Skin Colonization in a Skilled Nursing Facility." *Nature Medicine* 27 (8): 1401–9. https://doi.org/10.1038/S41591-021-01383-W.

R Core Team. 2020. “R: A Language and Environment for Statistical Computing.” https://www.gbif.org/tool/81287/r-a-language-and-environment-for-statistical-computing.

Reedy, Jennifer L., Anna M. Floyd, and Joseph Heitman. 2009. “Mechanistic Plasticity of Sexual Reproduction and Meiosis in the *Candida* Pathogenic Species Complex.” *Current Biology : CB* 19 (11): 891. https://doi.org/10.1016/J.CUB.2009.04.058.

Rhodes, Johanna, Alireza Abdolrasouli, Rhys A. Farrer, Christina A. Cuomo, David M. Aanensen, Darius Armstrong-James, Matthew C. Fisher, and Silke Schelenz. 2018. “Genomic Epidemiology of the UK Outbreak of the Emerging Human Fungal Pathogen *Candida auris* Article.” *Emerging Microbes and Infections* 7 (1): 43. https://doi.org/10.1038/S41426-018-0045-X.

Ross, Zoe K., and Alexander Lorenz. 2020. “Is *Candida auris* Sexual?” *PLOS Pathogens* 16 (12): e1009094. https://doi.org/10.1371/JOURNAL.PPAT.1009094.

Safari, Fatemeh, Mahboobeh Madani, Hamid Badali, Amir Abbas Kargoshaie, Hamed Fakhim, Majid Kheirollahi, Jacques F. Meis, and Hossein Mirhendi. 2022. “A Chronic Autochthonous Fifth Clade Case of *Candida auris* Otomycosis in Iran.” *Mycopathologia* 187 (1): 121–27. https://doi.org/10.1007/s11046-021-00605-6.

Sahl, Jason W., Darrin Lemmer, Jason Travis, James M. Schupp, John D. Gillece, Maliha Aziz, Elizabeth M. Driebe, et al. 2016. “NASP: An Accurate, Rapid Method for the Identification of SNPs in WGS Datasets That Supports Flexible Input and Output Formats.” *Microbial Genomics* 2 (8): e000074. https://doi.org/10.1099/MGEN.0.000074.

Salah, Husam, Sathyavathi Sundararaju, Lamya Dalil, Sarah Salameh, Walid Al-Wali, Patrick Tang, Fatma Ben Abid, and Clement K.M. Tsui. 2021. “Genomic Epidemiology of *Candida auris* in Qatar Reveals Hospital Transmission Dynamics and a South Asian Origin.” *Journal of Fungi (Basel, Switzerland)* 7 (3). https://doi.org/10.3390/JOF7030240.

Sandor, Sarah, Hanchen Wang, Lumin Vaario, Steven Trudell, and jianping Xu. 2020. “Mitochondrial Multilocus DNA Sequence Analyses Reveal Limited Genetic

Variability within and Consistent Differences between Species of the Global *Matsutake* Species Complex." *Acta Edulis Fungi* 27 (1): 1–19. https://jglobal.jst.go.jp/en/detail?JGLOBAL_ID=202002217764653746.

Sandor, Sarah, Yongjie Zhang, and Jianping Xu. 2018. "Fungal Mitochondrial Genomes and Genetic Polymorphisms." *Applied Microbiology and Biotechnology 2018 102:22* 102 (22): 9433–48. https://doi.org/10.1007/S00253-018-9350-5.

Sathyapalan, Dipu Thareparambil, Remya Antony, Vrinda Nampoothiri, Anil Kumar, Nandita Shashindran, Jini James, Jisha Thomas, et al. 2021. "Evaluating the Measures Taken to Contain a *Candida auris* Outbreak in a Tertiary Care Hospital in South India: An Outbreak Investigational Study." *BMC Infectious Diseases* 21 (1). https://doi.org/10.1186/S12879-021-06131-6.

Satoh, Kazuo, Koichi Makimura, Yayoi Hasumi, Yayoi Nishiyama, Katsuhisa Uchida, and Hideyo Yamaguchi. 2009. "*Candida auris* Sp. Nov., a Novel Ascomycetous Yeast Isolated from the External Ear Canal of an Inpatient in a Japanese Hospital." *Microbiology and Immunology* 53 (1): 41–44. https://doi.org/10.1111/J.1348-0421.2008.00083.X.

Saville, Barry J., Yatika Kohli, and James B. Anderson. 1998. "MtDNA Recombination in a Natural Population." *Proceedings of the National Academy of Sciences of the United States of America* 95 (3): 1331–35. https://doi.org/10.1073/pnas.95.3.1331.

Sekizuka, Tsuyoshi, Shigekazu Iguchi, Takashi Umeyama, Yuba Inamine, Koichi Makimura, Makoto Kuroda, Yoshitsugu Miyazaki, and Ken Kikuchi. 2019. "Clade II *Candida auris* Possess Genomic Structural Variations Related to an Ancestral Strain." *PLOS ONE* 14 (10): e0223433. https://doi.org/10.1371/JOURNAL.PONE.0223433.

Sharma, C., N. Kumar, R. Pandey, J. F. Meis, and A. Chowdhary. 2016. "Whole Genome Sequencing of Emerging Multidrug Resistant *Candida auris* Isolates in India Demonstrates Low Genetic Variation." *New Microbes and New Infections* 13 (September): 77–82. https://doi.org/10.1016/J.NMNI.2016.07.003.

Sharma, Cheshta, Nitin Kumar, Jacques F. Meis, Rajesh Pandey, and Anuradha Chowdhary. 2015. "Draft Genome Sequence of a Fluconazole-Resistant *Candida*

auris Strain from a Candidemia Patient in India." *Genome Announcements* 3 (4): 722–37. https://doi.org/10.1128/GENOMEA.00722-15.

Sharp, Ashley, Berit Muller-Pebody, Andre Charlett, Bharat Patel, Rebecca Gorton, Jonathan Lambourne, Martina Cummins, et al. 2021. "Screening for *Candida auris* in Patients Admitted to Eight Intensive Care Units in England, 2017 to 2018." *Euro Surveillance : Bulletin Europeen Sur Les Maladies Transmissibles = European Communicable Disease Bulletin* 26 (8). https://doi.org/10.2807/1560-7917.ES.2021.26.8.1900730.

Shelest, Ekaterina. 2008. "Transcription Factors in Fungi." *FEMS Microbiology Letters* 286 (2): 145–51. https://doi.org/10.1111/J.1574-6968.2008.01293.X.

Sherwood, Racquel Kim, Christine M. Scaduto, Sandra E. Torres, and Richard J. Bennett. 2014. "Convergent Evolution of a Fused Sexual Cycle Promotes the Haploid Lifestyle." *Nature 2014 506:7488* 506 (7488): 387–90. https://doi.org/10.1038/nature12891.

Skrzypek, Marek S., Jonathan Binkley, Gail Binkley, Stuart R. Miyasato, Matt Simison, and Gavin Sherlock. 2017. "The Candida Genome Database (CGD): Incorporation of Assembly 22, Systematic Identifiers and Visualization of High Throughput Sequencing Data." *Nucleic Acids Research* 45 (Database issue): D592. https://doi.org/10.1093/NAR/GKW924.

Tan, Yen Ee, Jocelyn Qi Min Teo, Nurdyana Binte Abdul Rahman, Oon Tek Ng, Marimuthu Kalisvar, Ai Ling Tan, Tse Hsien Koh, and Rick Twee Hee Ong. 2019. "*Candida auris* in Singapore: Genomic Epidemiology, Antifungal Drug Resistance, and Identification Using the Updated 8.01 VITEK ®2 System." *International Journal of Antimicrobial Agents* 54 (6): 709–15. https://doi.org/10.1016/J.IJANTIMICAG.2019.09.016.

Tian, Sufei, Jian Bing, Yunzhuo Chu, Jingjing Chen, Shitong Cheng, Qihui Wang, Jingping Zhang, et al. 2021. "Genomic Epidemiology of *Candida auris* in a General Hospital in Shenyang, China: A Three-Year Surveillance Study." *Emerging Microbes and Infections* 10 (1): 1088–96. https://doi.org/10.1080/22221751.2021.1934557.

Tse, Herman, Alan K. L. Tsang, Yiu-Wai Chu, and Dominic N. C. Tsang. 2021. "Draft Genome Sequences of 19 Clinical Isolates of *Candida auris* from Hong Kong." *Microbiology Resource Announcements* 10 (1). https://doi.org/10.1128/MRA.00308-20.

Villanueva-Lozano, Hiram, Rogelio de J. Treviño-Rangel, Gloria M. González, María Teresa Ramírez-Elizondo, Reynaldo Lara-Medrano, Mary Cruz Aleman-Bocanegra, Claudia E. Guajardo-Lara, et al. 2021. "Outbreak of *Candida auris* Infection in a COVID-19 Hospital in Mexico." *Clinical Microbiology and Infection* 27 (5): 813–16. https://doi.org/10.1016/J.CMI.2020.12.030.

Vogelzang, Erik H., Annemarie J.L. Weersink, Rosa Van Mansfeld, Nancy A. Chow, Jacques F. Meis, and Karin Van Dijk. 2019. "The First Two Cases of *Candida auris* in the Netherlands." *Journal of Fungi* 5 (4): 91. https://doi.org/10.3390/JOF5040091.

Wasi, Mohd, Nitesh Kumar Khandelwal, Alexander J. Moorhouse, Remya Nair, Poonam Vishwakarma, Gustavo Bravo Ruiz, Zoe K. Ross, et al. 2019. "ABC Transporter Genes Show Upregulated Expression in Drug-Resistant Clinical Isolates of *Candida auris*: A Genome-Wide Characterization of ATP-Binding Cassette (ABC) Transporter Genes." *Frontiers in Microbiology* 10 (January). https://doi.org/10.3389/FMICB.2019.01445.

Whiteway, Malcolm, Daniel Dignard, and David Y. Thomas. 1992. "Dominant Negative Selection of Heterologous Genes: Isolation of *Candida albicans* Genes That Interfere with *Saccharomyces Cerevisiae* Mating Factor-Induced Cell Cycle Arrest." *Proceedings of the National Academy of Sciences of the United States of America* 89 (20): 9410. https://doi.org/10.1073/PNAS.89.20.9410.

Woodworth, Michael H., David Dynerman, Emily D. Crawford, Sarah B. Doernberg, Lynn Ramirez-Avila, Paula Hayakawa Serpa, Amy Nichols, et al. 2019. "Sentinel Case of *Candida auris* in the Western United States Following Prolonged Occult Colonization in a Returned Traveler from India." *Microbial Drug Resistance* 25 (5): 677–80. https://doi.org/10.1089/MDR.2018.0408.

Xu, Jianping. 2021. “Is Natural Population of *Candida tropicalis* Sexual, Parasexual, and/or Asexual?” *Frontiers in Cellular and Infection Microbiology* 11 (October): 1066. https://doi.org/10.3389/FCIMB.2021.751676.

Xu, Jianping, and He Li. 2015. “Current Perspectives on Mitochondrial Inheritance in Fungi.” *Cell Health and Cytoskeleton* 7 (August): 143–54. https://doi.org/10.2147/CHC.S59508.

Xu, Jianping, Zhun Yan, and Hong Guo. 2009. “Divergence, Hybridization, and Recombination in the Mitochondrial Genome of the Human Pathogenic Yeast *Cryptococcus Gattii*.” *Molecular Ecology* 18 (12): 2628–42. https://doi.org/10.1111/J.1365-294X.2009.04227.X.

Xu, Jianping, Ying Zhang, and Nicholas Pun. 2013. “Mitochondrial Recombination in Natural Populations of the Button Mushroom *Agaricus Bisporus*.” *Fungal Genetics and Biology* 55 (June): 92–97. https://doi.org/10.1016/J.FGB.2012.09.004.

Yadav, Anamika, Kusum Jain, Yue Wang, Kalpana Pawar, Hardeep Kaur, Krishan Kumar Sharma, Vandana Tripathy, Ashutosh Singh, Jianping Xu, and Anuradha Chowdhary. 2022. “*Candida auris* on Apples: Diversity and Clinical Significance.” Edited by Leah E. Cowen. *MBio* 13 (2). https://doi.org/10.1128/MBIO.00518-22.

Yadav, Anamika, Anubhav Singh, Yue Wang, Merlijn Hi Van Haren, Ashutosh Singh, Theun De Groot, Jacques F. Meis, Jianping Xu, and Anuradha Chowdhary. 2021. “Colonisation and Transmission Dynamics of *Candida auris* among Chronic Respiratory Diseases Patients Hospitalised in a Chest Hospital, Delhi, India: A Comparative Analysis of Whole Genome Sequencing and Microsatellite Typing.” *Journal of Fungi* 7 (2): 81. https://doi.org/10.3390/JOF7020081.

Yan, Zhun, Sheng Sun, Mori Shahid, and Jianping Xu. 2007. “Environment Factors Can Influence Mitochondrial Inheritance in the Fungus *Cryptococcus Neoformans*.” *Fungal Genetics and Biology* 44 (5): 315–22. https://doi.org/10.1016/J.FGB.2006.10.002.

Yue, Huizhen, Jian Bing, Qiushi Zheng, Yulong Zhang, Tianren Hu, Han Du, Hui Wang, and Guanghua Huang. 2018. “Filamentation in *Candida auris*, an Emerging Fungal

Pathogen of Humans: Passage through the Mammalian Body Induces a Heritable Phenotypic Switch." *Emerging Microbes and Infections* 7 (1). https://doi.org/10.1038/S41426-018-0187-X.

Zordan, Rebecca E., Mathew G. Miller, David J. Galgoczy, Brian B. Tuch, and Alexander D. Johnson. 2007. "Interlocking Transcriptional Feedback Loops Control White-Opaque Switching in *Candida albicans*." *PLOS Biology* 5 (10): e256. https://doi.org/10.1371/JOURNAL.PBIO.0050256.

Chapter 6

Genome-Wide Association for Antifungal Drug Susceptibility in Individual Clades of *Candida auris*

Candida auris is a recently emerged human fungal pathogen that has posed a significant threat to public health. Since its first identification in 2009, this fungus has caused nosocomial infections in over 47 countries across all inhabited continents. Previous studies usually reported the antifungal profiles of their isolated strains and mutations identified in known antifungal related genes. However, the statistical significance of the relationships between those mutations and antifungal susceptibilities in *C. auris* remains unknown. In this study, we conducted genome-wide association studies on individual clades of previously published *C. auris* isolates to examine the genomic variants that are statistically associated with antifungal susceptibility. Genome wide association studies were performed using both FarmCPU and BLINK methods. As a result, we identified 12 SNPs associated with tested antifungal drugs in Clade I, 24 SNPs in Clade III, and 13 SNPs in Clade IV.

6.1 Introduction

Candida auris is an ascomycete fungus that has recently gained lots of attention due to its pathogenicity and ability to cause nosocomial outbreaks. In October 2022, this species was classified as one of the four critical human fungal pathogens by the World Health Organization. Although *C. auris* was first reported in 2009 (Satoh et al., 2009a), its earliest presence in clinical settings can date back to 1996 in South Korea (Lee et al., 2011). Since *C. auris* has not been widely reported from clinics until 2009, its emergence has been related to climate changes (Casadevall et al., 2019). This fungus has been isolated from environments, such as tropical wetlands (Arora et al., 2021), suggesting that global warming may boost its adaptation to high temperatures and salinity conditions that are similar to human bodies (Ellwanger et al., 2022). In addition, *C. auris* has been successfully isolated from the surface of stored apples, stray dog ears, and other surfaces, indicating a

potential risk of colonization or infection in individuals exposed to these sources. (Yadav et al., 2021; 2022).

Furthermore, the substantial antifungal resistance of *C. auris* exacerbates the situation. Currently, only 4 classes of antifungal drugs are widely prescribed to treat fungal infections in clinics, which include azoles, polyenes, echinocandins and antimetabolite, each with its unique mode of action. In particular, azoles disrupt the ergosterol biosynthesis pathway and ergosterol serves as a vital component of the fungal cell membrane (Maertens, 2004). Polyenes exert their mechanism of action by directly binding to ergosterol and forming channels within the cell membrane, disrupting its integrity (Zotchev, 2003). On the other hand, echinocandins suppress beta-(1,3)-D-glucan synthase, which is an enzyme for the synthesis of a vital component of the fungal cell wall (Morris et al., 2006). Lastly, antimetabolite prevents nucleotide acid synthesis by acting as false metabolites so as to incorporate into the DNA strand or block essential enzymes (Silverman et al., 2015). However, unlike other *Candida* species, *C. auris* contains strains that are often resistant to multiple commonly used antifungal drugs. As reported by a multicentre study on 350 clinical *C. auris* isolates in India, 90% isolates were resistant against fluconazole, 15% against 5-fluorocytosine, 8% against amphotericin B, and 2% against echinocandins (Chowdhary et al., 2018). Remarkably, a quarter of these isolates exhibited resistance to multiple classes of antifungal drugs (Chowdhary et al., 2018). Indeed, previous studies have explored and elucidated the molecular basis of antifungal resistance in *C. auris*, which involves the mutations and/or overexpression of drug target genes and drug efflux gene. Examples included *EGR* family genes and ATP binding cassette alterations conferring resistance to azoles and polyenes, mutations in the gene *FCY1, FCY2*, and *FUR1* leading to 5FC resistance, and mutations in *FKS* family genes causing resistance to echinocandins (Frías-De-león et al., 2020).

A genome-wide association study (GWAS) is an approach to identify genomic variants that are linked to specific phenotypic traits. GWAS usually involves collecting genomic data

from a large sample with a wide range of phenotypic trait values, identifying genomic variants such as single nucleotide polymorphisms (SNPs) in individuals, and statistically testing the association between identified genomic variants and trait values. The Genome Association and Prediction Integrated Tool (GAPIT) is a popular R package that offers a wide range of models to perform GWAS analysis. The two most current developed models are Fixed and Random Model Circulating Probability Unification (FarmCPU) (Liu et al., 2016) and Bayesian-information and Linkage-disequilibrium Iteratively Nested Keyway (BLINK) (Huang et al., 2019). Both utilize mixed linear models and use principal component analysis to account for population structure. FarmCPU uses a bin method as it assumes that quantitative trait related SNPs are evenly distributed across the genome. And their associated genetic markers are used as covariates to adjust for false positive. Then, quantitative trait related SNPs with the most significant P value in each determined bin are causative SNPs. In contrast, BLINK drops this assumption and accounts for SNP interactions by taking linkage disequilibrium information into consideration.

Genomic analyses have classified strains of *C. auris* into five distinct clades, with each clade showing clonal expansion (Muñoz et al., 2018b; Lockhart et al., 2017b). Genomic divergence between different clades can range from tens of thousands to hundreds of thousands of SNPs (Chow et al., 2020) . To eliminate the effects of population structures for strains from different clades, we conducted GWAS analyses on individual clades to investigate antifungal related variants in populations of *C. auris*.

6.2 Materials and Methods

6.2.1 Data collection

As of May 18, 2023, the NCBI database contains a total of 4,304 *C. auris* samples with paired-end genomic data available. We performed literature search to retrieve the corresponding minimum inhibitory concentrations (MIC) against antifungal drugs for those

samples from relevant publications. The distribution of MICs for each clade against different drugs was visualized using ggplot2 (Wickham, 2016) in the form of histograms.

6.2.2 Genomic variant calling and annotation

Genomic data of samples from Clades I, III, and IV with available MIC information were obtained from the NCBI database. B8441 (I; GCA_002759435.2), B11221 (III; GCA_002775015.1), and B11245 (IV; GCA_008275145.1) were selected as reference genomes for their respective clades, due to the high level of genome annotation. MICs were only available for B8441 and B11221 against 6 drugs (Table 6. S1). Whole genome SNPs were called and filtered using NASP pipeline (Sahl et al., 2016) for samples from individual clades. Briefly, raw reads of samples were adapter and quality trimmed using Trimmomatic (Bolger et al., 2014). Then trimmed reads were aligned to the selected reference genome for their respective clades. Next, genomic variants were called using GATK UnifiedGenotyper (McKenna et al., 2010). Lastly, SNPs were filtered out if they failed to meet any of the following criteria: a) located in unduplicated regions of the reference genomes; b) with a read depth no lower than 10; c) with a minimum read proportion of 0.9.

The SNPs and their effects were annotated and predicted using SnpEff (Cingolani et al., 2012). The gene homology and function annotation for Clade I were obtained from the Candida Genome Database (Skrzypek et al., 2017). SNPs and genes of Clades III and IV were annotated by blasting the sequences containing the SNPs with the reference B8441.

6.2.3 SNPs in antifungal related genes for individual clades

Several antifungal related genes reported for *Candida* species were investigated, including *FUR1*, *TAC1B*, *ERG3*, *ERG4*, *ERG5*, *ERG11*, *CDR1*, *MDR1*, *MSH2*, *PMS1*, *PDR1*, *HOG1*,

STE6, YMC1, *MLH1*, *CDR2*, *CDR4*, *FKS1*, and *FKS2*. We performed SNP screening for these genes within each clade to explore shared resistance mutations across all clades.

6.2.4 Genome-wide association study

Association analysis was performed on each of the 9 antifungal drugs within the individual clades using both FarmCPU and BLINK from the GAPIT package (Jiabo Wang et al., 2021).

The MIC values of each drug were considered as the dependent variable in individual analysis. Samples with a MIC range against certain antifungals were assigned to an adjusted value. If the MIC was "> the maximum value" or "< the minimum value" for a certain drug, the sample was assigned the adjusted value of the maximum value plus one unit or the minimum value minus one unit, either -1, -0.1, or -0.01, depending on the number of digits present in the value. For instance, a sample with MIC >256 mg/L was assigned a value of 257 mg/L, and a sample with <0.06 mg/L was assigned 0.05 mg/L. In cases where the MIC was a closed interval, the mean value was assigned to those samples. In the following scenarios, samples were excluded. For example, in a clade, if strain A has a MIC for drug1 greater than v1, but v1 is not the maximum MIC value for drug1 in this clade, then strain A will be excluded from the analysis for that drug. Similarly, if strain B has a MIC for drug1 less than v2, but v2 is not the minimum MIC value for that drug, strain B will also be excluded. After MIC adjustment, we determined the final number of samples from each clade that would be used for GWAS analysis.

The genomic variants were treated as the independent variables and the minimum allele frequencies were set as 0.01. Principal components of genomic variants were included as covariates to account for population structure, and the optimum number was determined based on QQ plot for individual analyses. A GWAS was considered validated if the overall distribution of observed p-values, or at least most observed p-values, showed no deviation from expected p-values, i.e., the points on the QQ plot aligns to the diagonal line (with a

tail). The significance of SNPs in relation to antifungal susceptibility were assessed using FDR adjusted p-value.

6.2.5 Analysis of SNPs associated with antifungal susceptibility

For Clade I, genes harboring significant SNPs were annotated according to the *Candida* genome database, which provides comprehensive and curated information on the genes and genomes of Clade I reference B8441. For Clades III and IV, SNPs and genes were compared to B8441 genome using BLAST (Camacho et al., 2009) to obtain the annotation and function details. As for intergenic SNPs, four gamete tests and linkage disequilibrium tests were performed as described in (Wang et al., 2022) to examine whether they are linked to other identified significant SNPs. To gain insights into the potential roles of these SNPs in antifungal susceptibility, we carried out Gene Ontology (GO) enrichment analysis on the genes flanking the intergenic SNPs that were not linked to other significant SNPs using Fungifun (Priebe et al., 2011).

6.3 Results

6.3.1 MIC Distribution

Collectively, MIC values were obtained for 408 strains, consisting of 178 Clade I, 12 Clade II, 119 Clade III, 99 Clade IV, 5 Clade V *C. auris* strains (Table 6. S1). These strains come from 22 countries across 6 continents encompassing 215 from Asia, 82 from South America, 49 from North America, 47 from Europe, 11 from Oceania, 7 from Africa, and 2 with unknown country of origin. Each of these strains contains MIC value against at least one of the following 9 antifungal drugs: 5-fluorocytosine (5FC), amphotericin B (AMB), fluconazole (FLU), voriconazole (VOR), itraconazole (ITR), posaconazole (POS), anidulafungin (AFG), caspofungin (CAS), and micafungin (MCF). Due to the limited availability of strains from Clades II and V, data analysis was exclusively carried out on the remaining three clades. In total, MICs of nine antifungal drugs were collected for Clade

I, III, and IV (Table 6. 1) and their distributions for each clade have been visualized in Figure 6. 1.

Table 6. 1. Sample distribution and MIC statistics for GWAS analysis across individual clades, categorized by antifungal drugs.

Antifungal drugs	Clade I	Mean (range)	Clade III	Mean (range)	Clade IV	Mean (range)
5FC	131	8.05 (0.03 - 65)	110	0.12 (0.05 - 0.5)	1	0.5 (0.5 - 0.5)
AMB	174	1.99 (0.125 - 16)	119	0.95 (0.125 - 2)	96	1.04 (0.25 - 4)
FLU	152	142.29 (0.5 - 256)	111	246.66 (8 - 256)	96	13.20 (1 - 256)
VOR	172	2.44 (0.008 - 16)	119	1.53 (0.06 - 8)	88	0.29 (0.015 - 8)
ITR	158	2.09 (0.015 - 16)	115	0.28 (0.06 - 1)	86	0.19 (0.02 - 1)
POS	155	1.07 (0.008 - 8)	114	0.08 (0.015 - 0.25)	86	0.09 (0.015 - 0.5)
AFG	165	0.56 (0.015 - 9)	119	0.41 (0.032 - 8)	88	0.57 (0.016 - 4)
CAS	159	1.37 (0.008 - 16)	118	0.27 (0.06 - 4)	96	0.35 (0.016 - 9)
MFG	169	0.53 (0.015 - 9.0)	116	0.28 (0.06 - 8.0)	92	0.42 (0.03 9.0)

5FC: 5-fluorocytosine; AMB: amphotericin B; FLU: fluconazole; VOR: voriconazole; ITR: itraconazole; POS: posaconazole; AFG: anidulafungin; CAS: caspofungin; MCF: micafungin.

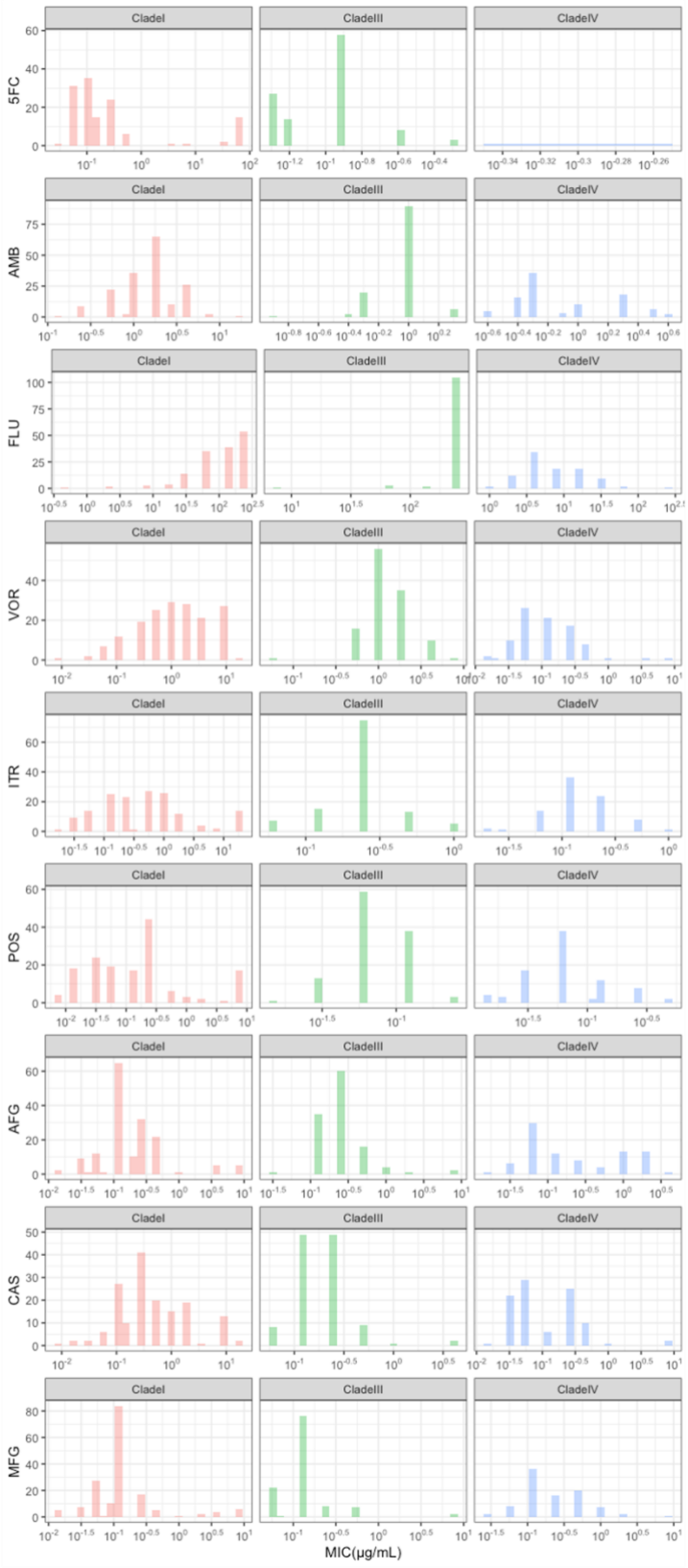
CladeI
CladeIII
CladeIV
5FC
AMB
FLU
VOR
ITR
POS
AFG
CAS
MFG
MIC(μg/mL)

Figure 6. 1. Histograms depicting the distribution of MICs for each clade against different drugs.

6.3.2 Variant calling and SNPs in known antifungal related genes

Overall, the Clade I, III and IV populations had 983, 1,687, and 1,031 genomic loci with SNPs as compared to their respective reference genomes.

We investigated SNPs in 19 genes that have been reported associated with antifungal resistance in each clade. Overall, we identified 10, 8, and 9 SNPs present in those genes in Clades I, III, and IV subpopulations respectively (Table 6. S3). We compared SNP positions among clades and found several SNPs occur at the same positions between clades in genes *EGR11* and *FKS1* (Table 6. 2).

Table 6. 2. Clade-shared SNPs in reported antifungal related genes.

Clade	Gene	Chr	Pos	Corresponding SNP in Clade I	REF	ALT	Mutations	REF_n	ALT_n
I	*ERG11*	PEKT02000003.1	833880	PEKT02000003.1_833880	T	C	Lys143Arg	119	59
I	*ERG11*	PEKT02000003.1	833913	PEKT02000003.1_833913	T	A	Tyr132Phe	62	116
I	*FKS1*	PEKT02000002.1	1006624	PEKT02000002.1_1006624	G	T, A	Ser639Phe, Tyr	170	5
I	*FKS1*	PEKT02000002.1	1006625	PEKT02000002.1_1006625	A	G	Ser639Pro	176	2
III	*FKS1*	NW_021640162.1	2137612	PEKT02000002.1_1006624	G	A	Ser639Phe	117	2
IV	*ERG11*	CP043444.1	1566724	PEKT02000003.1_833880	T	C	Lys143Arg	97	2
IV	*ERG11*	CP043444.1	1566757	PEKT02000003.1_833913	A	T	Phe132Tyr	3	96
IV	*FKS1*	CP043443.1	2100709	PEKT02000002.1_1006625	A	G	Ser639Pro	97	2

Chr: scaffold; Pos: position; REF: reference allele; REF_n: count of reference allele; ALT: alternative allele; ALT_n: count of alternative allele; Rows in same color indicate the same SNP loci among different clades.

6.3.3 Clade I genome-wide association study

GWAS was performed on Clade I strains to investigate genomic variants associated with antifungal susceptibility. Various numbers of principal components were examined to adjust the population structure. Except for 5FC, GWAS analyses for the rest of the examined antifungals drugs generated optimal QQplots. However, no significant SNPs were identified linked to ITR, VOR, and POS susceptibility in Clade I of *C. auris*.

We observed significant associations between genetic variants and antifungal tolerance for FLU, AMB, CAS, MFG, and AFG. The findings of the 5 GWAS analyses are summarized in Figure 6. 2, which include both QQ Plot and Manhattan plot for each antifungal drug. Details of significant SNPs are presented in Table 6. 3. The table shows the details of SNPs associated with antifungal susceptibility, including antifungal agent, SNP ID, minor allele frequency, number of strains involved in each GWAS analysis, adjusted p-value, the effect of the presence of the SNPs on the MIC value, parameters for GWAS analysis, mutation type, the gene containing the SNP and its ortholog in *C. albicans*. Specifically, we observed putative associations of 4 SNPs with FLU, 3 with AMB, 1 with CAS, 4 with MFG, and 5 with AFG susceptibility.

Of note, none of the 4 SNPs associated with FLU susceptibility were in protein-coding regions. The SNP PEKT02000001.1_925494 was found linked to AMB susceptibility, and the presence of this mutation is associated with an increase in AMB MICs. This SNP resulted in a conversion of arginine to glycine at position 274 in the product of gene *B9J08_000441*, whose function and properties have not been fully characterized. When performing a BLAST search of this protein against *C. albicans*, the amino acid sequence showed a sequence coverage of 41% with a 37.23% identity against gene *C5_00510W_A*, but no hits were found when comparing the nucleotide sequence. Similarly, *C5_00510W_A* is also uncharacterized in *C. albicans*.

Regarding the three echinocandins, SNP PEKT02000003.1_355435 was found to be significantly related to all of them. Interestingly, the negative effect values of -7.6, -2.698, and -3.3 indicated this SNP was mainly present in strains with low echinocandins MICs. This SNP resulted in a premature stop codon in *B9J08_001232*, which shows homology to *FCR1*, a zinc cluster transcription factor in *C. albicans*. Of note, *FCR1* has been found to repress azole and brefeldin resistance (Hui Shen et al., 2007; Talibi et al., 1999). Additionally, the SNP PEKT02000002.1_1006624 was identified to significantly increase

MICs against both MFG and AFG. It caused a serine-to-phenylalanine/tyrosine mutation at position 639 in the product of gene *B9J08_000964*, which is known as 1,3-beta-D-glucan synthase subunit *Fks1p*, an essential synthase necessary for the synthesis of the main component of the fungal cell wall. The identified mutation has been proven to confer echinocandins resistance in a murine model of infection (Sharma et al., 2022). Another SNP PEKT02000004.1_9898 was found to have a minor positive effect on AFG and MFG MICs. This SNP resulted in a synonymous variant in an uncharacterized gene *B9J08_001531*. The homolog of this gene in *C. albicans* is *IFF4*, encoding an adhesin-like cell surface protein (Kempf et al., 2007). The other synonymous variant that contributes to the increase of echinocandins MICs was PEKT02000002.1_804575 in gene B9J08_000876. This gene's ortholog, *GWT1*, is known to be involved in the glycosylated proteins biosynthetic process. Study has shown that this gene had the potential to be a drug target in *C. albicans* and *Aspergillus fumigatus* (Watanabe et al., 2012).

Table 6. 3. Significant SNPs associated with antifungal drugs identified in Clade I GWAS.

Drug	SNP ID	MAF	nobs	FDR adjusted p-value	Effect	Parameters	Annotation	HGVS.c	HGVS.p	Gene	*Candida albicans* ortholog
FLU	PEKT02000001.1_897129	0.03	152	1.14E-05	-84.241	FarmCPU, PCA:12	intergenic	c.-3672G>T			
	PEKT02000003.1_642734	0.03	152	4.08E-05	181.497		intergenic	c.-4186G>A			
	PEKT02000003.1_1045994	0.023	152	8.23E-05	181.022		intergenic	c.-4975T>A			
	PEKT02000004.1_361235	0.079	152	0.00789	-72.382		intergenic	c.-1790T>A			
AMB	PEKT02000001.1_925494	0.029	174	0.00151	2.9	FarmCPU, PCA:45	missense	c.820C>G	p.Arg274Gly	*B9J08_000441*	*C5_00510W_A*
	PEKT02000003.1_1045418	0.06	174	0.0002	-1.816		intergenic	c.-4399A>C			
	PEKT02000003.1_1045419	0.049	174	0.00151	4.424		intergenic	c.-4400A>C			
CAS	PEKT02000003.1_355435	0.013	159	3.72E-09	-7.6	FarmCPU, PCA:53	stop_gained	c.1012C>T	p.Gln338*	*B9J08_001232*	*FCR1*
MFG	PEKT02000002.1_1006624	0.021	169	3.94E-42	6.865	FarmCPU, PCA:5	missense	c.1916C>T	p.Ser639Phe	*B9J08_000964*	*FKS1*
	PEKT02000003.1_355435	0.012	169	1.92E-14	-2.698		stop_gained	c.1012C>T	p.Gln338*	*B9J08_001232*	*FCR1*
	PEKT02000004.1_9898	0.036	169	5.64E-06	0.845		synonymous	c.3261C>T	p.Thr1087Thr	*B9J08_001531*	*IFF4*
	PEKT02000002.1_1006624	0.021	169	9.66E-55	7.096	BLINK, PCA:5	missense	c.1916C>W	p.Ser639Phe/Tyr	*B9J08_000964*	*FKS1*
	PEKT02000003.1_355435	0.012	169	1.02E-15	-2.756		stop_gained	c.1012C>T	p.Gln338*	*B9J08_001232*	*FCR1*
	PEKT02000004.1_9898	0.036	169	2.66E-06	0.848		synonymous	c.3261C>T	p.Thr1087Thr	*B9J08_001531*	*IFF4*
	PEKT02000002.1_804575	0.038	169	5.84E-05	0.827		synonymous	c.369G>A	p.Lys123Lys	*B9J08_000876*	*GWT1*
AFG	PEKT02000002.1_1006624	0.021	165	2.90E-42	6.655	FarmCPU, PCA:8	missense	c.1916C>T	p.Ser639Phe	*B9J08_000964*	*FKS1*
	PEKT02000003.1_355435	0.012	165	1.02E-16	-3.385		stop_gained	c.1012C>T	p.Gln338*	*B9J08_001232*	*FCR1*
	PEKT02000002.1_804575	0.027	165	0.00012	1.781		synonymous	c.369G>A	p.Lys123Lys	*B9J08_000876*	*GWT1*
	PEKT02000004.1_9898	0.036	165	0.00193	0.658		synonymous	c.3261C>T	p.Thr1087Thr	*B9J08_001531*	*IFF4*
	PEKT02000002.1_1006624	0.021	165	5.95E-41	6.744	BLINK, PCA:8	missense	c.1916C>T	p.Ser639Phe	*B9J08_000964*	*FKS1*
	PEKT02000003.1_355435	0.012	165	2.05E-15	-3.347		stop_gained	c.1012C>T	p.Gln338*	*B9J08_001232*	*FCR1*
	PEKT02000002.1_804575	0.027	165	1.18E-05	1.545		synonymous	c.369G>A	p.Lys123Lys	*B9J08_000876*	*GWT1*
	PEKT02000001.1_212518	0.03	165	0.00224	-0.69		intergenic	c.-471G>A			

Shared SNPs are highlighted in the same colors. MAF: Minor allele frequency; nobs: sample size; Effect: the increase of phenotype values due to the increase of genotype values per unit; Parameters: GWAS methods, numbers of principal components as covariates; HGVS: Human Genome Variation Society; HGVS.c: Variant using HGVS notation (DNA level); HGVS.p: Variant using HGVS notation (Protein level); Gene: the genes in which the specific coding-region SNPs are located.

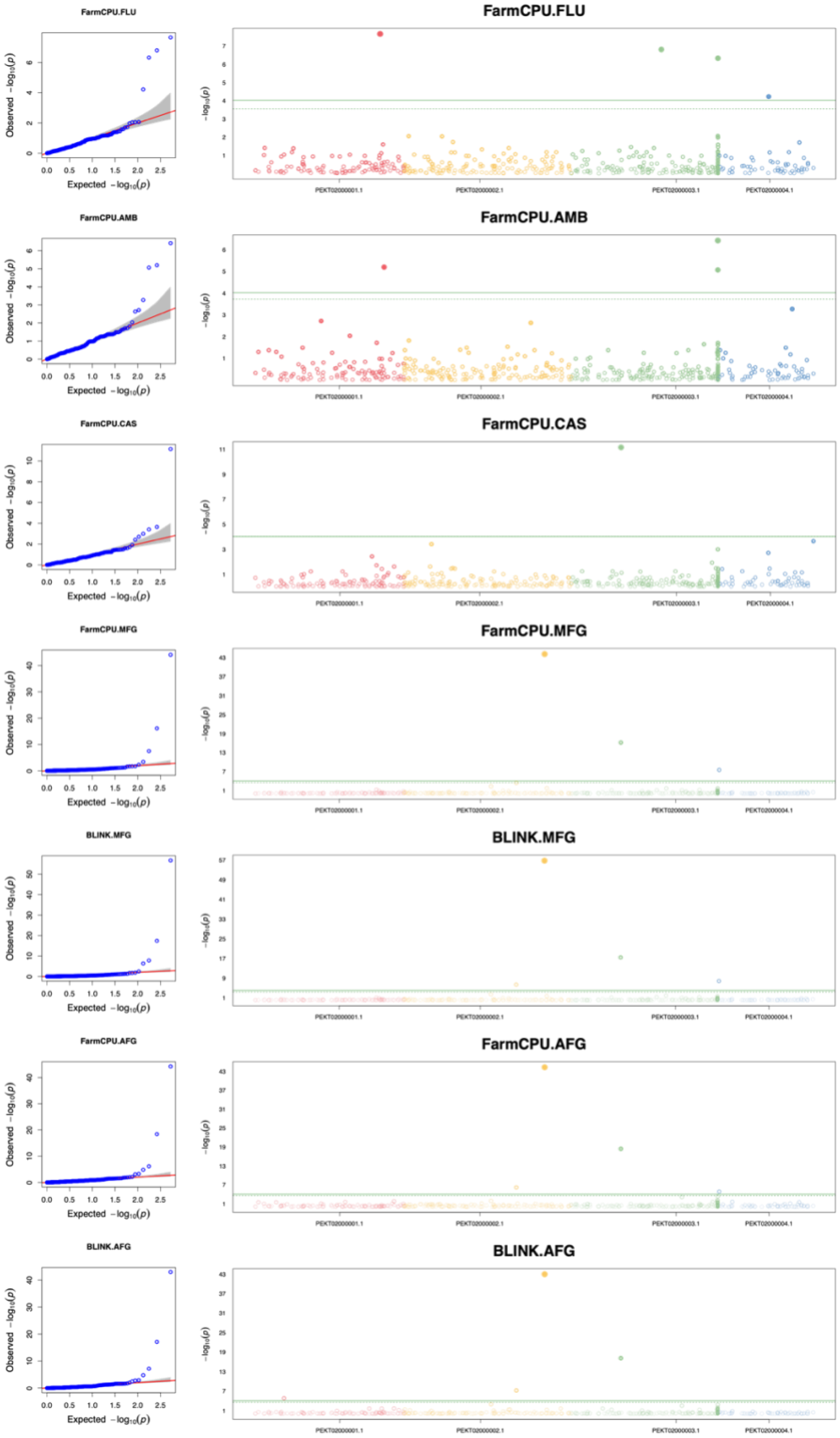
FarmCPU.FLU
FarmCPU.AMB
FarmCPU.CAS
FarmCPU.MFG
BLINK.MFG
FarmCPU.AFG
BLINK.AFG
Observed $-\log_{10}(p)$
Expected $-\log_{10}(p)$
$-\log_{10}(p)$

Figure 6. 2. Clade I QQ plots and Manhattan plots showing genome-wide SNPs associated with antifungal susceptibility. The left panel displays the QQ plots for five GWAS analyses, while the right panel presents the Manhattan plots. Plots are arranged from top to bottom in the following order: FLU, AMB, CAS, MFG, and AFG. The QQ plots display the expected -$\log_{10}$(p-value) on the X-axis and the observed -$\log_{10}$(p-value) on the Y-axis. The Manhattan plots are depicted with scaffold position on the X-axis and the -$\log_{10}$(p-value) on the Y-axis. The significant p-value threshold for the SNPs is represented by green lines on the Manhattan plots.

6.3.4 Clade III genome-wide association study

GWAS was performed for 9 antifungal drugs in Clade III, and significant associations were observed for 4 of these drugs. They are FLU, CAS, MFG, and AFG as shown in Figure 6. 3. Both BLINK and FarmCPU methods identified several SNPs linked to echinocandins susceptibility. However, due to discrepancies in the results obtained from these methods, the significant SNPs identified by both approaches were retained for further analysis (Table 6. 4).

We observed 10 SNPs that showed significant associations with FLU susceptibility in Clade III. Out of these 10 SNPs, two resulted in missense mutations, another two led to synonymous mutations, and the remaining six located in intergenic regions. All variants that located in coding regions were positively related to FLU MICs except for the SNP NW_021640165.1_3471968, which altered glycine to valine at position 756 of B9J08_003726p. The ortholog of the gene *B9J08_003726* in *C. albicans* is *C2_04360W_A*, which encodes a putative protein kinase involved in stress response (Nobile et al., 2003; Luther et al., 2023). The other missense SNP led to the conversion from alanine to serine at position 42 of B9J08_000558p. This gene has been predicted to be involved in transmembrane transport and an integral component of membrane localization (Skrzypek et al., 2017). Apart from the missense variants, two synonymous variants in *B9J08_004201* and *B9J08_000516* contributed to the increase of FLU MICs. Orthologs of the former gene are known to be involved in intracellular membrane transport and regulation of GTPase activity, while orthologs of the latter gene exhibit phospholipase A2 activity and play a role in cardiolipin acyl-chain remodeling (Skrzypek et al., 2017).

With respect to the three echinocandins, 15 SNPs were identified to have significant associations. The GWAS analysis for CAS identified 5 SNPs, among which the SNP NW_021640163.1_1501688 was found to be positively associated with both AFG and CAS tolerance. This SNP introduced a synonymous mutation in *B9J08_001552*, a gene with an undetermined function. Meanwhile, a missense variant, NW_021640164.1_366204, was solely identified associated CAS using FarmCPU, but with a weak effect. This variant converted arginine to serine at position 221 in B9J08_002399p. Its ortholog in *C. albicans* is Sup35p, a translation factor eRF3 (Resende et al., 2002). Another variant with weak association is NW_021640168.1_1068005 from gene *B9J08_005386*, which caused a premature stop codon. *B9J08_005386* was an uncharacterized gene but its protein product was predicted to have zinc ion binding activity (Skrzypek et al., 2017). On the other hand, a missense variant, NW_021640163.1_505104, was found associated with CAS susceptibility using BLINK. This SNP resulted in a Tyr236His mutation in the product of gene *B9J08_001308*. Its ortholog *EIP1* encodes a separase-binding protein in *C. albicans* and has been implicated in regulating cell wall integrity, filamentation, and response to antifungals (Sparapani et al., 2019).

Table 6. 4. Significant SNPs associated with antifungal susceptibility identified in Clade III GWAS.

Drug	SNP	MAF	nobs	FDR adjusted p-value	Effect	Parameters	Annotation	HGVS.c	HGVS.p	Gene	*Candida albicans* ortholog
FLU	NW_021640166.1_27489	0.04	111	1.05E-130	63.924	BLINK, PCA:8	synonymous	4041T>A	Thr1347Thr	*B9J08_004201*	*C4_05790W_A*
	NW_021640163.1_757345	0.03	111	1.44E-99	261.051		intergenic	-4102G>T			
	NW_021640164.1_51689	0.49	111	1.44E-99	260.855		intergenic	-781C>T			
	NW_021640164.1_51692	0.5	111	8.53E-99	261.523		intergenic	-784C>T			
	NW_021640168.1_1173685	0.01	111	3.69E-53	111.826		intergenic	-2970A>G			
	NW_021640164.1_773750	0.45	111	1.28E-49	-68.521		upstream	-867C>T			
	NW_021640162.1_73156	0.02	111	3.17E-49	34.103		synonymous	993C>T	Cys331Cys	*B9J08_000516*	*C6_00490W_A*
	NW_021640165.1_3471968	0.01	111	4.53E-36	-22.502		missense	2267G>T	Gly756Val	*B9J08_003726*	*C2_04360W_A*
	NW_021640162.1_147544	0.02	111	2.23E-26	21.65		missense	124G>T	Ala42Ser	*B9J08_000558*	*CR_09700W_A*
	NW_021640164.1_37868	0.02	111	1.01E-10	20.514		intergenic	-1343C>G			
CAS	NW_021640163.1_1501688	0.02	118	1.80E-83	1.922	FarmCPU, PCA:5	synonymous	1245C>T	Cys415Cys	*B9J08_001552*	*orf19.3701*
	NW_021640164.1_366204	0.02	118	4.70E-12	0.712		missense	663A>T	Arg221Ser	*B9J08_002399*	*SUP35*
	NW_021640168.1_1068005	0.01	118	0.0096	0.16		stop_gained	879C>A	Tyr293*	*B9J08_005386*	*C6_01620W_A*
	NW_021640163.1_1501688	0.02	118	5.38E-82	1.896	BLINK, PCA:5	synonymous	1245C>T	Cys415Cys	*B9J08_001552*	*orf19.3701*
	NW_021640163.1_505104	0.02	118	2.58E-06	0.591		missense	706T>C	Tyr236His	*B9J08_001308*	*EIP1*
	NW_021640164.1_51605	0.32	118	0.0138	-0.053		intergenic	-697C>T			
MFG	NW_021640162.1_404574	0.02	116	2.86E-124	-3.939	FarmCPU, PCA:5	intergenic	-4910C>G			
	NW_021640162.1_1734842	0.11	116	0.0045	0.069		intergenic	-1408A>G			
	NW_021640165.1_1713220	0.02	116	0.00036	0.111		missense	6345T>G	Asp2115Glu	*B9J08_002877*	*C4_06130W_A*
	NW_021640162.1_404574	0.02	116	5.63E-124	-3.942	BLINK, PCA:5	intergenic	-4910C>G			
	NW_021640162.1_564168	0.03	116	0.0019	0.145		synonymous	1203C>T	Pro401Pro	*B9J08_000751*	*CR_01410C_A*
	NW_021640165.1_1713220	0.02	116	0.0029	0.101		missense	6345T>G	Asp2115Glu	*B9J08_002877*	*C4_06130W_A*
AFG	NW_021640162.1_692140	0.02	119	1.15E-11	1.418	FarmCPU, PCA:5	missense	520A>T	Ser174Cys	*B9J08_000805*	*ZCF19*
	NW_021640163.1_1501688	0.02	119	1.00E-100	3.877		synonymous	1245C>T	Cys415Cys	*B9J08_001552*	*orf19.3701*
	NW_021640168.1_217077	0.03	119	0.0055	0.298		intergenic	-4324G>A			
	NW_021640165.1_1276391	0.05	119	2.29E-06	0.381		intergenic	-2259A>T			
	NW_021640163.1_1501688	0.02	119	1.74E-98	3.87	BLINK, PCA:5	synonymous	1245C>T	Cys415Cys	*B9J08_001552*	*orf19.3701*
	NW_021640162.1_1360735	0.18	119	0.0024	-0.393		intron	-2009G>A			
	NW_021640166.1_397189	0.03	119	0.00312	0.244		intergenic	-1210T>A			

Shared SNPs are highlighted in the same colors. MAF: Minor allele frequency; nobs: sample size; Effect: the increase of phenotype values due to the increase of genotype values per unit; Parameters: GWAS methods, numbers of principal components as covariates; HGVS: Human Genome Variation Society; HGVS.c: Variant using HGVS notation (DNA level); HGVS.p: Variant using HGVS notation (Protein level); Gene: the genes in which the specific coding-region SNPs are located.

Four SNPs were found to be associated with MFG susceptibility, and two of them were detected by both the BLINK and FarmCPU methods. Among the two shared SNPs, one, NW_021640165.1_1713220, resulted in a missense mutation, resulting in an amino acid change from aspartic acid to glutamic acid in the product of gene *B9J08_002877*. Its orthologs have tubulin binding activity (Skrzypek et al., 2017). In addition, BLINK found another SNP in coding sequence, but it produced a synonymous mutation in a putative gene of unknown function.

A missense variant and a synonymous variant were identified in a positive relationship to AFG tolerance. The missense SNP NW_021640162.1_692140 triggered a Ser174Cys mutation in the protein product of gene *B9J08_000805*. Its ortholog in *C. albicans* is *ZCF19*, which is predicted to be a Zn(II)2Cys6 transcription factor (Maicas et al., 2005). Additionally, the synonymous variant related to AFG susceptibility was also found to be associated with CAS susceptibility.

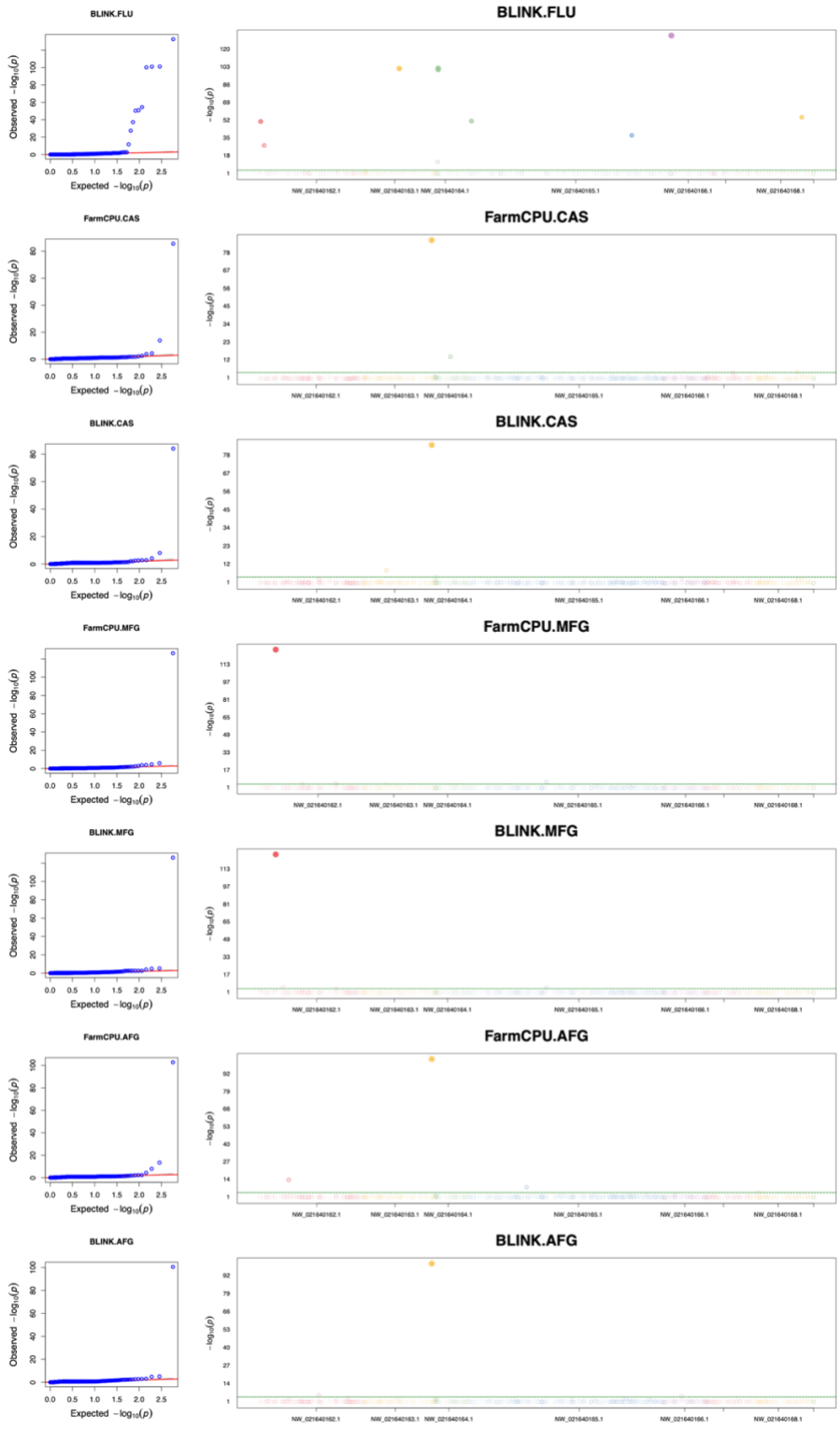

Figure 6. 3. Clade III QQ plots and Manhattan plots showing genome-wide SNPs associated with antifungal susceptibility. The left panel displays the QQ plots for five GWAS analyses, while the right panel presents

the Manhattan plots. Plots are arranged from top to bottom in the following order: FLU, CAS (FarmCPU; BLINK), MFG (FarmCPU; BLINK), and AFG (FarmCPU; BLINK). The QQ plots display the expected -$\log_{10}$(p-value) on the X-axis and the observed -$\log_{10}$(p-value) on the Y-axis. The Manhattan plots are depicted with scaffold position on the X-axis and the -$\log_{10}$(p-value) on the Y-axis. The significant p-value threshold for the SNPs is represented by green lines on the Manhattan plots.

6.3.5 Clade IV genome-wide association study

GWAS analysis was conducted on 8 antifungals for Clade IV strains and significant associations were identified for three antifungal drugs. They include VOR, CAS, and MFG, among which CAS associated SNPs were identified using both methods (Figure 6. 4). The details of the significant SNPs are listed in Table 6. 5.

Three SNPs were found to be associated with VOR susceptibility in Clade IV and all of them introduced missense mutations. In particular, the SNP CP043444.1_1566757 resulted in a Phe132Tyr mutation in gene *ERG11*, which encodes lanosterol 14-alpha-demethylase, an essential enzyme for ergosterol biosynthesis. This mutation has been frequently reported from FLU resistant *C. auris* strains (Aljindan et al., 2020; Anuradha Chowdhary et al., 2018; Healey et al., 2018). However, the other two missense variants have not been reported associated with antifungal susceptibility. One of these variants, CP043442.1_1367963, led to a Ser1443Leu mutation in gene *B9J08_003473*. While this gene has not been fully characterized, its orthologs have been discovered to have diverse roles and activities, such as binding to signal sequences and participating in different transport processes (Skrzypek et al., 2017). The second variant identified to be associated with VOR is CP043444.1_1393470, which caused a Asn39Ile mutation in gene *B9J08_001368*. Its orthologs show glycerone kinase activity and affect cellular response to toxic substance (Skrzypek et al., 2017).

Five SNPs each were identified linked to CAS susceptibility using both FarmCPU and BLINK methods. Among the five SNPs, three were detected by both methods. They are intergenic variant CP043443.1_1796780, missense variant CP043443.1_2100709, and

stop-gained variant CP043444.1_498630. The variant CP043443.1_2100709 resulted in a replacement of serine to proline at position 639 in Fks1p. This mutation has been reported to be exclusively present in strains not susceptible to caspofungin (Kordalewska et al., 2018; Chaabane et al., 2019). On the other hand, FarmCPU identified two extra missense variants. One is CP043442.1_1778999 converting phenylalanine to leucine at position 1098 in the protein product of gene *B9J08_003281*. Its orthologs have protein kinase activity. The other one, CP043446.1_343550, in *B9J08_004612* led to a Pro163Leu mutation. Orthologs of *B9J08_004612* exhibit mRNA binding activity (Jong Hwan Jung et al., 2014).

In the context of MFG GWAS, three variants were identified. Among them, one is SNP CP043444.1_498630, which was also identified associated with CAS susceptibility. In addition, two missense variants demonstrated a negative effect on MFG tolerance. They are located in two uncharacterized genes. *B9J08_002701* is associated with GTP binding, GTPase activity, and ribosome binding activity. *B9J08_003827*, on the other hand, has been predicted to be involved in ascospore formation and ascospore wall assembly. (Skrzypek et al., 2017)

Table 6. 5. Significant SNPs associated with antifungal susceptibility identified in Clade IV GWAS.

Drug	SNP	MAF	nobs	FDR adjusted p-value	Effect	Parameters	Annotation	HGVS.c	HGVS.p	Gene	*Candida albicans* ortholog
VOR	CP043444.1_1566757	0.023	88	7.66E-52	-1.76	FarmCPU, PCA:10	missense	c.395T>A	p.Phe132Tyr	*B9J08_001448*	*ERG11*
	CP043442.1_1367963	0.011	88	2.35E-15	0.367		missense	c.4328C>T	p.Ser1443Leu	*B9J08_003473*	*PEP1*
	CP043444.1_1393470	0.023	88	0.00041	0.111		missense	c.116A>T	p.Asn39Ile	*B9J08_001368*	*DAK2*
CAS	CP043442.1_1778999	0.01	96	7.77E-15	0.464	FarmCPU, PCA:12	missense	c.3292T>C	p.Phe1098Leu	*B9J08_003281*	*RIM15*
	CP043443.1_1796780	0.094	96	1.50E-05	0.228		intergenic	c.-4835A>G			
	CP043443.1_2100709	0.021	96	1.04E-32	4.725		missense	c.1915T>C	p.Ser639Pro	*B9J08_000964*	*FKS1*
	CP043444.1_498630	0.141	96	0.00044	0.144		stop_gained	c.964A>T	p.Arg322*	*B9J08_002136*	*WOR2*
	CP043446.1_343550	0.083	96	9.95E-05	0.093		missense	c.488C>T	p.Pro163Leu	*B9J08_004612*	*EDC3*
	CP043443.1_2100709	0.021	96	2.38E-34	4.551	BLINK, PCA:12	missense	c.1915T>C	p.Ser639Pro	*B9J08_000964 (FKS1)*	*FKS1*
	CP043443.1_1645903	0.01	96	2.33E-14	-0.464		synonymous	c.600G>A	p.Glu200Glu	*B9J08_000760*	*C4_01930C_A*
	CP043444.1_498630	0.141	96	9.68E-06	0.162		stop_gained	c.964A>T	p.Arg322*	*B9J08_002136*	*WOR2*
	CP043443.1_1796780	0.094	96	0.000367	0.206		intergenic	c.-4835A>G			
	CP043442.1_182935	0.083	96	0.00625	-0.077		intergenic	c.-4482C>T			
MFG	CP043442.1_514989	0.011	92	4.55E-53	-4.452	BLINK, PCA:5	missense	c.400G>C	p.Gly134Arg	*B9J08_002701*	*C7_04260W_A*
	CP043442.1_613136	0.011	92	1.05E-13	-0.797		missense	c.590C>T	p.Pro197Leu	*B9J08_003827*	*C2_10320C_A*
	CP043444.1_498630	0.147	92	3.14E-06	0.321		stop_gained	c.964A>T	p.Arg322*	*B9J08_002136*	*WOR2*

Shared SNPs are highlighted in the same colors. MAF: Minor allele frequency; nobs: sample size; Effect: the increase of phenotype values due to the increase of genotype values per unit; Parameters: GWAS methods, numbers of principal components as covariates; HGVS: Human Genome Variation Society; HGVS.c: Variant using HGVS notation (DNA level); HGVS.p: Variant using HGVS notation (Protein level); Gene: the genes in which the specific coding-region SNPs are located.

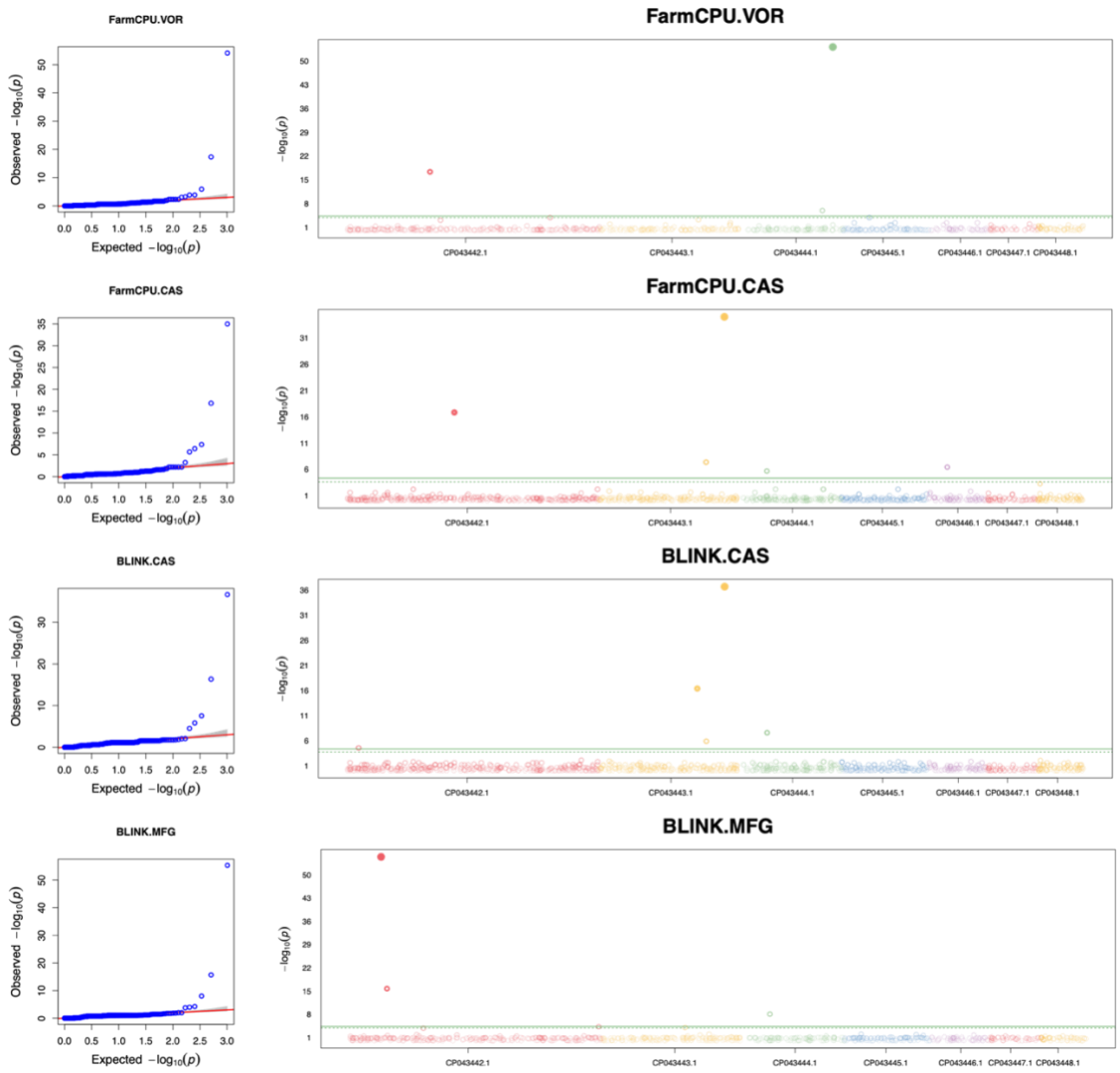

Figure 6. 4. Clade IV QQ plots and Manhattan plots showing genome-wide SNPs associated with antifungal susceptibility. The left panel displays the QQ plots for three GWAS analyses, while the right panel presents the Manhattan plots. Plots are arranged from top to bottom in the following order: VOR, CAS (FarmCPU; BLINK), and MFG. The QQ plots display the expected -$\log_{10}$(p-value) on the X-axis and the observed -$\log_{10}$(p-value) on the Y-axis. The Manhattan plots are depicted with scaffold position on the X-axis and the -$\log_{10}$(p-value) on the Y-axis. The significant p-value threshold for the SNPs is represented by green lines on the Manhattan plots.

6.3.6 Noncoding SNPs associated with antifungal susceptibility

Overall, there are 20 noncoding SNPs associated with antifungal susceptibility as uncovered by GWAS from individual clades (Table 6. 6). Noncoding SNPs located in gene

regulatory elements usually have impacts on the gene expression, thereby affecting traits of interest. However, it can be challenging to infer which genes are controlled by these noncoding SNPs based on the current data. In addition, some intergenic SNPs could be identified as quantitative trait nucleotides because they are linked to SNPs located within coding sequences. Therefore, we performed four-gamete tests and linkage disequilibrium tests between SNPs in noncoding and coding sequences. The four-gamete tests and linkage disequilibrium tests on individual clades discovered that four SNPs of Clade I, including PEKT02000001.1_897129, PEKT02000003.1_642734, PEKT02000004.1_361235, and PEKT02000001.1_212518, were linked to the SNP PEKT02000002.1_1006624 which has been demonstrated to confer echinocandin resistance in *C. auris*. Of note, two of them had negative effects on FLU MICs, whereas one had a positive effect on FLU MICs. The last one had a mild negative effect on AFG MICs. On top of that, two intergenic SNPs were found to be linked with each other in Clade III.

Table 6. 6. Details of noncoding SNPs in linkage disequilibrium with other significant SNPs.

Clade	Drug	SNP	MAF	nobs	FDR adjusted p-value	Effect	Significant linked SNPs	r2	FDR adjusted p-value for linked SNPs
I	FLU	PEKT02000001.1_897129	0.03	152	1.14E-05	-84.241	PEKT02000002.1_1006624	0.071	0.0022
		PEKT02000003.1_642734	0.03	152	4.08E-05	181.497	PEKT02000002.1_1006624	0.199	3.68E-08
		PEKT02000003.1_1045994	0.023	152	8.23E-05	181.022	-	-	
		PEKT02000004.1_361235	0.079	152	0.00789	-72.382	PEKT02000002.1_1006624	0.412	3.21E-14
	AMB	PEKT02000003.1_1045418	0.06	174	0.0002	-1.816	-	-	-
		PEKT02000003.1_1045419	0.049	174	0.00151	4.424	-	-	-
	AFG	PEKT02000001.1_212518	0.03	165	0.00224	-0.69	PEKT02000002.1_1006624	0.072	0.00215
III	FLU	NW_021640163.1_757345	0.027	111	1.44E-99	261.051	-	-	-
		NW_021640164.1_51689	0.4865	111	1.44E-99	260.855	-	-	-
		NW_021640164.1_51692	0.4955	111	8.53E-99	261.523	-	-	-
		NW_021640168.1_1173685	0.0135	111	3.69E-53	111.826	-	-	-
		NW_021640164.1_773750	0.4505	111	1.28E-49	-68.521	-	-	-
		NW_021640164.1_37868	0.018	111	1.01E-10	20.514	-	-	-
	CAS	NW_021640164.1_51605	0.3178	118	0.0138	-0.053	NW_021640165.1_1276391	0.135	0.0119
	MFG	NW_021640162.1_404574	0.0172	116	2.86E-124	-3.939	-	-	-
		NW_021640162.1_1734842	0.1121	116	0.0045	0.069	-	-	-
		NW_021640162.1_404574	0.0172	116	5.63E-124	-3.942	-	-	-
	AFG	NW_021640168.1_217077	0.0252	119	0.0055	0.298	-	-	-
		NW_021640165.1_1276391	0.0462	119	2.29E-06	0.381	NW_021640164.1_51605	0.135	0.0119
		NW_021640162.1_1360735	0.1807	119	0.0024	-0.393	-	-	-
		NW_021640166.1_397189	0.0294	119	0.00312	0.244	-	-	-
IV	CAS	CP043443.1_1796780	0.094	96	1.50E-05	0.228	-	-	-
		CP043443.1_1796780	0.094	96	0.000367	0.206	-	-	-
		CP043442.1_182935	0.083	96	0.00625	-0.077	-	-	-

Shared SNPs are highlighted in the same colors. MAF: Minor allele frequency; nobs: sample size; Effect: the increase of phenotype values due to the increase of genotype values per unit; r2: linkage disequilibrium measure.

The linkage disequilibrium analysis showed that 16 noncoding SNPs were not linked to the identified drug associated SNPs in coding sequences. Therefore, we hypothesized that those SNPs could affect the expression of adjacent genes (Table 6. S2). We then carried out GO enrichment analysis on 26 adjacent genes to investigate their relationship with antifungal susceptibility. Due to that *C. auris* annotation was not incorporated in Fungifun, we performed GO enrichment analysis on their orthologs in *C. albicans* SC5314. 24 orthologs were identified using BLAST. Genes orf19.6520, orf19.4779, and orf19.4031 were enriched in 6 GO terms. They include transmembrane transport, drug transmembrane transport, drug transmembrane transporter activity, hydrolase activity, and integral component of membrane (Table 6. 7). SNPs adjacent to these genes were NW_021640164.1_37868, and NW_021640164.1_773750 associated with FLU MICs in Clade III as well as all the three SNPs associated with FLU/AMB MICs in Clade I.

Table 6. 7. GO enrichment analysis genes flanking the 16 noncoding SNPs.

GO ID	GO name	Gene ID(s)	Exact p-value	Adjusted p-value	# genes | category	# genes | input
GO:0055085	transmembrane transport	orf19.6520 | orf19.4779	0.004520505	0.01679101	2 | 232	2 | 24
GO:0006855	drug transmembrane transport	orf19.4779	0.005597002	0.01679101	1 | 11	1 | 24
GO:0015238	drug transmembrane transporter activity	orf19.4779	0.005597002	0.01679101	1 | 11	1 | 24
GO:0004553	hydrolase activity, hydrolyzing O-glycosyl compounds	orf19.4031	0.01471062	0.02738752	1 | 29	1 | 24
GO:0016798	hydrolase activity, acting on glycosyl bonds	orf19.4031	0.01521529	0.02738752	1 | 30	1 | 24
GO:0016021	integral component of membrane	orf19.6520 | orf19.4779	0.02426908	0.03640362	2 | 547	2 | 24

Exact p-value: Exact p-value which is calculated by Fisher's exact test; # genes | category: Number of assigned genes to this category; # genes | input: Number of assigned genes out of the entered gene IDs.

6.4 Discussion

In this study, we investigated molecular mechanisms underlying the antifungal susceptibility differences in *C. auris*. To the best of our knowledge, this study encompasses all documented *C. auris* samples containing genomic data and MIC profiles. We examined the SNPs in genes known to confer or related to antifungal resistance for individual clades

and identified clade-shared SNPs between clades. Totally, there are three shared SNPs between Clades I and IV, 1 between Clades I and III, and 0 between Clades III and IV. Although Clades I and IV exhibit greater genetic distance compared to Clades I and III, more antifungal related SNPs are shared between Clades I and IV.

We specifically analyzed the genomic variants within individual clades to eliminate the effect of population structure in this fungus.

For each clade, a range of 11 to 24 candidate antifungal-related SNPs were identified. Interestingly, Ser639 mutation in *FKS1* was found associated with echinocandins MICs for both Clades I and IV. Notably, other SNPs related to specific antifungal drugs didn't overlap between clades, indicating the existence of distinct genomic variations that influence drug susceptibility within each clade. This highlights the importance of considering clade-specific genomic variations when studying the mechanisms of drug resistance in the development of antifungal treatments.

The mechanisms of several newly identified mutations underlying antifungal tolerance could not be inferred due to the incomplete annotation of *C. auris* genome. Furthermore, it is worth noting that certain genomic regions lack orthologs in closely related species. This phenomenon is not limited at species level but has also been observed at clade level within species (Lockhart et al., 2017b). Therefore, improved annotation of *C. auris* genomes, encompassing not only a single clade but all the clades within the species are needed.

This study also has some limitations. For example, the antifungal susceptibility profiles in previous research were generated using different standards. They include Clinical and Laboratory Standards Institute (CLSI), European Committee on Antimicrobial Susceptibility Testing (EUCAST), Sensititre YeastOne panels (SYO), Etest, and the Vitek system. Therefore, slight variations in MIC values can still occur when using different standards. Essential agreement (EA) and categorical agreement (CA) are two indexes used

to assess the agreement between different standards. The former refers to the discrepancies in MICs with no more than +/– 2-fold dilutions, while the latter indicates the agreement in the categorization of samples as susceptible or resistant. In our dataset, 57.8% of the samples had their profiles determined using the CLSI, and 38.2% using SYO. The two methods, SYO and CLSI, showed great CA and EA consistence for echinocandins but a low CA value for azoles, as reported for *Candida spp.* by various studies (Altinbaş et al., 2020; Cuenca-Estrella et al., 2010; Espinel-Ingroff et al., 1999). Therefore, the MICs for echinocandins may be more accurate as compared to azoles. This could potentially explain why a higher number of genomic variants were identified associated with echinocandins compared to azoles. Additionally, we observed minimal variation in the MICs of individual drugs within each clade (Figure 6. 1), which might explain why we did not identify quantitative trait related SNPs for several other drugs. Another factor is that there is no MIC data for many strains with genome sequence data. Among the total of 4,303 strains with available genomic data, antifungal susceptibility profiles were only collected for 408 strains.

The other limitation is the sample size, with five clades available for this species, we only collected sufficient samples for Clades I, III and IV. Currently, there are only 5 Clade V strains with available genomic data and MIC data. Regarding Clade II, antifungal susceptibility profiles were only available for 12 strains. Therefore, to achieve a comprehensive understanding of the antifungal resistance mechanisms in this species, it is essential to obtain more samples from Clades II and V as well.

6.5 Conclusions

In this study, we performed GWAS analyses on Clades I, III, and IV strains of *C. auris* with published MIC values and genomic data. For each clade, we examined 8 or 9 antifungal drugs and identified 48 antifungal related SNPs in *C. auris*. Specifically, within Clade I, a total of 12 SNPs were identified, with 5 occurring in coding regions and 7 in noncoding regions. In Clade III, 24 SNPs were identified, with 11 in coding regions and 13

in noncoding regions. Clade IV exhibited 12 identified SNPs, with 10 in coding regions and 2 in noncoding regions. Those SNPs were shown to have various impacts on antifungal susceptibility, some with positive effects, while others with negative effects. Some SNPs occurring in coding regions have been proved to confer antifungal resistance according to previous research. Some occurring in noncoding regions with their flanking genes exhibiting activities in drug transmembrane transport, hydrolase activity and integral component of membrane. Many novel SNPs have been identified and their roles in antifungal resistance need to be further validated. Taken together, our findings contributed to a better understanding of the antifungal mechanisms employed by *C. auris*. Furthermore, these identified antifungal related variants could serve as diagnostic markers for quick drug resistance detection and/or new drug targets in clinics.

Supplementary Data

Table 6. S1. Details of samples used in this study.

Table 6. S2. Genes adjacent to the 16 noncoding SNPs independent of linkage to coding SNPs.

Table 6. S3. SNPs in reported antifungal resistance genes.

Data can be accessed at: https://docs.google.com/spreadsheets/d/1n1wb_pvj4ZKBADFq-zqdQ6o3sVcCCEEgDsxRe2MVoYY/edit?usp=sharing

References

Aljindan, Reem, Doaa M. Aleraky, Nehal Mahmoud, Baha Abdalhamid, Mashael Almustafa, Sayed Abdulazeez, and J. Francis Borgio. 2020. “Drug Resistance-Associated Mutations in *ERG11* of Multidrug-Resistant *Candida auris* in a Tertiary Care Hospital of Eastern Saudi Arabia.” *Journal of Fungi (Basel, Switzerland)* 7 (1): 1–9. https://doi.org/10.3390/JOF7010018.

Altinbaş, Rabiye, Ayşe Bariş, Sümeyye Şen, Recep Öztürk, and Nuri Kiraz. 2020. “Comparison of the Sensititre YeastOne Antifungal Method with the CLSI M27-A3 Reference Method to Determine the Activity of Antifungal Agents against Clinical

Isolates of *Candida* Spp." *Turkish Journal of Medical Sciences* 50 (8): 2024. https://doi.org/10.3906/SAG-1909-97.

Arora, Parth, Prerna Singh, Yue Wang, Anamika Yadav, Kalpana Pawar, Ashutosh Singh, Gadi Padmavati, Jianping Xu, and Anuradha Chowdhary. 2021. "Environmental Isolation of *Candida auris* from the Coastal Wetlands of Andaman Islands, India." Edited by Leah E. Cowen. *MBio* 12 (2): 1–9. https://doi.org/10.1128/mBio.03181-20.

Bolger, Anthony M., Marc Lohse, and Bjoern Usadel. 2014. "Trimmomatic: A Flexible Trimmer for Illumina Sequence Data." *Bioinformatics* 30 (15): 2114–20. https://doi.org/10.1093/BIOINFORMATICS/BTU170.

Camacho, Christiam, George Coulouris, Vahram Avagyan, Ning Ma, Jason Papadopoulos, Kevin Bealer, and Thomas L. Madden. 2009. "BLAST+: Architecture and Applications." *BMC Bioinformatics* 10 (1): 1–9. https://doi.org/10.1186/1471-2105-10-421.

Casadevall, Arturo, Dimitrios P. Kontoyiannis, and Vincent Robert. 2019. "On the Emergence of *Candida auris*: Climate Change, Azoles, Swamps, and Birds." *MBio* 10 (4). https://doi.org/10.1128/MBIO.01397-19/

Chaabane, Farid, Artan Graf, Léonard Jequier, and Alix T. Coste. 2019. "Review on Antifungal Resistance Mechanisms in the Emerging Pathogen *Candida auris*." *Frontiers in Microbiology* 10 (November). https://doi.org/10.3389/FMICB.2019.02788.

Chow, Nancy A., José F. Muñoz, Lalitha Gade, Elizabeth L. Berkow, Xiao Li, Rory M. Welsh, Kaitlin Forsberg, et al. 2020. "Tracing the Evolutionary History and Global Expansion of *Candida auris* Using Population Genomic Analyses." *MBio* 11 (2). https://doi.org/10.1128/MBIO.03364-19.

Chowdhary, Anuradha, Anupam Prakash, Cheshta Sharma, Milena Kordalewska, Anil Kumar, Smita Sarma, Bansidhar Tarai, et al. 2018. "A Multicentre Study of Antifungal Susceptibility Patterns among 350 *Candida auris* Isolates (2009-17) in India: Role of the *ERG11* and *FKS1* Genes in Azole and Echinocandin Resistance." *The Journal of Antimicrobial Chemotherapy* 73 (4): 891–99. https://doi.org/10.1093/JAC/DKX480.

Cingolani, Pablo, Adrian Platts, Le Lily Wang, Melissa Coon, Tung Nguyen, Luan Wang, Susan J. Land, Xiangyi Lu, and Douglas M. Ruden. 2012. "A Program for Annotating and Predicting the Effects of Single Nucleotide Polymorphisms, SnpEff: SNPs in the Genome of *Drosophila Melanogaster* Strain W1118; Iso-2; Iso-3." *Fly* 6 (2): 80–92. https://doi.org/10.4161/fly.19695.

Cuenca-Estrella, Manuel, Alicia Gomez-Lopez, Ana Alastruey-Izquierdo, Leticia Bernal-Martinez, Isabel Cuesta, Maria J. Buitrago, and Juan L. Rodriguez-Tudela. 2010. "Comparison of the Vitek 2 Antifungal Susceptibility System with the Clinical and Laboratory Standards Institute (CLSI) and European Committee on Antimicrobial Susceptibility Testing (EUCAST) Broth Microdilution Reference Methods and with the Sensititre YeastOne and Etest Techniques for In Vitro Detection of Antifungal Resistance in Yeast Isolates." *Journal of Clinical Microbiology* 48 (5): 1782. https://doi.org/10.1128/JCM.02316-09.

Ellwanger, Joel Henrique, and José Artur Bogo Chies. 2022. "*Candida auris* Emergence as a Consequence of Climate Change: Impacts on Americas and the Need to Contain Greenhouse Gas Emissions." *The Lancet Regional Health - Americas* 11 (July). https://doi.org/10.1016/j.lana.2022.100250.

Espinel-Ingroff, A., M. Pfaller, S. A. Messer, C. C. Knapp, S. Killian, H. A. Norris, and M. A. Ghannoum. 1999. "Multicenter Comparison of the Sensititre YeastOne Colorimetric Antifungal Panel with the National Committee for Clinical Laboratory Standards M27-A Reference Method for Testing Clinical Isolates of Common and Emerging *Candida* spp., Cryptococcus Spp., and Other Yeasts and Yeast-Like Organisms." *Journal of Clinical Microbiology* 37 (3): 591–95. https://doi.org/10.1128/JCM.37.3.591-595.1999.

Frías-De-león, María Guadalupe, Rigoberto Hernández-Castro, Tania Vite-Garín, Roberto Arenas, Alexandro Bonifaz, Laura Castañón-Olivares, Gustavo Acosta-Altamirano, and Erick Martínez-Herrera. 2020. "Antifungal Resistance in *Candida auris*: Molecular Determinants." *Antibiotics* 9 (9): 1–16. https://doi.org/10.3390/ANTIBIOTICS9090568.

Healey, Kelley R., Milena Kordalewska, Cristina Jiménez Ortigosa, Ashutosh Singh, Indira Berrío, Anuradha Chowdhary, and David S. Perlin. 2018. "Limited *ERG11* Mutations Identified in Isolates of *Candida auris* Directly Contribute to Reduced Azole Susceptibility." *Antimicrobial Agents and Chemotherapy* 62 (10). https://doi.org/10.1128/AAC.01427-18.

Huang, Meng, Xiaolei Liu, Yao Zhou, Ryan M. Summers, and Zhiwu Zhang. 2019. "BLINK: A Package for the next Level of Genome-Wide Association Studies with Both Individuals and Markers in the Millions." *GigaScience* 8 (2): 1–12. https://doi.org/10.1093/GIGASCIENCE/GIY154.

Jung, Jong Hwan, and Jinmi Kim. 2014. "Roles of Edc3 in the Oxidative Stress Response and CaMCA1-Encoded Metacaspase Expression in *Candida albicans*." *The FEBS Journal* 281 (21): 4841–51. https://doi.org/10.1111/FEBS.13022.

Kempf, Marie, Véronique Apaire-Marchais, Patrick Saulnier, Patricia Licznar, Corinne Lefrançois, Raymond Robert, and Jane Cottin. 2007. "Disruption of *Candida albicans* IFF4 Gene Involves Modifications of the Cell Electrical Surface Properties." *Colloids and Surfaces. B, Biointerfaces* 58 (2): 250–55. https://doi.org/10.1016/J.COLSURFB.2007.03.017.

Kordalewska, Milena, Annie Lee, Steven Park, Indira Berrio, Anuradha Chowdhary, Yanan Zhao, and David S. Perlin. 2018. "Understanding Echinocandin Resistance in the Emerging Pathogen *Candida* auris." *Antimicrobial Agents and Chemotherapy* 62 (6). https://doi.org/10.1128/AAC.00238-18.

Lee, Wee Gyo, Jong Hee Shin, Young Uh, Min Gu Kang, Soo Hyun Kim, Kyung Hwa Park, and Hee Chang Jang. 2011. "First Three Reported Cases of Nosocomial Fungemia Caused by *Candida* auris." *Journal of Clinical Microbiology* 49 (9): 3139–42. https://doi.org/10.1128/JCM.00319-11.

Liu, Xiaolei, Meng Huang, Bin Fan, Edward S. Buckler, and Zhiwu Zhang. 2016. "Iterative Usage of Fixed and Random Effect Models for Powerful and Efficient Genome-Wide Association Studies." *PLOS Genetics* 12 (2): e1005767. https://doi.org/10.1371/JOURNAL.PGEN.1005767.

Lockhart, Shawn R., Kizee A. Etienne, Snigdha Vallabhaneni, Joveria Farooqi, Anuradha Chowdhary, Nelesh P. Govender, Arnaldo Lopes Colombo, et al. 2017. "Simultaneous Emergence of Multidrug-Resistant *Candida auris* on 3 Continents Confirmed by Whole-Genome Sequencing and Epidemiological Analyses." *Clinical Infectious Diseases* 64 (2): 134–40. https://doi.org/10.1093/CID/CIW691.

Luther, Christian H., Philipp Brandt, Slavena Vylkova, Thomas Dandekar, Tobias Müller, and Marcus Dittrich. 2023. "Integrated Analysis of SR-like Protein Kinases Sky1 and Sky2 Links Signaling Networks with Transcriptional Regulation in *Candida albicans*." *Frontiers in Cellular and Infection Microbiology* 13: 1108235. https://doi.org/10.3389/FCIMB.2023.1108235.

Maertens, Johan A. 2004. "History of the Development of Azole Derivatives." *Clinical Microbiology and Infection* 10 (SUPPL. 1): 1–10. https://doi.org/10.1111/j.1470-9465.2004.00841.x.

Maicas, Sergi, Inmaculada Moreno, Almudena Nieto, Micaela Gómez, Rafael Sentandreu, and Eulogio Valentín. 2005. "In Silico Analysis for Transcription Factors with Zn(II)(2)C(6) Binuclear Cluster DNA-Binding Domains in *Candida albicans*." *Comparative and Functional Genomics* 6 (7–8): 345–56. https://doi.org/10.1002/CFG.492.

McKenna, Aaron, Matthew Hanna, Eric Banks, Andrey Sivachenko, Kristian Cibulskis, Andrew Kernytsky, Kiran Garimella, et al. 2010. "The Genome Analysis Toolkit: A MapReduce Framework for Analyzing next-Generation DNA Sequencing Data." *Genome Research* 20 (9): 1297–1303. https://doi.org/10.1101/GR.107524.110.

Morris, Michele I., and Mark Villmann. 2006. "Echinocandins in the Management of Invasive Fungal Infections, Part 2." *American Journal of Health-System Pharmacy : AJHP : Official Journal of the American Society of Health-System Pharmacists* 63 (19): 1813–20. https://doi.org/10.2146/AJHP050464.P2.

Muñoz, José F., Lalitha Gade, Nancy A. Chow, Vladimir N. Loparev, Phalasy Juieng, Elizabeth L. Berkow, Rhys A. Farrer, Anastasia P. Litvintseva, and Christina A. Cuomo. 2018. "Genomic Insights into Multidrug-Resistance, Mating and Virulence

in *Candida auris* and Related Emerging Species." *Nature Communications*. https://doi.org/10.1038/s41467-018-07779-6.

Nobile, Clarissa J., Vincent M. Bruno, Mathias L. Richard, Dana A. Davis, and Aaron P. Mitchell. 2003. "Genetic Control of Chlamydospore Formation in *Candida albicans*." *Microbiology (Reading, England)* 149 (Pt 12): 3629–37. https://doi.org/10.1099/MIC.0.26640-0.

Priebe, Steffen, Jörg Linde, Daniela Albrecht, Reinhard Guthke, and Axel A. Brakhage. 2011. "FungiFun: A Web-Based Application for Functional Categorization of Fungal Genes and Proteins." *Fungal Genetics and Biology* 48 (4): 353–58. https://doi.org/10.1016/J.FGB.2010.11.001.

Resende, Catarina, Steven N. Parham, Caroline Tinsley, Paulo Ferreira, Júlio A.B. Duarte, and Mick F. Tuite. 2002. "The *Candida albicans* Sup35p Protein (CaSup35p): Function, Prion-like Behaviour and an Associated Polyglutamine Length Polymorphism." *Microbiology (Reading, England)* 148 (Pt 4): 1049–60. https://doi.org/10.1099/00221287-148-4-1049.

Sahl, Jason W., Darrin Lemmer, Jason Travis, James M. Schupp, John D. Gillece, Maliha Aziz, Elizabeth M. Driebe, et al. 2016. "NASP: An Accurate, Rapid Method for the Identification of SNPs in WGS Datasets That Supports Flexible Input and Output Formats." *Microbial Genomics* 2 (8): e000074. https://doi.org/10.1099/MGEN.0.000074.

Satoh, Kazuo, Koichi Makimura, Yayoi Hasumi, Yayoi Nishiyama, Katsuhisa Uchida, and Hideyo Yamaguchi. 2009. "*Candida auris*, a Novel Ascomycetous Yeast Isolated from the External Ear Canal of an Inpatient in a Japanese Hospital." *Microbiology and Immunology* 53 (1): 41–44. https://doi.org/10.1111/J.1348-0421.2008.00083.X.

Sharma, Dipti, Raees A. Paul, Shivaprakash M. Rudramurthy, Nisha Kashyap, Sanjay Bhattacharya, Rajeev Soman, Shamanth A. Shankarnarayan, et al. 2022. "Impact of FKS1 Genotype on Echinocandin In Vitro Susceptibility in *Candida auris* and In Vivo Response in a Murine Model of Infection." *Antimicrobial Agents and Chemotherapy* 66 (1). https://doi.org/10.1128/AAC.01652-21.

Shen, Hui, Mao Mao An, De Jun Wang, Zheng Xu, Jun Dong Zhang, Ping Hui Gao, Ying Ying Cao, Yong Bing Cao, and Yuan Ying Jiang. 2007. "Fcr1p Inhibits Development of Fluconazole Resistance in *Candida albicans* by Abolishing *CDR1* Induction." *Biological & Pharmaceutical Bulletin* 30 (1): 68–73. https://doi.org/10.1248/BPB.30.68.

Silverman, Richard B., and Mark W. Holladay. 2015. "The Organic Chemistry of Drug Design and Drug Action: Third Edition." *The Organic Chemistry of Drug Design and Drug Action: Third Edition*, 1–517. https://doi.org/10.1016/C2009-0-64537-2.

Skrzypek, Marek S., Jonathan Binkley, Gail Binkley, Stuart R. Miyasato, Matt Simison, and Gavin Sherlock. 2017. "The *Candida* Genome Database (CGD): Incorporation of Assembly 22, Systematic Identifiers and Visualization of High Throughput Sequencing Data." *Nucleic Acids Research* 45 (Database issue): D592. https://doi.org/10.1093/NAR/GKW924.

Sparapani, Samantha, and Catherine Bachewich. 2019. "Characterization of a Novel Separase-Interacting Protein and *Candida*te New Securin, Eip1p, in the Fungal Pathogen *Candida albicans*." *Molecular Biology of the Cell* 30 (19): 2469. https://doi.org/10.1091/MBC.E18-11-0696.

Talibi, Driss, and Martine Raymond. 1999. "Isolation of a Putative *Candida albicans* Transcriptional Regulator Involved in Pleiotropic Drug Resistance by Functional Complementation of a Pdr1 Pdr3 Mutation in Saccharomyces Cerevisiae." *Journal of Bacteriology* 181 (1): 231. https://doi.org/10.1128/JB.181.1.231-240.1999.

Wang, Jiabo, and Zhiwu Zhang. 2021. "GAPIT Version 3: Boosting Power and Accuracy for Genomic Association and Prediction." *Genomics, Proteomics & Bioinformatics* 19 (4): 629–40. https://doi.org/10.1016/J.GPB.2021.08.005.

Wang, Yue, and Jianping Xu. 2022. "Population Genomic Analyses Reveal Evidence for Limited Recombination in the Superbug *Candida auris* in Nature." *Computational and Structural Biotechnology Journal* 20 (January): 3030–40. https://doi.org/10.1016/J.CSBJ.2022.06.030.

Watanabe, Nao Aki, Mamiko Miyazaki, Takaaki Horii, Koji Sagane, Kappei Tsukahara, and Katsura Hata. 2012. "E1210, a New Broad-Spectrum Antifungal, Suppresses *Candida albicans* Hyphal Growth through Inhibition of Glycosylphosphatidylinositol Biosynthesis." *Antimicrobial Agents and Chemotherapy* 56 (2): 960–71. https://doi.org/10.1128/AAC.00731-11.

Yadav, Anamika, Kusum Jain, Yue Wang, Kalpana Pawar, Hardeep Kaur, Krishan Kumar Sharma, Vandana Tripathy, Ashutosh Singh, Jianping Xu, and Anuradha Chowdhary. 2022. "*Candida auris* on Apples: Diversity and Clinical Significance." Edited by Leah E. Cowen. *MBio* 13 (2). https://doi.org/10.1128/MBIO.00518-22.

Yadav, Anamika, Anubhav Singh, Yue Wang, Merlijn Hi Van Haren, Ashutosh Singh, Theun De Groot, Jacques F. Meis, Jianping Xu, and Anuradha Chowdhary. 2021. "Colonisation and Transmission Dynamics of *Candida auris* among Chronic Respiratory Diseases Patients Hospitalised in a Chest Hospital, Delhi, India: A Comparative Analysis of Whole Genome Sequencing and Microsatellite Typing." *Journal of Fungi* 7 (2): 81. https://doi.org/10.3390/JOF7020081.

Zotchev, Sergey. 2003. "Polyene Macrolide Antibiotics and Their Applications in Human Therapy." *Current Medicinal Chemistry* 10 (3): 211–23. https://doi.org/10.2174/0929867033368448.

Chapter 7

Conclusions and Future Research Directions

7.1 Conclusions and Perspectives

My PhD thesis makes significant contributions to the expansion of our knowledge on *C. auris* by investigating its origin, discovering new ecological niches, detecting evidence of recombination, and identifying mechanisms of antifungal resistance.

In chapter 2, we reported the isolation of *C. auris* from tropical marine ecosystems in India, marking a significant finding as this yeast had previously only been identified in hospital environments. Interestingly, we isolated *C. auris* from two distinct habitats, namely salt marsh wetlands and sandy beaches of the Andaman Islands, India. The presence of *C. auris* in the salt marsh wetlands, which are untouched natural habitats abundant with sea birds and seagrass, is remarkable. This finding supports the hypothesis that *C. auris* might have existed as an environmental fungus before its emergence as a human pathogen (Casadevall et al., 2019). Furthermore, this discovery has motivated us to investigate additional non-clinical ecological niches of *C. auris*. However, further research is needed to understand the ecological implications of *C. auris* presence in these habitats in relation to human infections.

In chapter 3, we investigated a wide range of tropical and temperate fruit and identified that the surfaces of stored apples serve as a previously unrecognized reservoir for *C. auris*. Importantly, our results revealed that certain strains isolated from stored apples share clonal relationships with clinical isolates from India, indicating the existence of a potential transmission route between the surfaces of stored apples and clinical settings. Meanwhile, antifungal resistance as well as fungicides was frequently observed among *C. auris* isolates obtained from apples and clinical resistant strains. Additionally, metabarcoding analysis revealed a negative results of *C. auris*. Through genetic analysis, susceptibility testing of

environmental isolates from apple surfaces, and metabarcoding analysis of freshly picked apples, our study uncovered that the stored apples could act as a reservoir for the selection and transmission of azole-resistant *C. auris*. Based on our findings, we proposed that the contamination of apples by *C. auris* occurs through contact with human fingers and palms, particularly from individuals colonized with the yeast during postharvest treatment, storage, and distribution processes. The postharvest treatments, including the use of fungicides on stored apples and potentially other fruits, may contribute to the emergence and enrichment of drug-resistant strains, which could eventually be transmitted to clinical settings. This study significantly enhances our comprehension of the ecological niches of *C. auris* and will serve as a valuable reference for future investigations into the presence and behavior of this yeast in natural environments.

In chapter 4, we reported the first documented isolation of live *C. auris* culture from an animal source. Among the 87 dogs examined, four showed evidence of *C. auris* infection or colonization in their ears and on their skin surface, identified through culture and ITS meta-barcode sequencing. Interestingly, eight dogs had otitis externa (OE), and two of them were found to have *C. auris*, indicating a possible association between *C. auris* and external ear canal infections. Previous studies have isolated *C. auris* from human ear infections in Korea, Japan, and Iran, primarily belonging to Clade II and Clade V (Satoh et al., 2009a; Armaki et al., 2021; Jiwon Jung et al., 2020). A recent study from Spain investigating the microbiota in the ear canal of dogs with OE also identified *C. auris* in one dog and colonization on the skin of another dog (Puigdemont et al., 2021). Genomic analysis of *C. auris* strains from the ears of two dogs revealed genetically distinct strains of Clade I, suggesting a clonal transmission of this yeast in the Indian subcontinent. The association of *C. auris* with the ears in humans and dogs suggests that the ear canal may serve as an important reservoir for this yeast. Furthermore, the close genetic relationships between isolates obtained from dogs and humans indicate a possible source of transmission between the two. Further investigations are needed to explore the prevalence of *C. auris* transmission between humans and domesticated animals.

In chapter 5, we identified clear evidence of recombination both within the total sample and within individual clades of *C. auris*. Recombination was observed in both nuclear and mitochondrial genomes, as well as between them. The overall prevalence of recombination in the total sample suggests that it occurred more frequently before the divergence of the four clades than after. The specific mechanisms responsible for this recombination are currently unknown but warrant further investigation. The findings highlight potential research directions, such as sampling for alternative mating types, conducting laboratory mating experiments, and exploring the adaptive significance of shared genetic variations within the clades. These investigations will enhance our understanding of the genetic basis of virulence and drug resistance evolution in *C. auris* across different environments.

In chapter 6, we conducted GWAS analyses on different clades of *C. auris* strains (Clades I, III, and IV) using genomic data and MIC values for several antifungal drugs. A total of 48 antifungal-related SNPs were identified in *C. auris* across the examined clades. Clade I had 12 SNPs, with 5 in coding regions and 7 in noncoding regions. Clade III exhibited 24 SNPs, with 11 in coding regions and 13 in noncoding regions. Clade IV showed 12 SNPs, with 10 in coding regions and 2 in noncoding regions. These SNPs were associated with varying impacts on antifungal susceptibility, with some having positive effects and others having negative effects. Some SNPs in coding regions were previously shown to confer antifungal resistance, while those in noncoding regions were linked to genes involved in drug transmembrane transport, hydrolase activity, and integral component of the membrane. These findings validate the utility of GWAS methods for identifying antifungal-related variants in *C. auris*. Additionally, several novel SNPs were discovered, warranting further validation of their roles in antifungal resistance. Overall, our study enhances the understanding of antifungal mechanisms employed by *C. auris* and highlights the potential of these identified variants as diagnostic markers for rapid drug resistance detection or as new drug targets in clinical settings. A future direction of research is to expand the GWAS analysis to include a larger sample size. While our study focused on three clades of *C. auris*,

it is important to collect sufficient samples from the remaining clades (Clade II and V) to achieve a comprehensive understanding of the antifungal resistance mechanisms in this species. Obtaining data from these additional clades will provide valuable insights into the genetic variations and associated antifungal resistance traits across the entire *C. auris* population.

References

Armaki, Mojtaba Taghizadeh, Saeid Mahdavi Omran, Keyvan Kiakojuri, Shaghayegh Khojasteh, Jalal Jafarzadeh, Mahin Tavakoli, Hamid Badali, et al. 2021. "First Fluconazole-Resistant *Candida auris* Isolated from Fungal Otitis in Iran." *Current Medical Mycology* 7 (1): 51. https://doi.org/10.18502/CMM.7.1.6243.

Casadevall, Arturo, Dimitrios P. Kontoyiannis, and Vincent Robert. 2019. "On the Emergence of *Candida auris*: Climate Change, Azoles, Swamps, and Birds." *MBio* 10 (4). https://doi.org/10.1128/mbio.01397-19

Jung, Jiwon, Min Jae Kim, Ja Young Kim, Jeong Young Lee, Sun Hee Kwak, Min Jee Hong, Yong Pil Chong, et al. 2020. "*Candida auris* Colonization or Infection of the Ear: A Single-Center Study in South Korea from 2016 to 2018." *Medical Mycology* 58 (1): 124–27. https://doi.org/10.1093/MMY/MYZ020.

Puigdemont, Anna, Sara D'Andreano, Laura Ramió-Lluch, Anna Cuscó, Olga Francino, and Pilar Brazis. 2021. "Effect of an Anti-Inflammatory Pomegranate Otic Treatment on the Clinical Evolution and Microbiota Profile of Dogs with Otitis Externa." *Veterinary Dermatology* 32 (2): 158-e37. https://doi.org/10.1111/VDE.12930.

Satoh, Kazuo, Koichi Makimura, Yayoi Hasumi, Yayoi Nishiyama, Katsuhisa Uchida, and Hideyo Yamaguchi. 2009. "*Candida auris*, a Novel Ascomycetous Yeast Isolated from the External Ear Canal of an Inpatient in a Japanese Hospital." *Microbiology and Immunology* 53 (1): 41–44. https://doi.org/10.1111/J.1348-0421.2008.00083.X.